THE UNIVERSITY OF CALGARY

# Respiratory Chemoreception and Rhythm Generation in the Tadpole Brainstem

by

Cory S. Torgerson

A DISSERTATION

SUBMITTED TO THE FACULTY OF GRADUATE STUDIES

IN PARTIAL FULFILMENT OF THE REQUIREMENTS FOR THE

DEGREE OF DOCTOR OF PHILOSOPHY

DEPARTMENT OF CARDIOVASCULAR/RESPIRATORY PHYSIOLOGY

CALGARY, ALBERTA

August 11, 1998

National Library
of Canada

Acquisitions and
Bibliographic Services

395 Wellington Street
Ottawa ON K1A 0N4
Canada

Bibliothèque nationale
du Canada

Acquisitions et
services bibliographiques

395, rue Wellington
Ottawa ON K1A 0N4
Canada

*Your file Votre référence*

*Our file Notre référence*



0-612-34705-2

Canada

## *ABSTRACT*

Neural mechanisms underlying the generation and maintenance of breathing remain elusive, reflecting the complexity of the neural phenomena and the relative inadequacy of the available techniques. Because neural mechanisms responsible for lung ventilation and central respiratory chemoreception are likely conserved among air-breathing vertebrates, understanding respiratory control in "primitive" air-breathing vertebrates could yield valuable insight into the basic principles underlying respiratory control in all vertebrates. The purpose of this thesis was to investigate central respiratory rhythm generation and chemoreception in larval amphibians during the transition from gill to lung ventilation.

An *in vitro* brainstem preparation of the bullfrog tadpole *Rana catesbeiana* was developed that retains the necessary neural circuitry to generate spontaneous rhythmic motor output in the absence of peripheral input. Measurements of tissue pH and $P_{O_2}$ demonstrate that the isolated tadpole brainstem, although moderately acidic, is well-oxygenated. Minimum values of tissue pH and $P_{O_2}$ ($7.34 \pm 0.12$ and $240 \pm 68$ Torr) were recorded at a depth of 850-900 mm below the ventral surface. Comparison of *in vitro* recordings from cranial and spinal nerve roots with

similar recordings from *in vivo* preparations establish the identity of gill and lung ventilation during fictive breathing.

Studies using global hypercapnic challenges reveal the existence of central chemoreceptive influences during gill ventilation and a transfer of this influence from gill to lung regulation during development. The location of central respiratory chemoreceptor (CRC) elements was assessed by discrete microinjection of hypercapnic artificial cerebrospinal fluid into the brainstem. These results show that CRCs become progressively more prevalent with development and are functionally translocated from caudal brainstem areas, at the level of CN IX and SN II roots, to rostral brainstem regions, from the level of CN IX to an area 500 μm rostral to CN V. Brainstem regions critical for lung burst generation were localized by progressive transection. These results establish that the neurons essential for the generation of lung motor output roughly correspond to the location of CRC elements and translocate rostrally with development.

## ACKNOWLEDGEMENTS

First and foremost, I would like to acknowledge the Lord Jesus Christ, who has been my "firm foundation". I can do all things through Christ who strengthens me (Phil. 4:13).

I wish to express my sincerest gratitude to my advisor, Dr. John Remmers, for his incredible investment into my life. John has been a mentor of the finest caliber, teaching me, by example, what it is to be a fine scientist. Thank you for your constant encouragement, constructive criticism and direction. Thank you for imparting to me your enthusiasm for science, your love of great words, and many pearls of wisdom such as: "Mother Nature never lies, you just have to listen carefully", and "Let your data speak for itself, you don't have to gild the lily".

I wish to thank my supervisory committee, Dr. Naweed Syed and Dr. Ray Turner, for their valuable insights and encouragement throughout my training. Thanks also to the members of my examining committees, Dr. Peter Scheid, Dr. Bill Whitelaw, Dr. Richard Walker and Dr. Quentin Pittman, for their helpful comments and suggestions.

I would also like to extend my appreciation to my lab mates and best buddies, Heather Eliason and Dr. Matthew Gdovin, without whom coffee, lunch, coffee and workout is unbearable. Heather, thank you for helping me to put things in perspective, helping me to remember to take a break, helping me all the time. Matt, thanks for believing in me, for showing me the ropes and making it exciting to come to the lab to do science.

I wish to especially thank my family for their overwhelming love and support, who made it possible for me to achieve this goal. Mom and Dad, I am what I am because of you.

## *TABLE OF CONTENTS*

## *LIST OF TABLES*

## *LIST OF FIGURES*

CHAPTER FIVE: CHARACTERIZATION OF SPONTANEOUS BURSTING ACTIVITY IN THE TADPOLE BRAINSTEM



CHAPTER SIX: ONTOGENY OF CENTRAL RESPIRATORY CHEMORECEPTION IN THE ISOLATED TADPOLE BRAINSTEM



CHAPTER SEVEN: LOCATION OF CENTRAL RESPIRATORY CHEMORECEPTORS IN THE ISOLATED TADPOLE BRAINSTEM DURING DEVELOPMENT

# *CHAPTER ONE*

## *General Introduction*

### 1.1 STRUCTURE-FUNCTION RELATIONSHIPS IN TETRAPODS

By the middle Devonian, the stage was set for the appearance of terrestrial vertebrates. The first vertebrate to set fin on land was a sarcopterygian (lobe-finned fish), giving rise to labyrinthodonts, the first tetrapods that migrated from water to land (Norris, 1985). The classic theory put forth by Romer (1958) proposed that the aquatic ancestor of air-breathing vertebrates inhabited warm swampy areas where fluctuations of oxygen and carbon dioxide levels in the water commonly occurred. In response to aquatic hypoxia these fish presumably could supplement oxygen uptake at the gills by swimming to the surface and gulping air, or in shallow water, by propping themselves on their pectoral fins to lift their heads to the surface (Randall *et al.*,

1981). The evolutionary transition from water to land is complex because water and air have such different properties: aquatic animals are supported by water; terrestrial animals need skeletons and limbs. Aquatic animals extract oxygen from a unidirectional flow of water across the gills; terrestrial animals breathe air that they pump in and out of sac-like lungs. Accordingly, the invasion of land required two pivotal innovations: aerial respiration and quadrapedal locomotion. As one wag put it, evolutionary movement from water to land required only lungs and legs (for review, see Dejours 1975).

The development of limbs adequate to bear the weight of an animal in the absence of aquatic buoyancy was a critical pre-adaptation for terrestrial life. In shallow water, an air-breathing upstanding fish could have lifted its head above the water. Certain air-breathing fish had limbs developed enough to allow them to crawl from evaporating ponds and move overland to other, larger bodies of water in which their chances of survival were better.

Development of air receptacles that efficiently exploited "$O_2$-rich" air was undoubtedly an adaptive asset that facilitated survival on land. The transition from water breathing with gills to air breathing with lungs provided a selective advantage, owing principally to the physico-chemical properties of the convective media. Air, much less dense and much less viscous than water, allowed mechanically efficient connective distribution of the ambient media through small airways into micro-alveoli. Further, the capacitance of $O_2$ in air is 30 times

greater than in water at 20 °C. As a result, air-breathers required lower rates of ventilation despite substantial increases in oxidative metabolism and the high mechanical efficiency of air breathing permitted large increases in oxygen consumption at low metabolic cost during muscular exercise. (Dejours, 1988).

However, these advantages were countered by problems posed by $CO_2$ elimination, resulting directly from the decreased solubility and diffusibility of $CO_2$ in air as compared to water. This is reflected in the appearance of $CO_2$ chemoreception, a key component of $CO_2$ homeostasis. To provide feedback information related to arterial $P_{CO_2}$, the peripheral chemoreceptor, which evolved from an $O_2$ receptor in the first gill arch, developed $CO_2$ chemosensitivity. In addition, a central chemoreceptor positioned in the brainstem appeared in amphibia (De Marneffe-Foulon, 1962). This receptor sensed a $P_{CO_2}$ value related to arterial $P_{CO_2}$, but was associated with a considerable delay caused by the slow dynamics of equilibration of arterial $CO_2$ with the relatively large $CO_2$ capacity of the brain. One reasonable hypothesis regarding the function of the central chemoreceptor is that its slow dynamics enhance stability of the potentially high gain ventilatory control system produced by the efficient lung breathing an $O_2$ rich media.

The form and function of the respiratory systems of extant air-breathing fishes and amphibians reflect a diversity of successful adaptations to the limits

imposed by differences in the physical properties of air and water. Amphibians, the modern descendents of labyrinthodonts, undergo metamorphosis from a water-breathing larval stage (tadpole), during which gas exchange takes place through the skin and the gills, to an air-breathing adult stage, where cutaneous and pulmonary respiration predominate (Dejours, 1988; Burggren and West, 1982). In amphibians, the shift from water to air ventilation required two essential additions to the respiratory control system: a rhythmic neuromuscular controller for tidal movement of air into the lungs, and a $CO_2$ chemoreceptor. Recent studies indicate that these two functions may be intimately associated at the neuronal level; $CO_2$ chemosensitivity occurs in regions of the brain having dense populations of respiratory neurons (Coates *et al.,* 1993), and respiratory neurons appear to possess intrinsic $CO_2$ chemosensitivity (Kawai *et al.,* 1996). The larval form of frogs, tadpoles, provide a remarkable opportunity to investigate the ontogeny of $CO_2$ chemosensitivity and lung ventilatory rhythmogenesis. To the extent that ontogeny may recapitulate phylogeny, gill and lung ventilation in the developing tadpole may provide a "rerun" of that momentous episode in evolution when lung ventilation replaced gill ventilation. Because neural mechanisms responsible for lung ventilation and central respiratory chemoreception are likely conserved among air-breathing vertebrates, understanding respiratory control in "primitive" air-breathers could yield valuable insight into the basic principles underlying respiratory control in all vertebrates.

## 1.2 ONTOGENY OF BREATHING IN AMPHIBIANS

In anuran development, breathing goes through important changes. Immediately after hatching, bullfrog tadpoles respire predominantly by the diffusion of $O_2$ and $CO_2$ through their well-perfused skin (Burggren, 1984). As the tadpole matures, supplemental respiration is provided by the active ventilation of the internal gills as the opercular membrane develops, internal branchial chambers are formed and the buccal musculature differentiates (DeJongh, 1968). Here, the buccal floor develops rhythmic dorso-ventral movements, which draw a unidirectional stream of water into the mouth, through the gills and out the single opercular spout (Gradwell, 1972a, b). With further development and increasing need for $O_2$ transport, gill arch VI provides blood to the developing pulmonary circulation, enabling the paired unicameral lungs to contribute to respiratory function (Burggren, 1984). Thus, the relative contributions of internal gills, lungs and skin to the total gas exchange changes during larval development (Burggren and West, 1982). Early in development (stages 4-5, Taylor and Köllros, 1946), the lungs are ventilated infrequently and do not contribute significantly to gas exchange. As shown in Fig. 1.1, the skin accounts for a greater percentage of both $O_2$ and $CO_2$ exchange than the gills or lungs through stage 14. However, $O_2$ uptake across the lungs increases at the onset of metamorphosis (stage 16) such that gills and lungs each account for 20% of oxygen exchange (Burggren and West, 1982). At this time, amphibian larvae show ventilatory patterns similar to

those described for air-breathing fishes, where regular branchial ventilations, producing continuous, unidirectional water flow over the gills, are coordinated with single air breaths (Smatresk, 1990). During metamorphic climax (stage 18-19), the gills and tail begin to degenerate and the lungs replace the skin as the primary site of $O_2$ exchange. In post-metamorphic larvae, as in adults, the skin plays a minor role in $O_2$ uptake (less than 20%), but persists as the major site of $CO_2$ excretion.

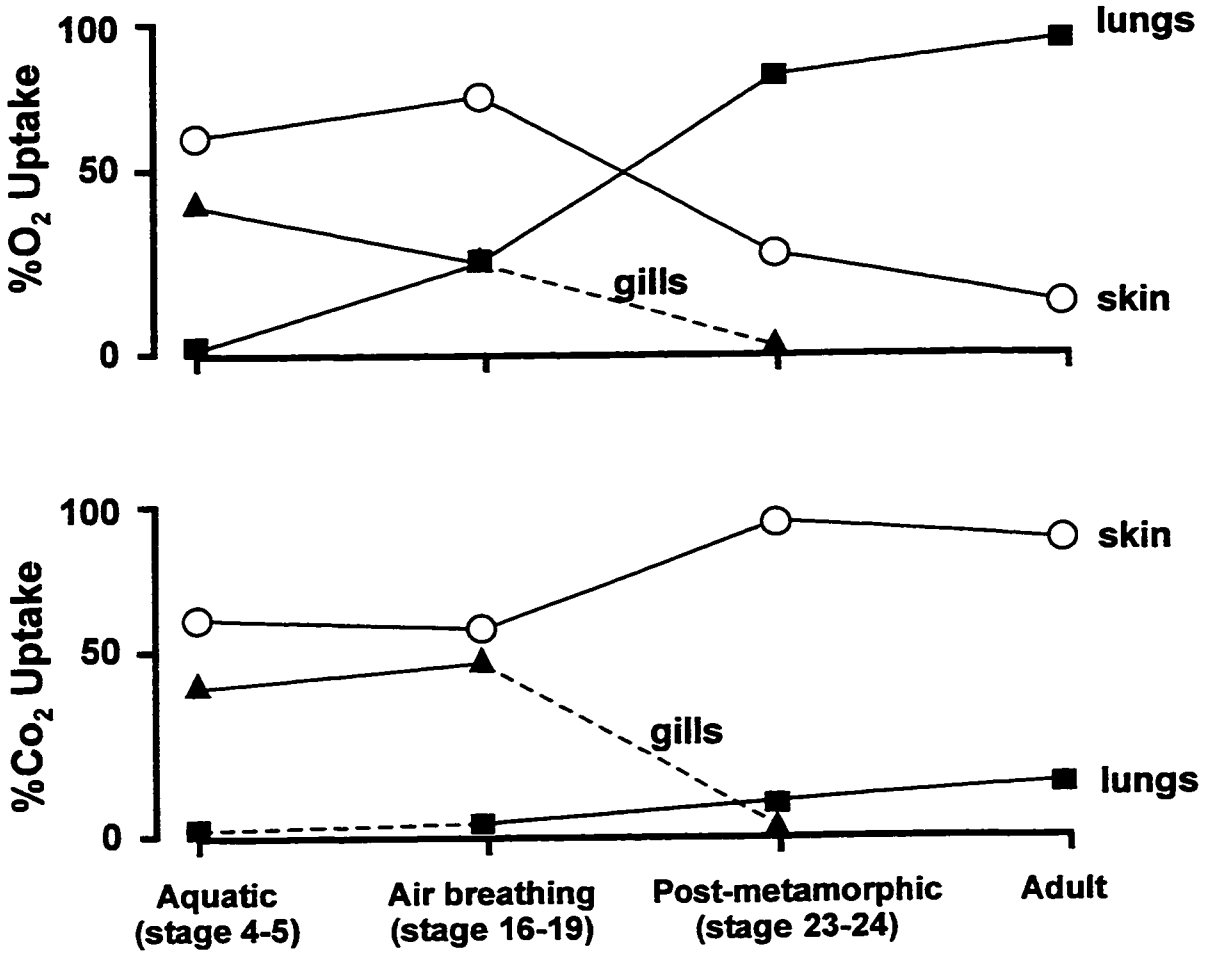


**Figure 1.1** Changes in gas exchange partitioning between gills, lungs and skin during metamorphosis at 20 °C in the bullfrog, Rana catesbeiana (adapted from Burggren and West, 1982).

## 1.3 MECHANISMS OF GILL VENTILATION

Gill ventilation in tadpoles is powered by antagonistic muscles in the oropharynx that drive oscillatory pumping movements, causing water to flow continuously over the gills. As illustrated in Fig. 1.2A, the buccal pressure pump aspirates water into the mouth and then forces it into the pharyngeal cavity and through the gills (Gradwell, 1971). This buccal pump alternates with a pharyngeal pump which receives water from the buccal cavity and forces it into the opercular cavity. As shown in Fig 1.2B, when the hydrostatic pressure in the buccal cavity increases through elevation of the buccal floor, pharyngeal pressure follows passively as the pharyngeal cavity expands, forcing water over the gills. When buccal pressure begins to decrease, the dorsal and ventral velum seal and obstruct flow between the two cavities and constriction of the pharyngeal pump musculature maintains a supra-atmospheric pharyngeal pressure, driving water over the gill clefts.

In the tadpole, Gradwell and Walcott (1971) described rhythmic bursts of neural activity, transmitted by branches of cranial nerves VII and X, that coordinated muscular activity during gill irrigation. During buccal filling (Gradwell's "inspiration"), activation of cranial nerve (CN) VII branches innervating the hyoidean muscles H2a and H2b cause a decompression of the buccal cavity and

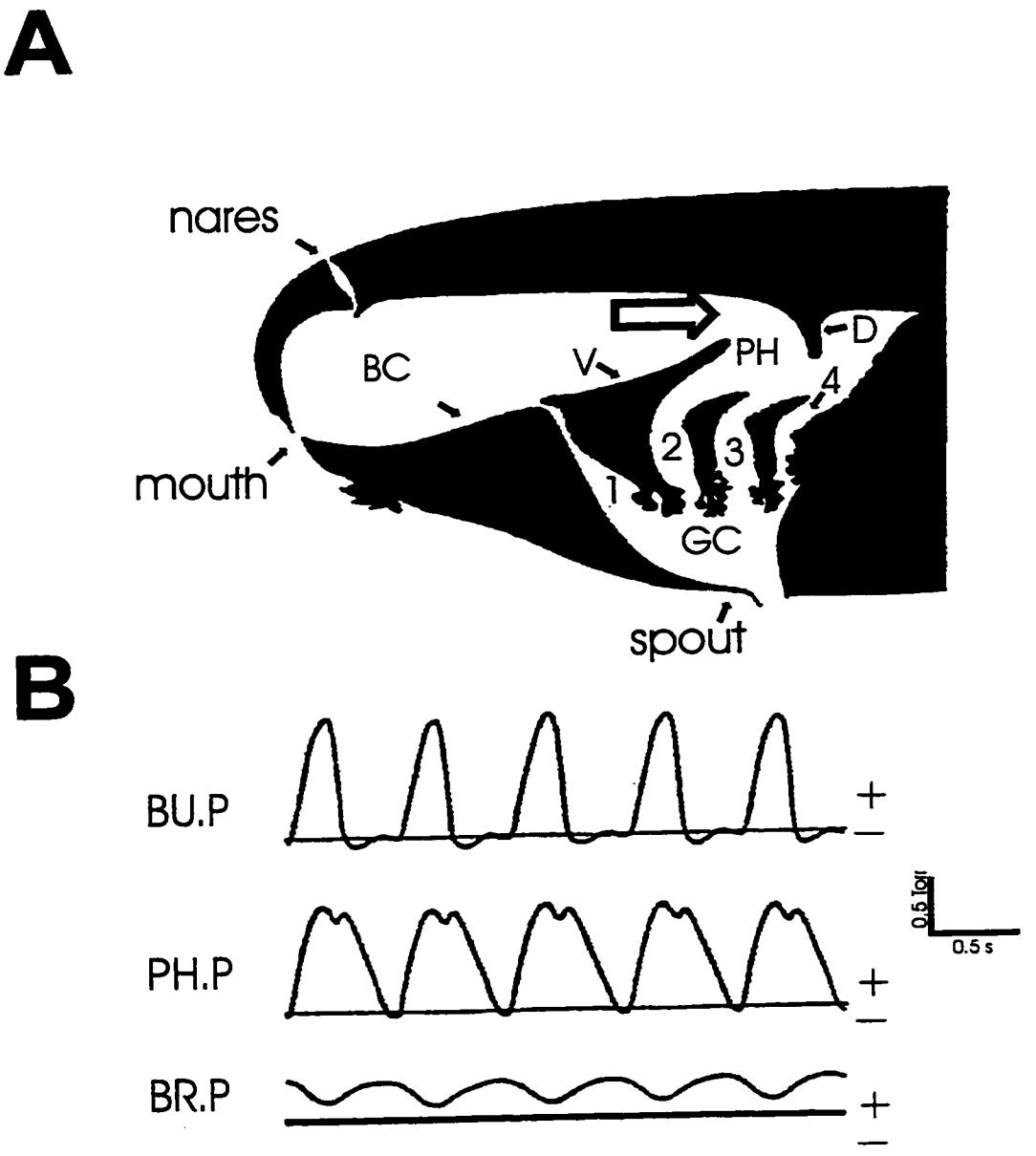


**Figure 1.2** Panel A: composite diagram of sagittal and parasagittal sections through the head of a bullfrog tadpole. The anatomy is shown in its orientation at the onset of expiration. The large arrow indicates water, which is beginning to flow over the ventral velum. BC, buccal cavity; D, dorsal velum; GC, gill cavity; PH, pharynx; V, ventral velum; 1 to 4, gill clefts 1 to 4. Panel B: correlated hydrostatic pressures in the buccal cavity (BU.P), pharynx (PH.P), gill cavity (BR.P) of a regularly breathing tadpole at 14°C.

subsequent increase in volume, while activation of branchial muscles B1a, B1b, B1c and B1d via action potentials in CN X produce pharyngeal constriction (Gradwell, 1971). In contrast, decreasing the volume of the buccal cavity (Gradwell's "expiration") is achieved through contraction of hyoidean muscle H3a, innervated by branches of CN VII, elevating the floor of the buccal cavity, along with expansion of the pharyngeal cavity caused by branchial muscles B3a, B3b and B4 innervated by branches of CN X.

## 1.4 MECHANISMS OF LUNG VENTILATION

Whereas the mechanics of internal gill irrigation in the tadpole is homologous to water-breathing fish, the basic mechanism for lung ventilation in anuran tadpoles is thought to be similar to that described in lung fish (McMahon, 1969) and in adult frogs (DeJongh and Gans, 1969; West and Jones, 1975; MacIntyre and Toews, 1976), and consists of modification of buccal movements normally used to continuously propel water through the branchial chambers. In the dipnoan lungfish Protopterus, McMahon (1969) described the mechanics of the aerial cycle as a series of consecutive aquatic movements modified to serve a specific phase of lung ventilation. The first event occurs as the animal approaches the surface prior to ventilation and the buccal floor is elevated, compressing the buccal cavity and subsequently removing the water. Next, as the mouth opens into the air, the buccal cavity expands, drawing in sufficient air to reinflate the lungs and the glottis opens, allowing expiration of the compressed gas in the lung, driven by elastic recoil. Finally, air in the buccal cavity is compressed by elevation of the buccal floor and forced through the pneumatic duct and into the lungs. Sufficient lung inflation is often accomplished through several oscillations of the buccal pump.

Adult bullfrogs display a comparatively complicated, but well-coordinated activation of oropharyngeal muscles that moves buccal and pharyngeal structures

to ventilate the oropharyngeal cavity continuously and the lung intermittently (Kogo *et al.*, 1994). As illustrated in Fig 1.3, ventilatory patterns analyzed in frogs were found to consist of three characteristic cycles: buccal ventilation, lung deflation and lung inflation (DeJongh and Gans, 1969; West and Jones, 1975; Milsom, 1991). In buccal ventilation, the presumed remnant of gill ventilation, rhythmic elevation and depression of the buccal floor produces tidal ventilation of the oropharynx with air entering and leaving through the nares (Gans, 1970). These high frequency ventilation cycles are periodically interrupted by lung ventilation cycles (1-3 breaths/minute) which begin with a deep depression of the buccal floor that draws a large volume of gas into the buccal cavity through the nares (DeJongh and Gans, 1969). The glottis is then opened, allowing gas to flow from the lung into an expanding oropharynx and out the nares. Following pulmonary expiration, the nares close and the floor of the buccal cavity is elevated, pushing the buccal air into the lung. The glottis then closes, trapping gas in the lung where it is held until the next lung ventilation cycle (DeJongh and Gans, 1969).

Although no study has focussed on the complex transition of lung ventilation mechanics from water-breathing anuran larvae to the air-breathing adult, hydrostatic pressure transients in the buccal cavity of bullfrog tadpoles indicate that air is drawn in through the mouth (rather than through the nares as in adults), and then is compressed by an exaggerated upward movement of the

buccal cavity (Burggren, 1984). At this time, lung filling occurs during the brief opening of the glottis and remains full until the beginning of the next cycle, where exhalation, powered by elastic recoil and hydrostatic pressure of the body wall, drives the air out of the lungs. Upon completion of metamorphosis, the branchial pump is modified exclusively for air breathing, and the branchial cavity is normally filled with air between breaths (Smatresk, 1990).

In the adult frog, Sakakibara (1984a, b) described in detail the respiratory output in specific branches of CN V, VII, X and the hypoglossal innervating buccal and laryngeal muscles, and correlated these neural patterns to electromyographic (EMG) data obtained by DeJongh and Gans (1969) and by West and Jones (1975). Similarly, studies from McLean *et al.* (1995a, b), Kogo *et al.* (1994), Kogo and Remmers (1994) and Ito *et al.* (1962) demonstrated that the patterns of efferent activity from brainstem neurons was synchronous with the buccal and pulmonary ventilatory cycles of adult bullfrogs. Here, two types of rhythmic bursting outputs were observed: 1) a high frequency, low amplitude reciprocal oscillation representing fictive oropharyngeal ventilation between branches of CN V and main branch of the hypoglossal nerve (buccal levator) and the sternohyoid branch of the hypoglossal nerve (buccal depressor); and 2) a low frequency, high amplitude synchronous bursting of branches of CN V, X and the main branch of the hypoglossal inferred to represent fictive pulmonary ventilation.

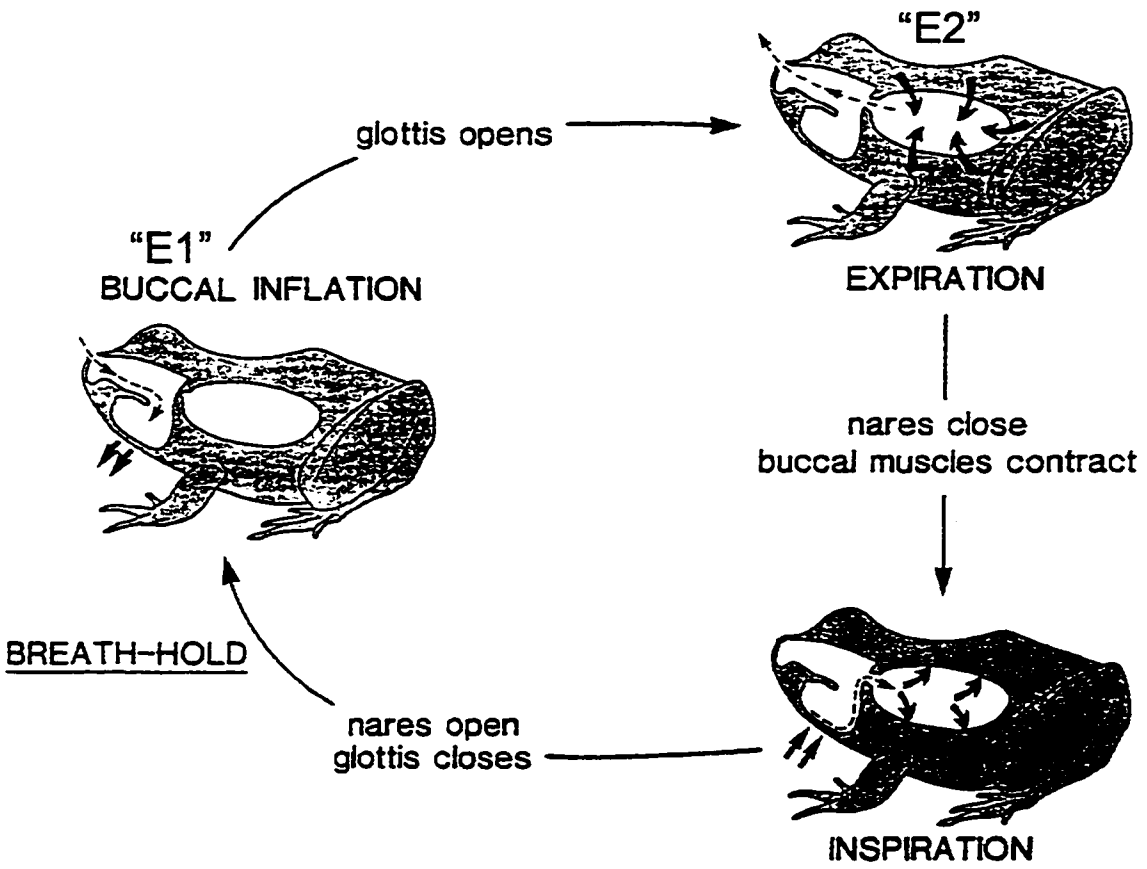


**Figure. 1.3** Breathing cycle of the adult frog (Adapted from Gans et al., 1969). E1, phase 1 of expiration; E2, phase 2 of expiration (see text).

## 1.5 CONTROL OF BREATHING IN AMPHIBIANS

While the functional and mechanical aspects of multi-modal gas exchange have been extensively described (DeJongh and Gans, 1969; West and Jones, 1975; Burggren and West, 1982; West and Burggren, 1982,1983), the corresponding knowledge of the central neural mechanisms of respiratory control is somewhat limited. The motor act of breathing in amphibians represents the final product of interplay of both voluntary and involuntary neural components at various levels of the central nervous system (CNS). The neural respiratory control system involves the interplay of these voluntary and involuntary components with chemical and proprioceptive feedback from the periphery. Although differences in central neural processes controlling breathing exist between mammals and amphibians, the basic features of the respiratory control system are conserved. These include: the respiratory central pattern generator (CPG), central and peripheral chemoreception, vagal volume feedback, and a 3-phase lung ventilatory cycle.

### 1.5.1 Central and peripheral chemoreception

The primary receptors involved in chemical homeostasis are the central and peripheral chemoreceptors. In adult amphibians, peripheral chemoreceptors that

monitor blood $O_2$ and $CO_2$ levels are found in the carotid labyrinth, a structure located at the bifurcation of the carotid artery (Ishii and Ishii, 1970; Ishii *et al.,* 1985; Van Vliet and West, 1992). These receptors are innervated by a branch of the glossophaymgeal nerve that projects its afferent fibers to the solitary tract in the brainstem (Stuesse *et al.,* 1984). While amphibians have some arterial receptors sensitive to $P_{CO_2}/[H^+]$ (Ishii and Ishii, 1976; 1985), arterial $P_{O_2}$ sensitive receptors seem to be more prevalent (Smatresk, 1990). Carotid labyrinth denervation caused a significant reduction of resting ventilatory activity in unanesthetized toads as compared with sham-denervated animals, but had no significant effect on the ventilatory response to hypoxia (Evans and Shelton, 1984; West *et al.,* 1987; Jones and Chu, 1988). These findings indicate that the carotid labyrinth influences respiratory drive but is not essential for the control of ventilation during hypoxia. Oxygen sensitive chemoreceptors residing in the aortic trunk and pulmocutaneous arteries have been established in both adult toad and frogs (Ishii *et al.,* 1985; Van Vliet and West, 1986;1987), however, the relative contribution of these sites to the hypoxic ventilatory response is unknown.

Peripheral chemoreception has also been identified in larval amphibians. Studies by West and Burggren (1983), Burggren and Doyle (1986) and Infantino (1992) demonstrate that exposure to aquatic hypoxia increased the frequency of both gill and lung ventilatory cycles in larvae younger than stage 22. However, the functional development of the carotid labyrinth remains unclear. Adams

(1958) reported that the labyrinth was absent in anuran larvae until after metamorphosis (stage 16-19). Further, in stage 5-7 tadpoles, Jia and Burggren (1989) showed gill ventilatory changes in response to step-wise changes in inspired water $P_{O_2}$ and suggested that an extrareceptor on the gills or within the oropharyngeal cavity contributed to the regulation of gill ventilation.

Central chemoreceptors reside within the medulla and respond to changes in $P_{CO_2}$ and/or $[H^+]$ of the extracellular fluid bathing the brain. Mitchell *et al.* (1963), Schläfke *et al.* (1970) and Cherniak *et al.* (1979) described three regions of the ventral lateral medulla in cats containing neural elements that function as central chemoreceptors: the rostral, intermediate and caudal chemosensitive zones. At present, however, neither the exact stimulus ($P_{CO_2}$ or $[H^+]$), nor the exact locations of medullary chemoreceptors are known. In anesthetized toads, indirect evidence for the existence of ventral medullary chemoreceptors which respond to acid hypercapnic challenge has been demonstrated by Smatresk and Smits (1991). These results have since been repeated in unanesthetized toads (Branco *et al.,* 1992), and confirm the early findings of De Marneffe-Foulon (1962) who also reported an increase in pulmonary ventilation when the brain of *Rana* was bathed in acidic saline. The response of gill ventilation to $CO_2$ has been previously described in fishes and tadpoles, however, there exists not compelling evidence for central chemosensitivity (Hughes and Shelton, 1962; Infantino,

1992). Acidic superfusion of isolated carp and lamprey brainstems, produced no response in fictive gill bursts (Hughes and Shelton, 1962; Rovainen, 1977).

The development of central chemoreceptors, in addition to peripheral chemoreceptors, most likely reflects the importance of defending the acid-base balance of the tissue (Tenney and Leiter, 1995). Once animals invaded land, they entered an environment with abundant oxygen, where high levels of ventilation were no longer necessary to obtain adequate oxygen. However, the removal of $CO_2$ became increasingly more difficult. Once air breathing was entrenched as the dominant mechanism of gas exchange, a quasi-reciprocal relation between $P_{CO_2}$ and $P_{O_2}$ was established. The particular value of tissue $P_{CO_2}$ probably became unimportant so long as adequate tissue oxygenation was maintained. Nonetheless, the particular $P_{CO_2}$ value was well defended because of the effect of $CO_2$ on acid-base balance. Effective protein function depends on maintaining protein conformation and relative charge state, requiring a stable ionic and pH environment. Hence, the development of central $CO_2$ chemoreception may have had less to do with ventilatory control and gas exchange than with protein function and acid-base balance.

### 1.5.2 Pulmonary stretch receptors

Pulmonary stretch receptors, resident in the connective tissue of the pulmonary walls and septa of large airways in amphibians (Knowlton and Larrabee, 1946) regulate lung volume feedback, thereby ensuring that the inspiratory and expiratory phases of the breathing cycle are consistent (Milsom and Jones, 1977). On the basis of their discharge characteristics, Milsom and Jones (1977) and Jones and Milsom (1982) identified three types of slowly adapting pulmonary mechanoreceptors that respond to static and dynamic changes in transmural pressure associated with changes in lung volume: 1) those which respond to the degree of lung inflation, 2) those that respond to the rate at which lung volume changes or 3) those which respond to both stimuli.

Mechanoreceptors of amphibians report to the CNS via afferent fibers in the pulmonary vagii (Milsom and Jones, 1977), which are thought to project to the nucleus of the tractus solitarius in the brainstem (Stuesse *et al.,* 1984). These inputs are thought to be important in determining the duration of breath holding in anurans, and also contribute to adjustments in tidal volume and frequency of lung ventilation. Evans and Shelton (1984) demonstrated that pulmonary deafferentation by vagotomy in *Xenopus,* increased the number of inspirations in a ventilatory period and caused overinflation of the lungs. Pulmonary stretch receptors are also thought to be important in the reflex regulation of gill

ventilation in larval *Rana catesbeiana* (West and Burggren, 1983). Lung inflation in stage 17-19 larvae resulted in a rapid decrease in both gill frequency and buccal cavity pressure independent of the $P_{O_2}$ of the inflation gas.

Additional information about the status of lung volume is also conveyed by chemosensitive mechanoreceptors. Kuhlmann and Fedde (1979) showed that mechanoreceptors decrease their firing rates when intrapulmonary $CO_2$ concentration was increased. It has also been suggested that intrapulmonary mechanoreceptors provide sensory input, which mediates adjustments in pulmonary blood flow as the degree of lung inflation changes (West and Burggren, 1984).

### 1.5.3 Breathing and central pattern generators

Neuronal elements that fundamentally generate and control normal resting breathing (eupnea) reside in the pons and medulla. In serial brainstem transection studies in cats, Lumsden (1923c) first documented that:

> "...the automatic respiratory center is in the lower part of the bulb, and the regulation of impulses sent out by it, is determined by impulses passing to it."

Subsequently, these original findings have been confirmed by similar brainstem transection experiments in lampreys, (Rovainen, 1985), frogs (Langendorff, 1887;

Oka, 1958a, b), turtles (Lumsden, 1924) and birds (Gleeson and Moloney, 1989), establishing that in all classes of vertebrates, the basic rhythm generator for breathing is situated in the caudal portion of the brainstem. More recently, the site of rhythmogenesis in mammals has been localized to the pre-Bötzinger complex (Smith *et al.,* 1991), situated in the reticular formation of the medulla near the rostral portion of the ventral respiratory group. Recordings of cranial and spinal nerves from completely isolated brainstem-spinal cord preparations of the neonatal rat (Suzue, 1984), lamprey (Rovainen, 1985), frog (McLean *et al.,* 1995b) and turtle (Douse and Mitchell, 1990) demonstrate spontaneous rhythmic respiratory motor output. That these preparations produce a respiratory rhythm in the absence of feedback from peripheral receptors, such as lung mechanoreceptors or peripheral chemoreceptors, provide considerable evidence that breathing is generated by a brainstem central pattern generator (CPG).

The concept of a CPG has emerged to facilitate an understanding of the relationship between respiratory rhythm and pattern. A CPG can be operationally defined as one or more neuronal processes that, acting together, generate a periodic bursting rhythm with defined spatio-temporal characteristics in the absence of peripheral afferent input. Thus, one component provides a rhythmogenic function and the other determines the shape and distribution of respiratory motor signals to various output stations (cranial and spinal motorneuron pools) (Funk and Feldman, 1995). In theory, 3 basic mechanisms

that govern rhythmogenic function have been identified, namely, networks that involve burster or pacemaker neurons (see Fig. 1.4A), networks that rely on synaptic connections between neurons to produce a rhythmic output (Fig. 1.4B) and networks that require both (Fig. 1.4C). As shown in Fig 1.4A, pacemaker neurons generate spontaneous rhythmic oscillations in membrane potential in the absence of synaptic inputs. Although conceptually interesting, no conclusive evidence shows that separate rhythm generating and pattern controlling functions underlie the generation of eupnea. Pacemaking and motor controlling functions may, alternatively, be combined so that the rhythmogenic function emerges from synaptic interconnections of a variety of respiratory interneurons that also control the spatio-temporal aspects of the respiratory pattern. Brown (1911) proposed the simplest demonstration of this arrangement in the "half-center" model (Fig. 1.4B), where inspiratory and expiratory neurons reciprocally inhibit each other. An additional mechanism, not shown in Fig 1.4B, is required to limit the duration of the inspiratory and expiratory phases and, thereby, cause switching between the two sequential phases.

Evidence from a variety of vertebrate preparations (Burggren and Doyle, 1986; Getting, 1988; Henke *et al.,* 1988; Orem and Vidruk, 1998) show that neural oscillations underlying respiratory rhythm generation require some external

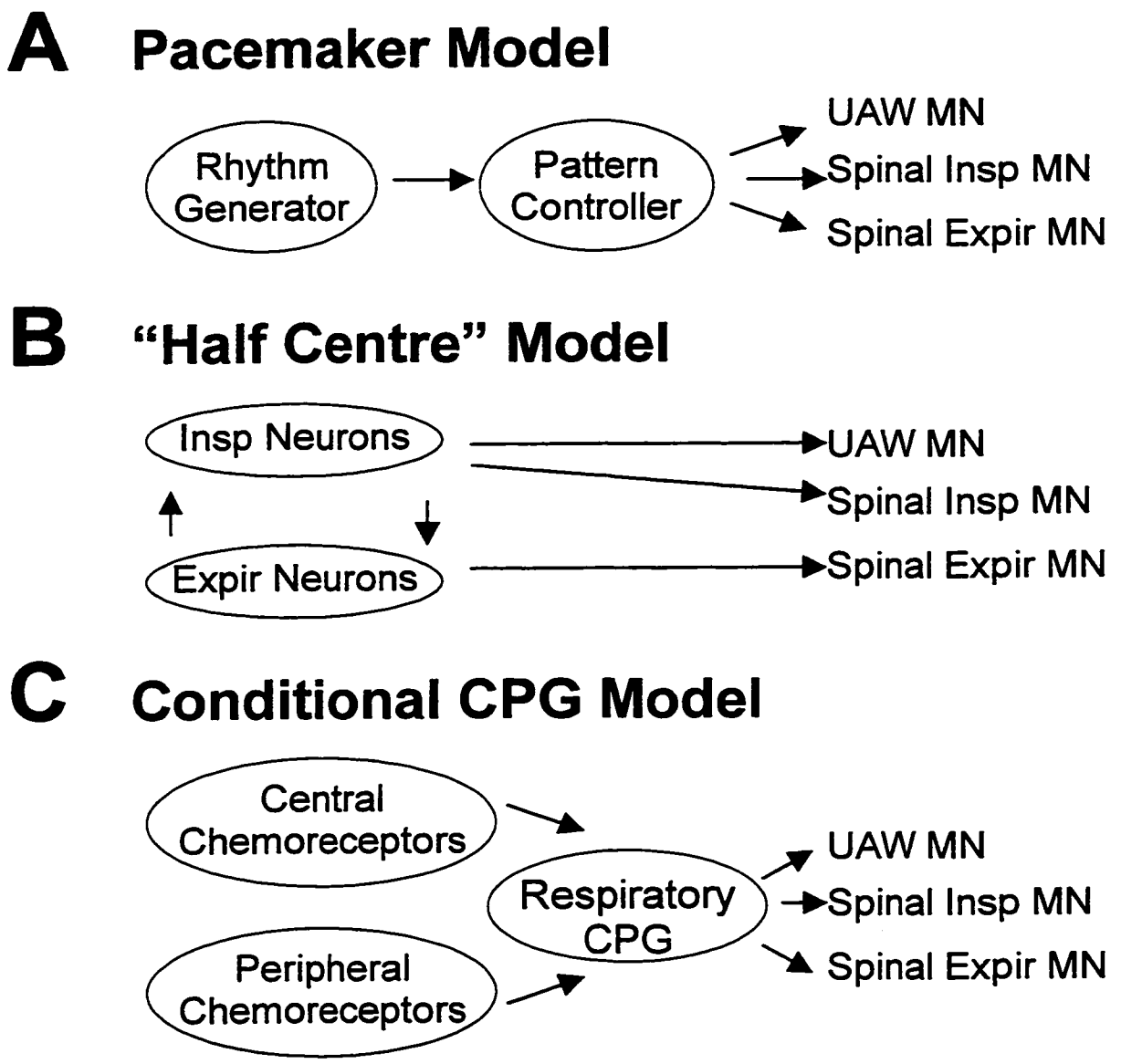


**Figure 1.4** Various central pattern generator (CPG) models are depicted. In all models, a respiratory CPG projects to upper airway (UAW) motor neurons (MN), spinal inspiratory (Insp) and spinal expiratory (Expir) motor neurons. A) Pacemaker Model: Rhythm generator (pacemaker) drives a functionally separate pattern controller which determines the precise timing and amplitude of respiratory bursts in various output stations. B) Half Center Model: Rhythm generation and pattern control are functionally inseparable and derived from inhibitory interconnections between inspiratory and expiratory neurons. Phase switching is provided by an additional neuronal circuit (not shown). C) Conditional CPG Model: The conditional CPG requires excitatory input from central and/or peripheral chemoreceptors in order to be physically active.

stimulus. This requirement indicates that respiratory CPGs in vertebrates are conditional oscillators, rather than endogenously active. Medullary CPGs that produce endogenous rhythmic bursts of activity responsible for gill and lung ventilation in amphibians require tonic influence from central and peripheral chemoreceptors, monitoring $O_2$ and $CO_2$/pH levels, mechanoreceptors in the lung and central nervous system structures in the forebrain and midbrain. Indeed, when adult frogs are subjected to hyperoxic gas mixtures and made hypocapnic by hyperventilation, thereby abolishing chemoreceptor activity, breathing stops (Smatresk, 1990; Kinkead, 1995). Additionally, gill ventilation in immature tadpoles insensitive to $CO_2$ ceases when the animal is exposed to hyperoxia (Burggren and Doyle, 1986). Thus, the amphibian brainstem respiratory controller is likely to include this conditional aspect of the oscillator as shown in Fig. 1.4C which is compatible with either general type of respiratory CPG, pacemaker (Fig 1.4A) or emergent behavior (Fig. 1.4B). Interestingly, chemoafferent input does not seem to be a critical source of drive to the gill rhythm generator in fish. Acidic superfusion of isolated carp and lamprey brainstems produced no effect on gill rhythmic motor output, suggesting the absence of central chemoreceptors (Hughes and Shelton, 1962; Rovainen, 1977). Also, hyperoxic fish continue to breathe rhythmically (Burleson and Smatresk, 1989).

Whether respiratory rhythmogenesis mirrors pacemaker functionality or network behavior is unresolved. Because breathing in mammals results from the

sequential activation of many populations of neurons to produce a three-phase motor act (see below) in which each process is conditioned by the previous one and initiates the next, Bianchi *et al.* (1995) suggested that the network model may be a better model to describe how respiratory rhythm is produced. Alternately, the coordination of the groups of respiratory neurons could be performed by an entity separate from the rhythm generator that was responsible for processing the relevant sensory signals and ensuring precise spatial and temporal patterns of muscle activation during each breath. Finally, both types of rhythmogenic mechanisms may coexist to form a hybrid mechanism able to adapt to varying conditions (Funk and Feldman, 1995).

### 1.5.4 Three-phase lung ventilatory cycle

Basic features of the respiratory pattern are conserved in air-breathing vertebrates. With regard to airflow, the tidal breathing cycle of mammals is two phase, comprised of inhalation and exhalation. However, examination of respiratory mechanics, muscle activities and neuronal synaptic events in mammals, amphibians and reptiles, suggest that the motor act of breathing is actually comprised of three distinct phases (Richter and Ballantyne, 1983; Kogo and Remmers, 1994; Takeda *et al.,* 1986). Richter (1982) defined these sequential phases in the mammal as active expiration (deflation of the lungs), inspiration

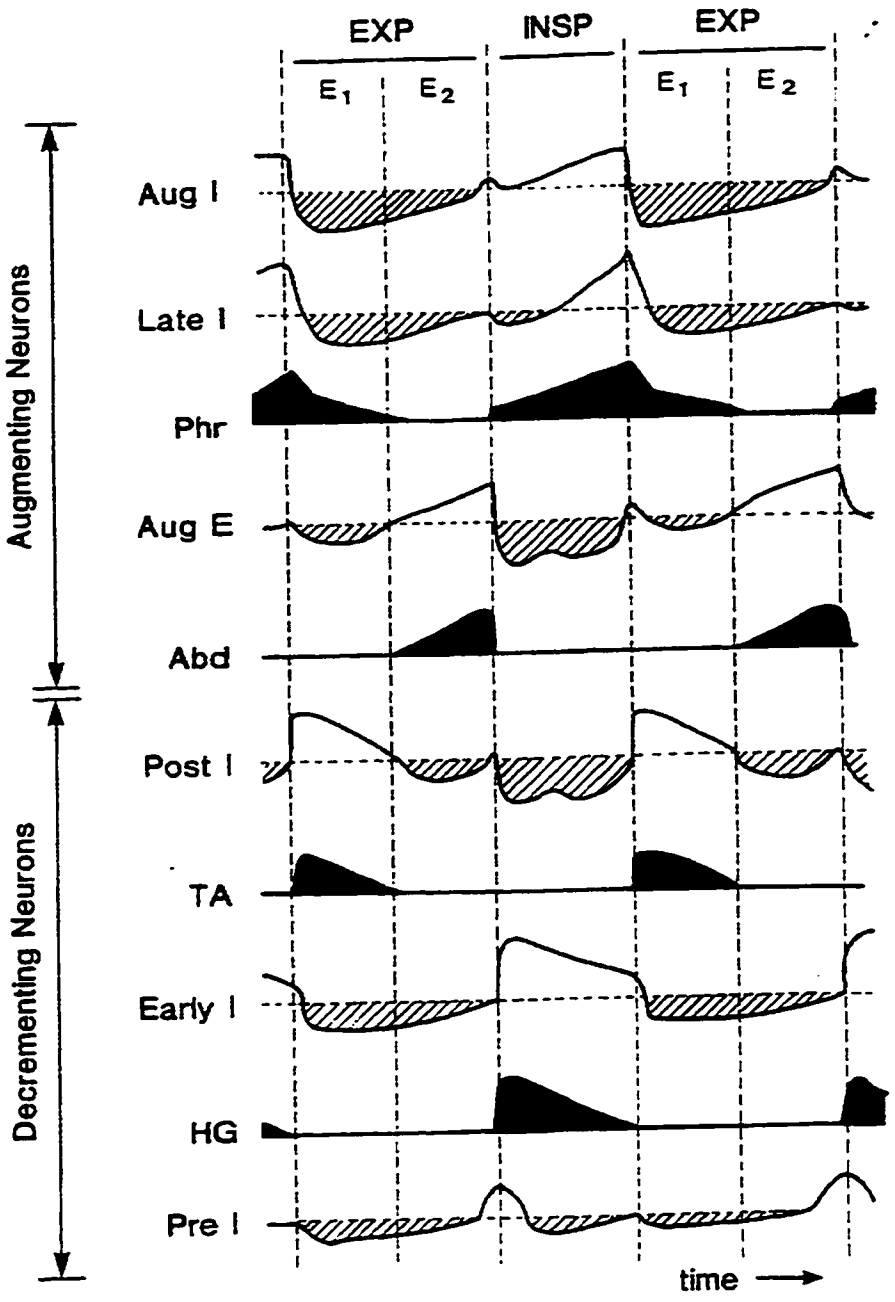


**Figure 1.5** Depiction of membrane potential trajectories from 6 bulbar respiratory neurons, together with relevant respiratory motor outputs recorded in phrenic (Phr), abdominal (Abd), thyroarytenoid (TA) and hypoglossal (HG) nerves. The respiratory cycle is divided into 3 phases, inspiration (Insp), and 2 phases of expiration (Exp), phase 1 of expiration (E1) and phase 2 of expiration (E2). Hyperpolarization by IPSPs indicated by the hatched areas. (Adapted from Bianchi et al., 1995)

(inflation of the lungs) and post-inspiration (breath-hold at end-inspiration or retardation of expiratory flow). The neurorespiratory circuit in mammals assumes one of three activity states, inspiration, post-inspiration and active expiration, corresponding to the three mechanical phases. Respiratory neurons display sequential activation of inspiratory, post-inspiratory and expiratory neurons, and these neurons receive post-synaptic inhibition during their inactive phases indicating that they are interconnected by inhibitory synaptic transmission. As shown in Fig. 1.5, inspiration is depicted by an augmenting pattern of discharge that is terminated abruptly. Post-inspiration follows the inspiration phase and is associated with expiratory braking (active control of expiratory airflow by the diaphragm and upper airway muscles) (Bartlett *et al.,* 1973) and relaxation of inspiratory muscles in the thorax and abdomen. The period of silence in phrenic nerve activity is associated with active expiration that may be facilitated by contraction of the abdominal expiratory muscles. The phase of post-inspiratory activity is often referred to as Stage I expiration (E1), and the period of silence is called stage II expiration (E2) (Richter and Ballantyne, 1983).

By recording intracellular and extracellular activity from inspiratory, post-inspiratory and expiratory respiratory neurons in adult frogs, Kogo and Remmers (1994) recently demonstrated that amphibians, like mammals, possess a three-phase neurorespiratory cycle. As shown in Fig 1.6, this neural cycle corresponded with the parallel three-phase mechanical respiratory cycle in which the first phase,

active expiration (E2), occurs when the glottis is first opened. Next, inspiration is produced by the brisk activation of the buccal levators to push air back into the lungs. The last phase, post-inspiration (E1), is associated with breath holding period, and occurs with complete closure of the glottis, trapping the lung gas after the end of inspiration. Similarly, in the fresh water turtle, Takeda *et al.* (1986) used intracellular recording techniques to examine the temporal discharge pattern and the patterns of postsynaptic activity of medullary respiratory-related neurons. In this study, Takeda *et al.* (1986) demonstrated that the pattern and timing of postsynaptic potentials in respiratory related neurons resembled the 3 phase neurorespiratory cycle observed in mammals. Thus, the three-phase cycle of reptiles and mammals probably takes origin from the 3 phase amphibian cycle consisting of expiration, inspiration and breath hold, where breath hold corresponds to the post-inspiratory phase of expiratory braking by the larynx.

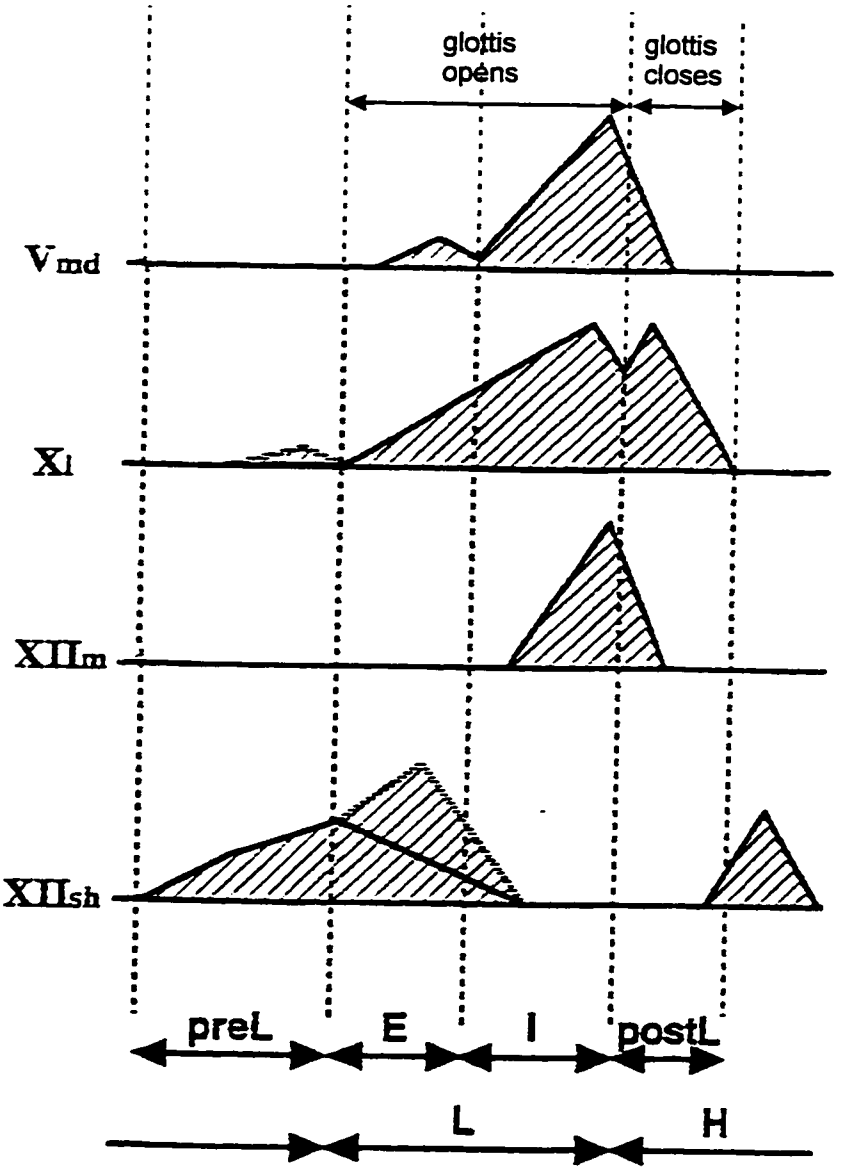


**Figure 1.6** The fictive breathing pattern of the decerebrate frog. Schematic diagram of the fictive breathing pattern showing lung ventilation cycles (pre-L, E, I, post-L). V md, mandibular branch of CN V; XI, layrngeal branch of CN X; XII m, main branch of the hypoglossal; XII sh, sternohyoid branch of the hypoglossal; L, ventilation; H, breath-holding; E, expiration; I, inspiration. (Adapted from Kogo and Remmers, 1994)

## 1.6 THESIS RESEARCH RATIONALE

The overall aim of the thesis was to examine the ontogenesis of central respiratory pattern generation and chemoreception in amphibians during the transition from gill to lung ventilation. The bullfrog *Rana catesbeiana* was chosen for this study because it undergoes extreme morphological and physiological changes during metamorphosis and because the respiratory behavior in the adult has been well documented. In order to compare central mechanisms controlling breathing during successive stages of development, I have investigated fictive gill and lung ventilation in an *in vitro* brainstem preparation from *Rana catesbeiana* tadpoles. This segment of the brain retains the necessary neural circuitry to generate the complex rhythmic neural output responsible for each type of breathing, thereby making it possible to conveniently trace the ontogeny of central respiratory mechanisms.

The generation of a putative respiratory motor output with the absence of peripheral input makes the *in vitro* tadpole brainstem an attractive model for studies of neurorespiratory control and central pattern generation. However, a key concern regarding any spontaneously bursting efferent activity generated by an *in vitro* neural preparation relates to the biological significance of such activity. In essence one must establish, by correlation with an *in vivo* preparation that such activity represents "fictive" behavior. In the case of tadpole breathing,

an additional difficulty remains, namely: lung and gill rhythms must be separately identified. Recent studies of *in vitro* tadpole brainstem preparations have begun to characterize the patterns of respiratory activity related to gill and lung ventilation (Galante *et al.*, 1996; Liao *et al.*, 1996; Pack *et al.*, 1993). Separate identification of lung and gill ventilatory activities in these studies, however, must be considered only tentative as an arbitrary amplitude criterion alone was used to identify putative gill and lung bursts in CN roots, i.e. large amplitude bursts were assumed to be fictive lung breaths and small amplitude bursts were assumed to be fictive gill bursts.

Another basic concern relates to the adequacy of respiratory gas exchange inasmuch as all $CO_2$ and $O_2$ transport must occur as diffusive exchange with the superfusate through the surface of the brainstem. Mammalian *in vitro* brainstem preparations sustain tissue acidosis (Okada *et al.*, 1990) and tissue hypoxia (Fujii *et al.,* 1982), both of which have been shown to alter neuronal membrane properties (Fugiwara *et al.,* 1987; Haddad and Donnelley, 1990), thereby possibly affecting normal behavior. Accordingly, if the isolated tadpole brainstem preparation is to be successfully utilized as a tool to investigate fundamental questions of rhythmogenesis and central chemoreception, brainstem tissue must be physiologically validated and fictive gill and lung ventilatory activity must be unmistakably and separately identified. I have investigated the gas exchange status of isolated tadpole brainstem (Chapter 3)

and then evaluated the biological meaning of the bursting efferent activity exhibited by this isolated brainstem. The latter was accomplished by observing the neural characteristics of mechanically-defined lung and gill motor activity in spontaneously breathing decerebrate tadpoles (Chapter 4) and correlating that activity with a detailed examination of cranial, spinal and peripheral nerve rhythmic efferent motor output generated by the *in vitro* brainstem (Chapter 5).

Following demonstration that rhythmic motor bursts produced in a well-oxygenated isolated tadpole brainstem are respiratory in nature, the ontogeny of central chemoreception in regards to gill and lung ventilation is assessed in Chapter 6. Because the results of this chapter indicate that amphibian tadpoles undergo complex developmental transitions of neural respiratory function from dominant gill CPG output and nascent lung CPG functionality in early larvae to highly functional lung CPG output and reduced gill CPG output in mature animals and that the transitions in respiratory output are associated with a shift in $CO_2$ chemoresponsiveness from gill to lung regulation, the subsequent study (chapter 7) tested the hypothesis that the location of central respiratory chemoreceptors changes as the shift from gill to lung chemoreceptive function occurs. Chapter 7 assesses the location of central respiratory chemoreceptors by microinjection of hypercapnic artificial cerebrospinal fluid (aCSF) into the brainstem while observing the fictive ventilatory response.

Previous studies in the adult frog, utilizing transection techniques, have localized neural elements essential for the generation of lung motor output to the rostral brainstem (between CN V and CN X) (Langendorff, 1887; Kimura and Remmers, 1997), however, the exact location and distribution of neurons responsible for the generation of gill and lung motor output in the tadpole has yet to be described. Recent studies by Onimaru *et al.* (1989), in isolated Pre-I neurons in the *in vitro* rat, Issa and Remmers (1992), in the ventral medulla of the *in vitro* rat, and Coates and Nattie (1991), in the rostral ventrolateral medulla of the *in vivo* cat, suggest that central respiratory chemoreception and lung burst rhythmogenesis are co-localized. In light of the results described in Chapter 7, Chapter 8 evaluates the hypothesis that central respiratory chemoreceptors and lung rhythmogenic regions anatomically tract each other. Here, brainstem regions with neurons critical for lung rhythmogenesis are identified by serial brainstem transection in the developing tadpole. Consequently, the study of central respiratory rhythm generation and chemoreception in larval amphibians offers a unique opportunity to gain insights into the origin and evolution of neural respiratory control systems.

# *CHAPTER TWO*

## *General Methods*

### 2.1 ANIMALS

Experiments were conducted on bullfrog tadpoles (*Rana catesbeiana*), of either sex, obtained from the Charles D. Sullivan Company Inc. (Nashville, TN, USA). Specimens were assigned to one of 25 stages based on external morphology as defined by Taylor and Köllros (1946). In general, tadpoles within stages 1-15 were characterized as "pre-metamorphic". Larvae ranging between stages 16-19 were labeled "metamorphic", and those ranging in stages 20-25 were termed "post-metamorphic". During the 5 days preceding experimentation, all tadpoles were housed in aerated, filtered aquariums (19-21 °C) and fed TetraFin Staple Food (TetraWerke, Germany). Experimental protocols used in the following chapters were approved by The Animal Care Committee of the University of Calgary, Canada.

## 2.2 SURGICAL PROCEDURES

Tadpoles were anaesthetized in tricaine methanesulfonate (1:10,000) and weighed. Once unresponsive, animals were decerebrated by transection just rostral to the eyes. This was followed by a caudal transection of the body: in pre-metamorphic and metamorphic animals, just caudal to the level of the opercular slit, and in post-metamorphic larvae, just behind the forelimbs. The dorsal cranium was removed and a laminectomy performed at the first and second vertebrae. With the aid of a dissecting microscope, the cranial and spinal nerves were severed at their respective ostia, leaving the rootlets as long as possible. The dura and arachnoid were then carefully removed from the dorsal and ventral surfaces, and the brainstem was transected 1 mm caudal to the root of the second spinal nerve (SN) and 1 mm rostral to the root of cranial nerve (CN) V. Throughout the dissection, which required 30-45 min, the brainstem was irrigated with a cold (5-10°C) bicarbonate-containing artificial cerebrospinal fluid (aCSF) of the following composition (in mM): NaCl, 104; KCl, 4; $MgCl_2$, 1.4; d-glucose, 10; $NaHCO_3$, 25 and $CaCl_2$, 2.4, and equilibrated with 98% $O_2$, 2% $CO_2$ (pH 7.8). Superfusate composition corresponded to that previously used by Liao *et al.* (1996) in the isolated tadpole brainstem and was similar to components of adult frog plasma (West *et al.*, 1987).

## 2.3 SUPERFUSION-RECORDING CHAMBER

The dissected brainstem was transferred to a superfusion recording chamber (total volume: 0.50 ml) at room temperature (22-24°C). Two superimposed disks (OD: 2.5cm, thickness: 1mm) with central elliptical holes (2.0 X 0.5 cm) partitioned the chamber into upper and lower compartments (Fig. 2.1). Fine netting (1.0 X 1.0 mm) spanned the holes attached to the inferior surface of the upper and lower disc, thereby creating a space between the netting for the brainstem. The brainstem was positioned between the two nets, ventral side up. Artificial CSF, having the composition listed above, was equilibrated with the 2% $CO_2$, 98% $O_2$ gas mixture in a room temperature tonometer, delivered into the chamber through an inflow aperture in the lower compartment at a rate of 10 ml/min and conducted from the upper compartment at the opposite end of the chamber via a paper wick.

Bolus injection of neutral red dye (Fischer Scientific) into the inflow aperture uniformly distributed throughout the recording chamber indicating streamline flow and no pockets of poorly mixed superfusate across upper and lower compartments. Thus, the brainstem suspended between the upper and lower chambers was uniformly superfused both ventrally and dorsally. The chamber was covered with a plexiglass coverslip with a central orifice, and the superfusate surface was maintained 1-2 mm below the coverslip. The space

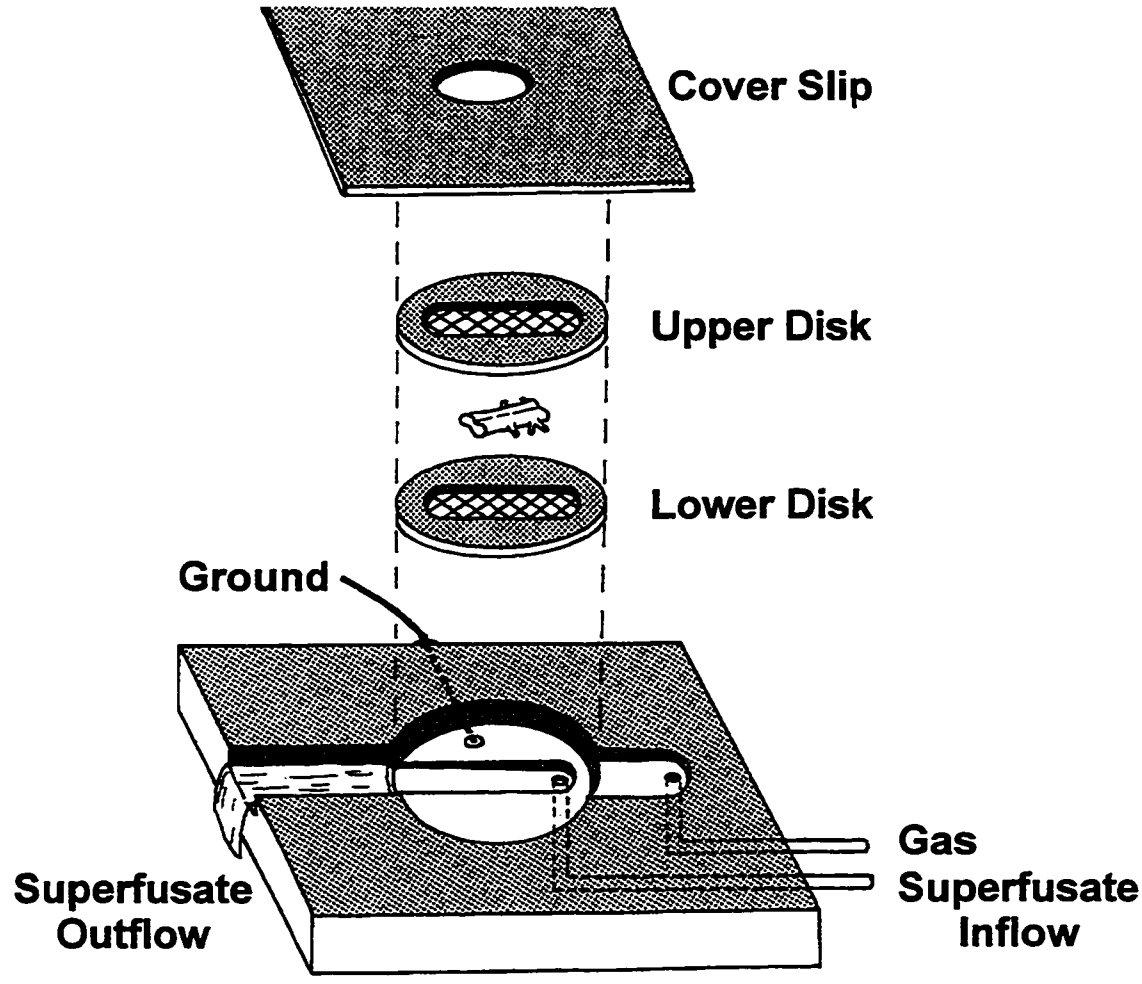


**Figure 2.1** Schematic diagram of brainstem superfusion chamber

between the superfusate surface and the coverslip was purged continuously with the same gas mixture as was flowing through the reservoir tonometer, thereby minimizing differences in the gas mixture composition at the air-water interface.

The superfusate was equilibrated in a tonometer with gas having a $P_{CO_2}$ of 45, 35, 17, 10 or 4 Torr (balance $O_2$) to produce pH values of 7.4, 7.6, 7.8, 8.0 and 8.4, respectively. In preliminary experiments, superfusate pH in the tonometer measured using a macro-pH electrode (Cole-Parmer, E-05591-10), was compared with simultaneously measured superfusate pH in the recording chamber using a small glass electrode (Cole-Parmer, E-05991-60). The $P_{CO_2}$ was adjusted until a stable measurement of the desired superfusate pH was recorded in the tonometer, and 2 min later, a shift in the recording chamber pH was observed, after which the recording chamber pH equalled reservoir tonometer pH to within $\pm$ 0.01 pH units.

## 2.4 NEURAL RECORDINGS

Neural recordings of spontaneous rhythmic motor output were obtained from the roots of cranial nerves (CN) V, VII, and X and spinal nerve (SN) II (develops into the hypoglossal nerve in the adult frog) using suction electrodes. The pipettes were made from 1 mm outer diameter, thin-walled borosilicate glass, then pulled to a fine tip with a horizontal micropipette puller (Brown-

Flaming, model P80). The tip was broken and bevelled (Shöhli, Lapp-Technik) to achieve various inner tip diameters ranging from 90-350 μm. Compound neural activity was amplified (AM Systems no.1700, Tektronix AM 502), filtered (100 Hz to 1 kHz), monitored on an oscilloscope (Gould, 4035), and recorded on video tape using a pulse code modulator (Neurodata no.890). The signals were full wave rectified and simultaneously averaged with a Paynter time averager, displayed on a polygraph (Gould) and digitized and analyzed on a Pentium PC (Datapac II software).

# *CHAPTER THREE*

## *Evaluation of Gas Exchange Status in the Isolated Tadpole Brainstem*

## 3.1 INTRODUCTION

The *in vitro* brainstem spinal cord preparation of the neonatal rat (Suzue, 1984) has been extensively used as an experimental model for neurophysiological and pharmacological studies of respiratory rhythmogenesis and central chemosensitivity (Suzue, 1984; Harada *et al.*, 1985; Smith and Feldman, 1987; Onimaru *et al.*, 1989; Issa and Remmers, 1992; Kawai *et al.*, 1996). Investigations using amphibian *in vitro* brainstem preparations have recently been undertaken to elucidate the central neural substrates of respiratory rhythm generation and regulation (Kogo *et al.*, 1994; Kogo and Remmers, 1994; McLean *et al.*, 1995a; McLean *et al.*, 1995b; Pack *et al.*, 1993; Galante *et al.*, 1996; Liao *et al.*, 1996; Kinkead *et al.*, 1997). I*n vitro* brainstem preparations

offer several advantages for studies of central respiratory control such as peripheral deafferentation, mechanical stability and control of the extracellular environment. However, because such models lack blood perfusion and respiratory gases are exchanged exclusively by diffusion at the brain surface, they are inherently susceptible to tissue hypoxia and acidosis. This can be of considerable importance to the results of *in vitro* investigations of rhythmogenesis and chemoreception. Hypoxia can induce gasping, a respiratory pattern fundamentally different from normal eupnic breathing (Lumsdem, 1923a, b, c), in addition to metabolic acidosis. Hypercapnia can distort tissue pH.

The critical depth of tissue of a superfused *in vitro* preparation can be defined as the distance from the surface at which the tissue $P_{O_2}$ reaches zero. In slices of adult mammalian brain at 37°C, the critical depth was found to be 400 μm (Fujii *et al.*, 1982). Critical depths are greater in hypothermic neonatal mammalian CNS preparations owing to increased oxygen solubility and reduced tissue $O_2$ consumption at lower temperatures (Dejours, 1988; Nishizaki *et al.*, 1988). Nonetheless, Okada *et al.* (1993) found a critical depth of 450 μm in a superfused neonatal rat brainstem at room temperature. They also found that the pH decreased 0.1 units for every 100 μm below the surface. Hence, the hypothermic neonatal rat brainstem preparation with an overall diameter of 2.5 mm has a large anoxic core and is profoundly acidic.

Amphibian *in vitro* brainstem preparations, by contrast, may offer a more robust, less hypoxic alternative to hypothermic mammalian preparations since frog brainstem tissue had a lower rate of oxygen consumption (Dittmer and Grebe, 1956). While *in vitro* mammalian brainstems are studied at comparatively hypothermic temperatures in order to reduce tissue oxygen consumption and improve oxygen solubility, ectothermic frog brainstem tissue maintains substantially lower rates of oxygen consumption at a given temperature (Dittmer & Grebe, 1956). In addition, diffusion distances within larval bullfrog brainstem preparations are considerably shorter than *in vitro* neonatal rat preparations; the tadpole brainstem is smaller (overall diameters: 1.0-1.5 mm) and the fourth ventricle is flatter. Preliminary experiments have shown that the fourth ventricle can be opened further by dorsal midline section of the caudal medulla producing a planar brainstem sheet without disturbing its neurorespiratory activity.

In order to evaluate the gas exchange status of the *in vitro* tadpole brainstem preparation, the $P_{O_2}$ and pH was measured as a function of depth in the metamorphic (Taylor-Köllros stages 15-19; see Taylor & Köllros, 1946) bullfrog tadpole, *Rana catesbeiana.* Accordingly, I hypothesized that the isolated brainstem is not hypoxic when superfused with artificial cerebrospinal fluid (aCSF) equilibrated with 98% $O_2$ and 2% $CO_2$ but is acidic in deep tissue layers as a result of $CO_2$ accumulation, owing to large diffusional distances.

## 3.2 MATERIALS AND METHODS

### 3.2.1 Animals and surgical preparation

Experiments were performed on 9 *Rana catesbeiana* tadpoles (stage 15-19; mean body mass: 9.86 g) of either sex, using 5 animals for $P_{O_2}$ measurements and 4 for pH recordings. Animals were purchased from a commercial supplier and cared for by methods previously detailed in Chapter 2. Surgical procedures for brainstem removal were performed according to the protocol previously described in Chapter 2.

### 3.2.2 Recording chamber and neural recordings

The brainstem was transferred to a superfusion recording chamber where spontaneous rhythmic motor output was recorded from the root of CN X using a suction electrode according to the protocol detailed in Chapter 2.

### 3.2.3 $P_{O_2}$ microelectrode

The $P_{O_2}$ of the brainstem tissue was measured with polarographic Clark-style oxygen microelectrodes (#737, Diamond General). Electrodes (tip diameter: 10, 60 μm) possessed an internal Ag/AgCl reference anode, a guard cathode to increase resolution and a 90% response time of less than 1 second. A linear relationship between electrode current and $P_{O_2}$ was observed between 0-

600 Torr when the cathode was polarized at - 800 mV. The current output of the electrode was fed into a polarographic amplifier (#1900, A-M Systems) and was approximately 300 pA at a $P_{O_2}$ of 135 Torr. Calibration was performed at the beginning, midpoint and end of each experiment in a tonometer filled with room temperature superfusate solutions equilibrated with 100% $N_2$, 21.95% $O_2$ and 100% $O_2$ respectively.

### 3.2.4 pH microelectrode

Brainstem extracellular pH was measured with a pH microelectrode (#823, Diamond General) constructed from 1.0 mm thick glass capillaries backfilled with a buffered (0.5 M phosphate) electrolytic reference solution (6.5 pH NaCl). The tips were beveled to a diameter of 2-10 μm. The electrical resistance of the pH electrode was approximately 1 GΩ with a 90% response time of less than 5 seconds, and the sensitivity averaged 59 mV/pH unit. The pH electrode and a Ag/AgCl reference electrode were connected to an electrometer (#2000, A-M Systems), where voltage differences were amplified and digitally displayed. Calibration was performed at the beginning, midpoint and end of the experiment in the recording chamber with superfusate of known pH measured with a standing pH electrode (Cole-Parmer, E-05591-10). The pH of the solution in the recording chamber was altered by equilibration with $CO_2$ of different partial pressures (balance $O_2$) in the tonometer.

### 3.2.5 Experimental protocol

Once positioned in the recording chamber, the brainstem was superfused with oxygenated aCSF for at least 60 min before beginning experiments. Viability of the brainstem preparation was monitored at the beginning and end of each experiment by recording the spontaneous rhythmic neural activity of cranial nerve X roots. The $P_{O_2}$ or pH microelectrode was attached to a vertical motorized positioner (Nanostepper, Type B, WPI), providing positioning resolution of < 1 μm. The positioner was mounted on a two-dimensional horizontal slide mechanism, which was manipulated by two manual micrometers (Newport Corp., Fountain Valley, CA) with a resolution of 5 μm. For each brainstem, a total of six tracts were made between CN V and CN X, three in the midline regions (denoted by the basilar artery) and three 500 μm lateral to the midline, with each penetration separated by a distance of 500 μm in the rostral-caudal dimension (Fig. 3.1).

Contact of the electrode tip with the surface of the tissue (zero depth) was determined visually with the aid of a dissecting microscope (x 313 magnification). Once the position of the surface had been identified, microelectrodes were withdrawn vertically 300 μm from the ventral brainstem surface, and measurements of superfusate $P_{O_2}$ and pH were made after advancing the electrode in 50 μm steps. Once the surface was contacted,

microelectrodes were advanced in steps of 5-15 μm into the ventral brainstem and $P_{O_2}$ or pH were measured every 50 μm.

### 3.2.6 Data analysis

Recordings of pH and $P_{O_2}$ from midline and lateral tracts were corrected for electrode drift, then averaged within each animal. These data were then averaged for all preparations and presented with their standard deviations. Following each experiment, the brainstem was fixed in 10% buffered formalin acetate (Fischer Scientific). Lateral-lateral width and dorsal-ventral thickness were measured in midline and lateral brainstem regions using a microscope (Zeiss, 31.25X) equipped with a fine reticule after complete tissue sectioning (Vibratome, Series 1000) between CN V and X. Values were corrected for tissue shrinkage based data from mammalian brain tissue (20%, Mourtizen, 1979) averaged and presented with their standard deviations.

Theoretical calculations of tissue $P_{CO_2}$ and pH were determined using averaged measurements of tissue $P_{O_2}$ and pH. By applying the equation of diffusion (see below), measured tissue $P_{O_2}$ values were used to calculate tissue $P_{CO_2}$. The Henderson-Hasselbalch equation (see below) was used to calculate tissue $P_{CO_2}$, using measured pH values, and, conversely, to calculate tissue pH from predicted $P_{CO_2}$ values. All calculations were made assuming that: 1) $O_2$

uptake and $CO_2$ output rates were equal (i.e., a respiratory quotient (R) of one), 2) specific tissue metabolic rates were uniform throughout the brainstem, and 3) bicarbonate levels were constant throughout the tissue.

Equation of Diffusion, assuming R=1:

$$(\textit{tissue}\ P_{CO_2} - \textit{superfusate}\ P_{CO_2})*(Dw_{CO_2}*\beta w_{CO_2}) = (Dw_{O_2}*\beta w_{O_2})*(\textit{superfusate}\ P_{O_2} - \textit{tissue}\ P_{O_2})$$

Dw = diffusion coefficient in water at 20°C (Dejours, 1975)
βw = solubility coefficient in water at 20°C (Dejours, 1975)
$Dw_{CO_2}$ = 0.000018 $cm^2*sec^{-1}$; $\beta w_{CO_2}$ = 51.9 $nMol*ml^{-1}*torr^{-1}$ (Dejours, 1975)
$Dw_{O_2}$ = 0.000025 $cm^2*sec^{-1}$; $\beta w_{O_2}$ = 1.82 $nMol*ml^{-1}*torr^{-1}$ (Dejours, 1975)

Henderson-Hasselbalch equation:

$$pH = pKa + \log([HCO_3^-]\ (\beta_{CO_2}\ P_{CO_2})^{-1})$$

first dissociation constant (pKa) = 6.14 (Dejours, 1975)
solubility of $CO_2$ ($\beta_{CO_2}$) = 0.04 mM $Torr^{-1}$ (Dejours, 1975)

## 3.3 RESULTS

Robust respiratory activity recorded from CN X was observed in all nine brainstem preparations at the beginning and end of each experiment. Mean brainstem dimensions, corrected for tissue shrinkage, are shown in Fig. 3.1. Between CN V and X, lateral width was 4.34 ± 0.57 mm, while dorsal-ventral thickness in midline and lateral regions was 0.92 ± 0.21 mm and 1.31 ± 0.22 mm respectively.

### 3.3.1 pH depth profile

Fig. 3.2 shows midline and lateral tract pH profiles as a function of ventral surface depth. At distances greater than 100 μm above the ventral brainstem surface, superfusate pH was uniform and equal to tonometer pH. Below 100 μm, however, a gradient of 0.07 pH units/100 μm was observed in the superfusate with pH levels reaching 7.73 (± 0.01) at the ventral surface. Immediately below the brainstem surface, a similar pH gradient was measured for the first 100 μm in midline tracts and for the first 200 μm in lateral tracts. pH gradients in both tracts decreased in a curvilinear manner below 200 μm with greater changes in slope observed in midline profiles. Minimal mean values of pH in midline tracts (7.58 ± 0.05) were observed between 500-700 μm below the

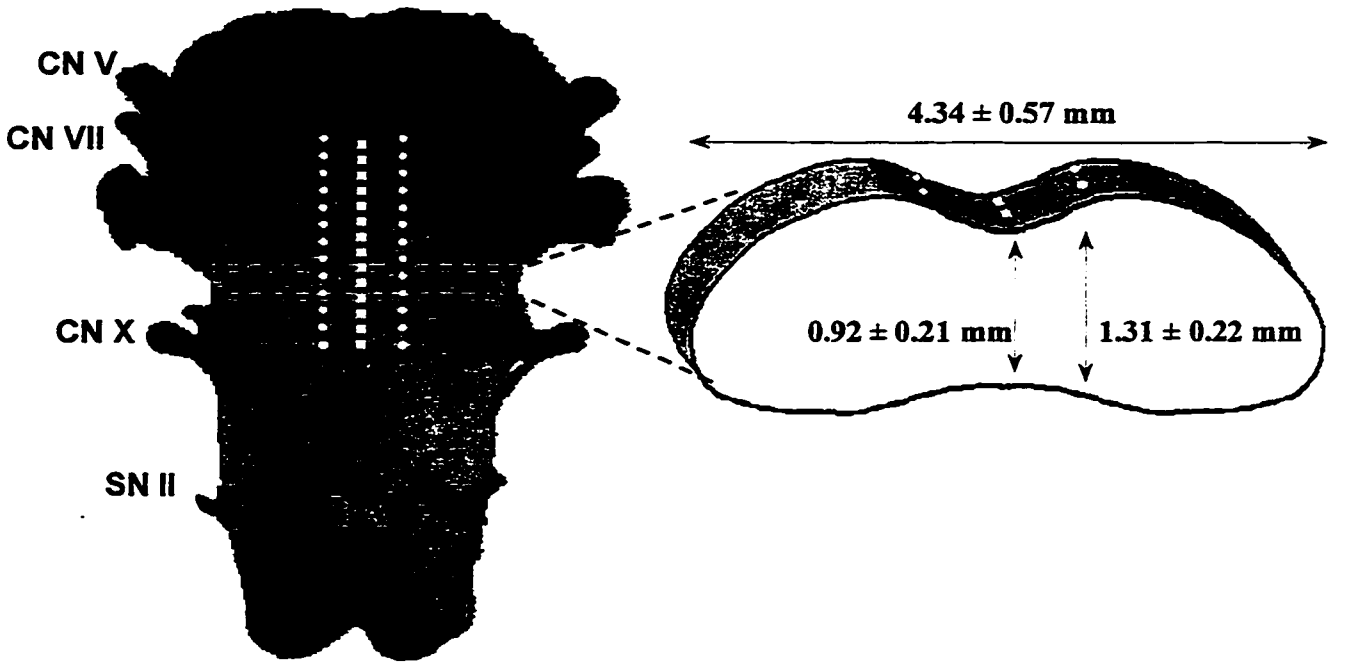


**Figure 3.1** Schema of the metamorphic in vitro tadpole brainstem preparation showing dorsal-ventral tissue thickness and sites of pH and $P_{O_2}$ measurements. Left: ventral surface of the preparation (squares indicate position of midline tracts; circles show lateral tracts). Right: Cross section of the medulla between CN V and X. BA, basilar artery.

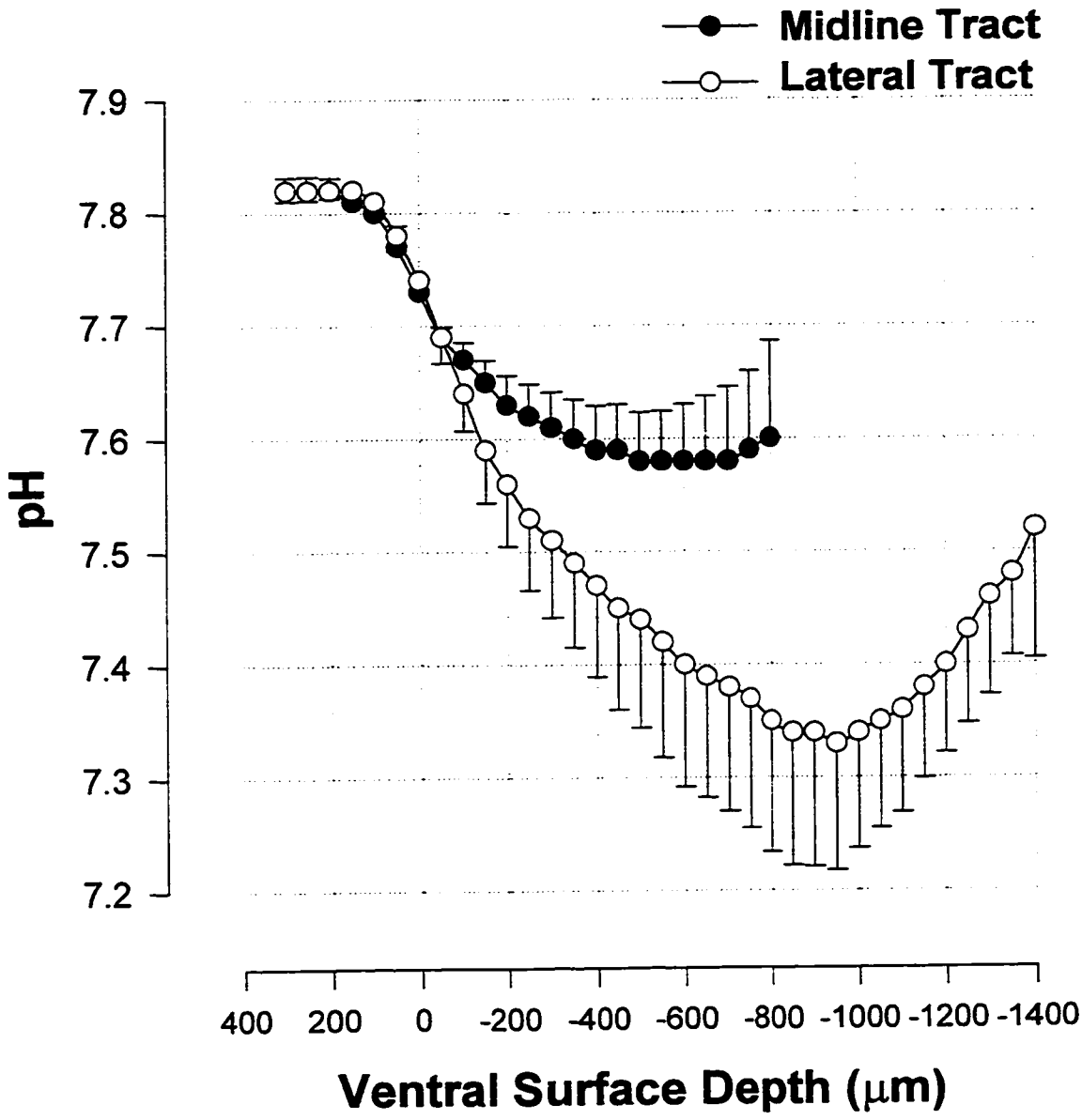


**Figure 3.2** Depth profiles of extracellular tissue pH in midline (closed circles) and lateral (open circles) medullary tracts of the *in vitro* tadpole brainstem preparation superfused with aCSF of pH = 7.8, $P_{CO_2}$= 17 Torr, $P_{O_2}$= 600 Torr at 23°C. Plotted are mean values (± SD), n=4.

surface. By contrast, pH levels in lateral tracts decreased more sharply below 200 μm than in to midline tracts, reaching a minimum mean value of 7.34 ± 0.12 at 900 μm. At depths greater than 700 μm in midline tracts and 900 μm in lateral tracts, the pH gradient reversed. Minimal midline and lateral pH levels occurred roughly 250 μm deeper than the corresponding measures of dorsal-ventral half-thickness (460 μm, 655 μm). Variability in pH recordings was minimal in superficial brainstem layers and increased as the electrode was advanced to deeper layers.

### 3.3.2 $P_{O_2}$ depth profile

Midline and lateral depth profiles of $P_{O_2}$ in the *in vitro* tadpole brainstem preparation are illustrated in Fig. 3.3. Substantial reductions in $P_{O_2}$ from the bulk of the solution began 200 μm above the brainstem surface, falling 60 Torr/100 μm, to reach 438 ± 52 Torr at the surface. A comparable gradient was observed for the first 100 μm below the ventral brainstem surface in midline tracts and for the first 200 μm in lateral tracts. With further electrode penetration below 200 μm, $P_{O_2}$ gradients in both midline and lateral tracts declined in a curvilinear fashion with increasing variability. However, greater changes in slope were measured in midline tracts as the $P_{O_2}$ levels in lateral tracts decreased more linearly. In midline tracts, $P_{O_2}$ levels fell to a mean minimum of 323 ± 31 Torr at

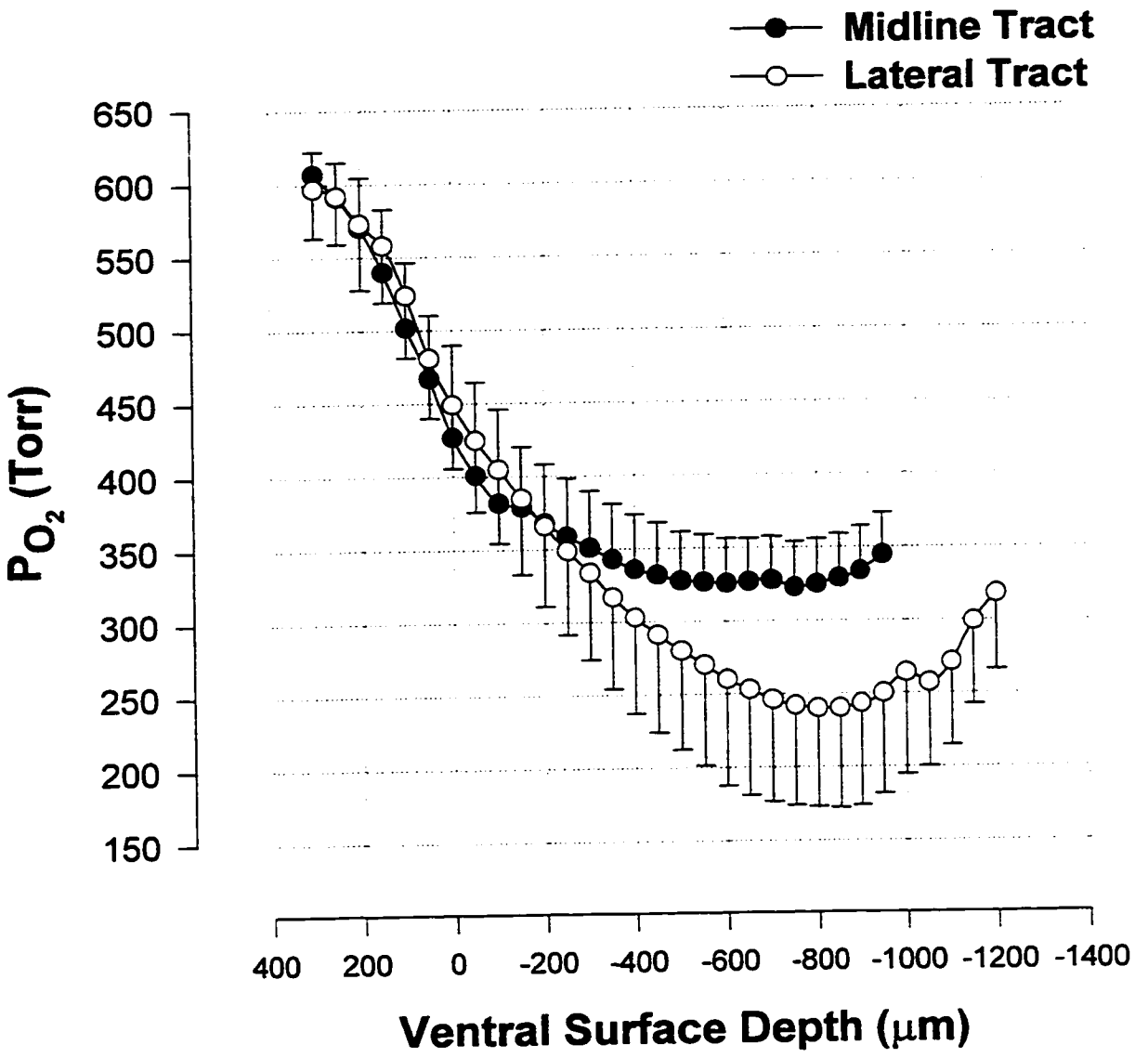


**Figure 3.3** Depth profiles of tissue $P_{O_2}$ in midline (closed circles) and lateral (open circles) medullary tracts of the *in vitro* tadpole brainstem preparation superfused with aCSF of pH = 7.8, $P_{CO_2}$= 17 Torr, $P_{O_2}$= 600 Torr at 23°C. Plotted are mean values (± SD), n=5.

depth of 750 μm. Below 750 μm, $P_{O_2}$ gradients reversed and appeared to increase with the same slope. $P_{O_2}$ levels in lateral tracts reached a mean minimal value of 240 ± 68 Torr at a depth of 850 μm. Thus, minimum midline and lateral $P_{O_2}$ values were approximately 250 μm less than corresponding half-thickness measurements. Like midline tracts, continued electrode advancement past 850 μm in lateral tracts showed reversal of $P_{O_2}$ gradients.

### 3.3.3 Theoretical pH and $P_{CO_2}$ profiles

Fig. 3.4 shows theoretical depth profiles of pH and $P_{CO_2}$ calculated for the lateral tracts. Panel A plots predicted and measured pH profiles as a function of ventral surface depth. Both pH profiles displayed similar shape, however, pH levels predicted from $P_{O_2}$ data decreased less sharply below the ventral surface compared to measured pH in lateral tracts, before reaching a minimum value of 7.46 at 750 μm. In Panel B, substantial tissue $P_{CO_2}$ gradients below the ventral surface are predicted using both $P_{O_2}$ and pH measurements. Compared to tissue $P_{CO_2}$ levels calculated from pH data that increased from 19 Torr at the surface to 49 Torr 950 μm below before slope reversal, $P_{CO_2}$ gradients determined from tissue $P_{O_2}$ were not as steep, rising from 26 Torr at the ventral surface tissue to 36 Torr, at a depth of 800 μm before gradient reversal.

A

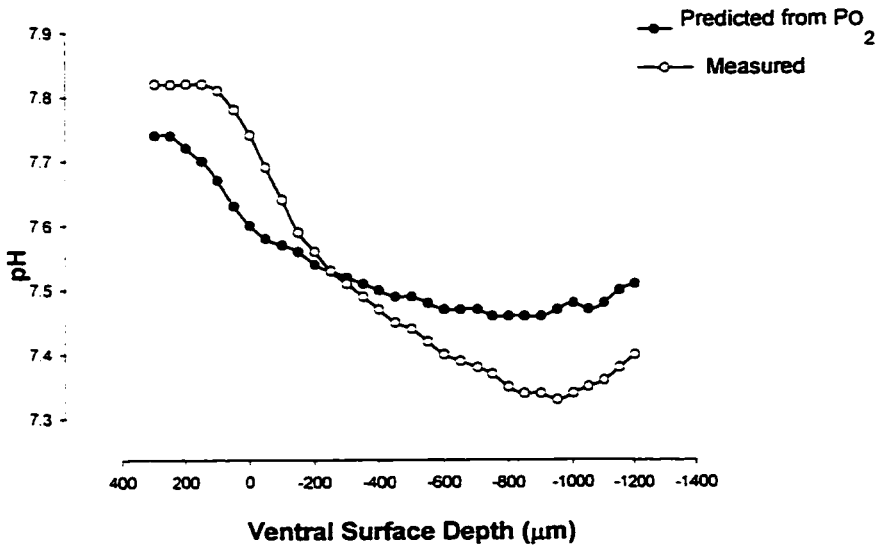


B

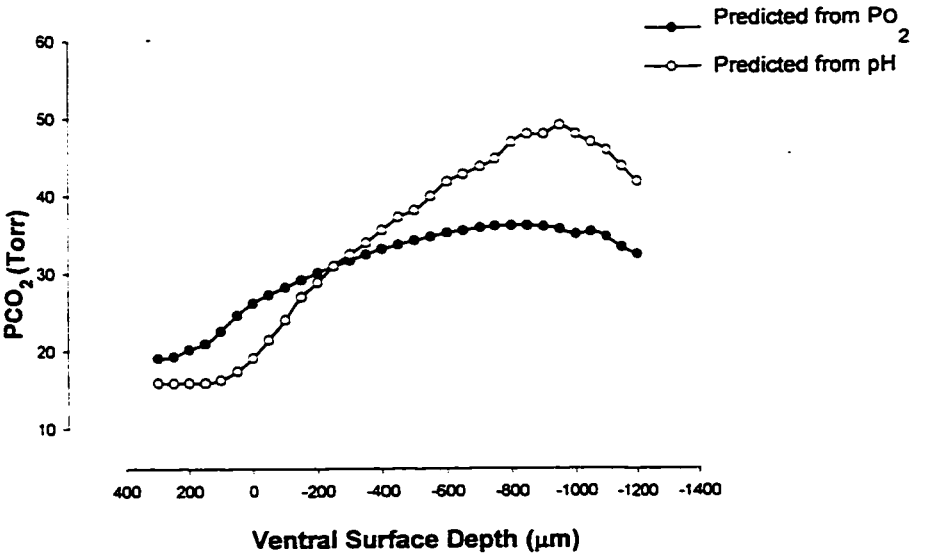


**Figure 3.4** Theoretical lateral depth profiles of $P_{CO_2}$ and pH. Panel B plots $P_{CO_2}$ profiles calculated from mean pH data (open circles) and $P_{O_2}$ measurements (filled circles). Panel A shows the mean pH profile measured in lateral tracts (open circles) and the predicted pH profile calculated from mean $P_{O_2}$ data.

## 3.4 DISCUSSION

### 3.4.1 Tissue $P_{O_2}$

$P_{O_2}$ measurements of *in vitro* tadpole brainstem tissue ranged from 438 ± 52 Torr on the ventral surface to a minimum of 323 ± 31 Torr in midline tracts (750 μm below the surface) and 240 ± 68 Torr in lateral tracts (at a depth of 850 μm). Therefore, recordings of $P_{O_2}$ no less than 240 ± 68 Torr in the thickest regions of the brainstem preparation indicate all tissue layers were fully supplied with oxygen. This finding provides the first evidence of an *in vitro* vertebrate brainstem preparation exhibiting rhythmic respiratory activity that is not associated with tissue hypoxia.

Previous studies by Okada *et al.* (1993), Brockhaus *et al.* (1993) and most recently by Voipio and Ballanyi (1997) evaluated the gas exchange status of the widely used isolated neonatal rat brainstem-spinal cord preparation developed by Suzue (1984). Using oxygenated aCSF, both Okada *et al.* (1993) and Brockhaus *et al.* (1993) reported $P_{O_2}$ gradients of 100 Torr per 100 μm in the superfusate 200 μm above the surface of the brainstem. By contrast, the present study demonstrates $P_{O_2}$ gradients of 30 Torr/100 μm in the superfusate 200 μm above the brainstem surface. The thickness of the unstirred layer for $O_2$ measured in the present study (>200 μm) approximated that reported by Okada *et al.* (1993) (>200 μm) and was greater than values given by Brockhaus *et al.* (1993) (200

μm), indicating variation in superfusion flow rates between preparations. Unstirred layer thickness influences the level of tissue oxygenation at the ventral brainstem surface. This effect is apparent when comparing brainstem surface $P_{O_2}$ in the isolated neonatal rat preparations; Okada *et al.* (1993) recorded a $P_{O_2}$ of 200 Torr, while Brockhaus *et al.* (1993) measured a $P_{O_2}$ of 400 Torr. By comparison, the present study showed ventral brainstem surface $P_{O_2}$ at 438 Torr, reflecting similar oxygen gradients in the unstirred layer compared to results by Brockaus *et al.* (1993) and substantially lower oxygen gradients in the unstirred layer compared to Okada *et al.* (1993).

Below the ventral surface, Okada *et al.* (1993) and Brockhaus *et al.* (1993) observed similar $P_{O_2}$ gradients of 100 Torr /100 μm for the first 200 μm and recorded anoxic tissue levels at 450 μm and 700 μm, respectively. By contrast, the present study showed lateral tract $P_{O_2}$ gradients of 60 Torr /100 μm for the first 200 μm with a minimum $P_{O_2}$ of 323 Torr in the midline and 240 Torr laterally at depths of 750 μm and 850 μm, respectively. Therefore, while differences between $P_{O_2}$ profiles of the neonatal rat brainstem and those of the present study may be attributed, in part, to the relatively low consumption of oxygen by amphibian CNS tissue (Dittmer and Grebe, 1956), they may also reflect variations in superfusion techniques, which, in turn, may influence the gradient in the unstirred layer.

Below 200 μm, differences between the slopes of the $P_{O_2}$ depth profiles in midline and lateral tracts reflect diffusional profiles of tissues with unequal thickness that uniformly metabolize oxygen at a constant rate (Hill, 1928). Because diffusion of oxygen into the brainstem is influenced as a function of the thickness and oxygen consumption of the tissue, the amount of oxygen available to each successive layer of tissue in the brainstem is reduced as the $P_{O_2}$ gradient decreases and oxygen is metabolized. Therefore, $P_{O_2}$ levels in thicker lateral tracts decreased with steeper slopes than those in midline regions.

In contrast to isolated anoxic mammalian brainstem preparations, tissue in the *in vitro* tadpole brainstem was hyperoxic. Compared with normoxic tissue $P_{O_2}$ values of 30-40 Torr, minimum tissue $P_{O_2}$ (240 Torr) demonstrated in the present study was considerably higher (Dejours, 1975). Although the effect of oxygen toxicity on respiratory neurons in brainstem tissue is unknown, recent studies have shown that oxidative stress induces cell death in cultured forebrain neurons (Enokido *et al.*, 1992) and impairs neuronal thermosensitivity in hypothalamic slices by free radical formation (Shibata and Blatteis, 1991).

Hyperoxia may have also effected the production of nitric oxide (NO), a neurotransmitter shown to enhance the excitability and spontaneous discharge rates of neurons within the nucleus tractus solitarii (Ma *et al.*, 1995), dorsal motor nucleus of the vagus (Travagli and Gillis, 1994) and in the pontine respiratory group (Ling *et al.*, 1992). Because molecular oxygen is a substrate

for NO synthesis (Leone *et al.*, 1991), tissue hyperoxia could increase NO production leading to stimulation of respiratory motor output frequency. Additionally, since NO binds to hemoglobin, the lack of NO removal by the blood in the isolated brainstem may contribute to the accumulation of tissue NO. Nevertheless, because rhythmic respiratory activity in the present study was maintained well over 10 hours, the tadpole brainstem appeared tolerant of hyperoxic conditions.

### 3.4.2 Tissue pH

Paralleling reductions in $P_{O_2}$, pH decreased from 7.74 ± 0.01 at the ventral surface to a minimum of 7.58 ± 0.05 in midline tracts and 7.34 ± 0.12 in lateral tracts. Minimum pH measurements occurred 700 μm below the midline surface and 900 μm below the lateral surface. Comparatively, when superfused with aCSF equilibrated with a $P_{CO_2}$ of 28 Torr (pH 7.5), Okada *et al.* (1993) demonstrated, in the isolated neonatal rat brainstem preparation, a nearly constant pH gradient of 0.1 pH unit per 100 μm beginning 200-300 μm above the ventral surface of the medulla which continued to a depth of 1000 μm below. A similar gradient (0.1 pH unit per 100 μm) was recently reported by Voipio and Ballanyi (1997) in the isolated neonatal rat brainstem preparation which corresponded to pH measurements in the isolated tadpole brainstem (0.07 pH units per 100 μm) from 100 μm above to 200 μm below the brainstem surface.

However, compared to the 100 μm thick unstirred layer for pH in the present study, both Okada *et al.* (1993) and Voipio and Ballanyi (1997) demonstrated unstirred layers for pH greater than 200 μm.

At the ventral brainstem surface, Okada *et al.* (1993) recorded a pH of 7.22 that reached a minimum value of 6.23 at a depth of 1000 μm. Similarly, Voipio and Ballanyi (1997) reported values of 7.2 and 6.6, respectively. By contrast, the tadpole preparation demonstrated greater pH levels at both the ventral surface (7.74) and its minimum value (7.34), 900 μm below. These differences show that the gradient for pH is less in the tadpole brainstem than in the neonatal rat brainstem preparation. In the tadpole brainstem, unstirred layer thickness for $P_{O_2}$ (200 μm) was twice that observed for pH (100 μm). Presuming that the extracellular pH gradient is established by $CO_2$ accumulation rather than lactate production, these differences may be accounted for by the greater diffusivity of $CO_2$ in water over $O_2$.

Development of substantial tissue pH gradients may result from two processes: 1) accumulation of $CO_2$ produced by aerobic metabolism; or 2) accumulation of acid metabolites from anaerobic metabolism. Both Okada *et al.* (1993) and Brockhaus *et al* (1993) postulated that the latter accounted for the extracellular pH gradient observed in the neonatal rat brainstem resulting from a steep $P_{O_2}$ gradient and anoxic center at tissue depths between 450 and 700 μm. By simultaneously measuring tissue pH and $P_{CO_2}$, Voipio and Ballanyi (1997)

confirmed this postulate, showing steady-state [$HCO_3^-$] gradients. Voipio and Ballanyi (1997) suggested that the $H^+$ load generated by cellular metabolism was buffered by the $CO_2$-$HCO_3^-$ buffer system within cells, as well as in the interstitial space. At steady state, these reactions were in balance with active transport of acid equivalents across cell membrane, creating a source of $CO_2$ and a sink of $HCO_3^-$ in the tissue.

By contrast, all tissue layers within the isolated tadpole brainstem were fully oxygenated, suggesting that $CO_2$ accumulation related to aerobic metabolism accounts for the extracellular pH gradient. Theoretical calculation of lateral tract pH gradients extrapolated from $P_{O_2}$ data, assuming uniform bicarbonate levels, were similar in shape to measured pH gradients, but less steep (Fig. 3.4A). Calculation of tissue $P_{CO_2}$ using mean pH and $P_{O_2}$ values from lateral tracts predicted substantial gradients, with maximum values between 36 and 49 Torr 800-950 μm below the ventral surface, however, $P_{CO_2}$ gradients calculated from $P_{O_2}$ were less steep. Hence, for the degree of $P_{O_2}$ change in the tissue, greater calculated changes in $P_{CO_2}$ were observed, suggesting another source of $H^+$ and the possibility of a bicarbonate gradient. Nonetheless, predicted $P_{CO_2}$ gradients in the tadpole were substantially lower than those reported by Voipio and Ballanyi (1997) in the isolated neonatal rat brainstem, with maximal values of 106 Torr, 1000 μm below the surface. This suggests that

in the neonatal rat, the consumption of bicarbonate in buffering the $H^+$ in the tissue is a significant source of $CO_2$ in addition to its production by aerobic metabolism.

Like $O_2$, $CO_2$ gradients within the brainstem tissue are influenced by tissue thickness, thereby mediating lower pH levels in lateral tracts compared to thinner midline tracts. At depths greater than 500 μm, pH levels in lateral tracts were maintained approximately 0.2 units lower than in the midline tracts (Fig. 3.3). The observed differences between midline and lateral pH levels may also result from regional differences in the metabolic rate. Intracellular hypercapnia produces transcellular transport of acid or acid equivalents. However, this transport is not likely to be a sustained phenomenon and, hence, could not contribute to the observed pH gradients. Overall, the lack of hypoxic and anoxic tissue with acid producing regions associated with the isolated neonatal rat brainstem-spinal cord preparation that was observed in the present study clearly demonstrates an advantage of the tadpole brainstem as a tool for *in vitro* studies.

While the acidotic tissue levels measured in deeper tissue layers were clearly outside normal pH ranges, more physiological tissue pH levels could have been easily achieved by utilizing a more alkaline superfusate. Because pH values within the brainstem tissue are also influenced by the superfusate pH, increasing

the pH level of the superfusate would produce concomitant elevations in extracellular tissue pH.

### 3.4.3 Tissue thickness

Mean medullary tissue width between CN V and X was measured at 4.34 ± 0.57 mm, with dorsal-ventral thicknesses in midline and lateral medullary regions of 0.92 ± 0.21 mm and 1.31 ± 0.22 mm respectively. By comparison, brainstem measurements of the *in vitro* neonatal rat preparation were similar in lateral width (4-5 mm), but were considerably greater in dorsal-ventral thickness (2.5 mm) (Okada *et al.*, 1993; Issa & Remmers, 1992). If the metamorphic tadpole brainstem preparation was completely uniform and homogeneously superfused, maximal diffusion distances would have been expected at 460 μm in midline tracts and 655 μm in lateral tracts. Minimum values of $P_{O_2}$ and pH, however, were observed nearly 250 μm deeper than predicted values. This discrepancy may have resulted from measurement artifacts, such as, inaccuracy of microelectrode positioning or greater than anticipated tissue shrinkage during fixation. More likely, smaller diffusional flow rates at the dorsal brainstem surface, producing greater unstirred layers at the ventral than dorsal surface, could have shifted minimal $P_{O_2}$ and pH values below the half-thickness of the medulla. While these dimensions apply to tadpoles of stage 15-19, preliminary

brainstem measurements of more immature tadpoles showed smaller diffusion distances.

Overall, the results serve to clarify the limitations of the isolated *in vitro* brainstem preparation of the larval bullfrog as a model for studies of neurorespiratory control. This study demonstrates a robust tadpole brainstem model that, although being moderately acidic, is well oxygenated throughout all tissue layers. Diffusion distances were reduced as a result of the increased uniformity of superfusion and diffusional homogeneity by creation of a planar brainstem sheet. Hence, recordings of spontaneous rhythmic motor output in the *in vitro* tadpole brainstem possess physiological validity, a considerable advancement from recordings of isolated neonatal rat brainstem-spinal cord preparations, and may prove an invaluable tool for studies of neurorespiratory control.

# *CHAPTER FOUR*

## *Characterization of the Neurorespiratory Pattern of the Decerebrate Tadpole*

The goal of Chapters 4 and 5 of the thesis research is to provide information regarding the biological significance of the spontaneous efferent bursting activity observed in the isolated tadpole brainstem preparation. To achieve this goal, the spontaneous bursting activity of the *in vitro* brainstem was compared to that observed in the semi-intact, *in vivo* preparation where simultaneous mechanical measurements provide unequivocal evidence regarding respiratory pattern. Validation of the spontaneous bursts as "fictive" is achieved by showing that cranial and spinal nerve activity, *in vitro,* shows a rhythmic sequence of motor activity that is comparable to the activity of bursting motor output generating gill and lung ventilation in the decerebrate preparation.

## 4.1 INTRODUCTION

Recent studies have described neural mechanisms of gill and lung ventilation in *in vitro* preparations of the brainstem of larval *Rana catesbeiana* which exhibit efferent bursting activity in CN VII motorneurons (Galante *et al.* 1996; Liao, *et al.* 1996; Pack *et al.* 1993). Such activity has been interpreted as being "fictive" gill and lung ventilation, however, in these studies, lung and gill bursts were separately identified using an amplitude criterion. The use of this criterion was based on a preliminary report by Pack *et al.* (1993) correlating patterns of mass action potentials recorded in the region of the facial nucleus with oscillations in opercular or intrapulmonary pressures in the decerebrate tadpole. Both opercular pressure and facial nucleus activity exhibited two distinct patterns of activity: 1) a high-frequency, low-amplitude rhythm, and 2) a low-frequency, high-amplitude pattern as shown in Fig. 4.1. In separate experiments, these investigators demonstrated that intrapulmonary pressure increased following the high-amplitude bursts of facial nucleus activity (Pack *et al.* 1993). Although Pack *et al.* (1993) did not record facial nucleus activity, opercular and intrapulmonary pressure simultaneously, they inferred that the high-frequency, low-amplitude rhythm represented gill ventilation, whereas the low-frequency, high-amplitude rhythm corresponded to pulmonary ventilation.

If the *in vitro* tadpole brainstem preparation is to be a useful preparation for investigating ontogenetic aspects of central respiratory pattern generation and chemoreception in vertebrates, the biological meaning of the rhythmic bursts appearing in cranial and spinal nerve roots must be unequivocally established. In other words, specific and separate neural correlates of gill and lung ventilation must be established. While the preliminary report by Pack *et al.* (1993) describing the relationship between facial motor neurons, opercular pressure, and intrapulmonary pressure provides an important first step in this process, these findings must be expanded upon if convincing neural correlates of fictive gill and lung ventilation are to be established. Specifically, description of the behavior of a number of motor pools during mechanically identified gill and lung ventilation (i.e. spatio-temporal relationships, recruitment of new motor outputs) is needed to provide more certain characterization of the patterns of neural activities associated with gill and lung breaths.

The purpose of the present study was to provide a more complete description of the activity patterns in the cranial and spinal nerve roots associated with mechanically identified gill and lung ventilation of the tadpole *in vivo*. Accordingly, I recorded, in the decerebrate, spontaneously breathing tadpole, pharyngeal muscle electromyogram (EMG), pressures in the pharynx and in the lungs, and efferent action potentials in the roots of CN V, VII and SN II.

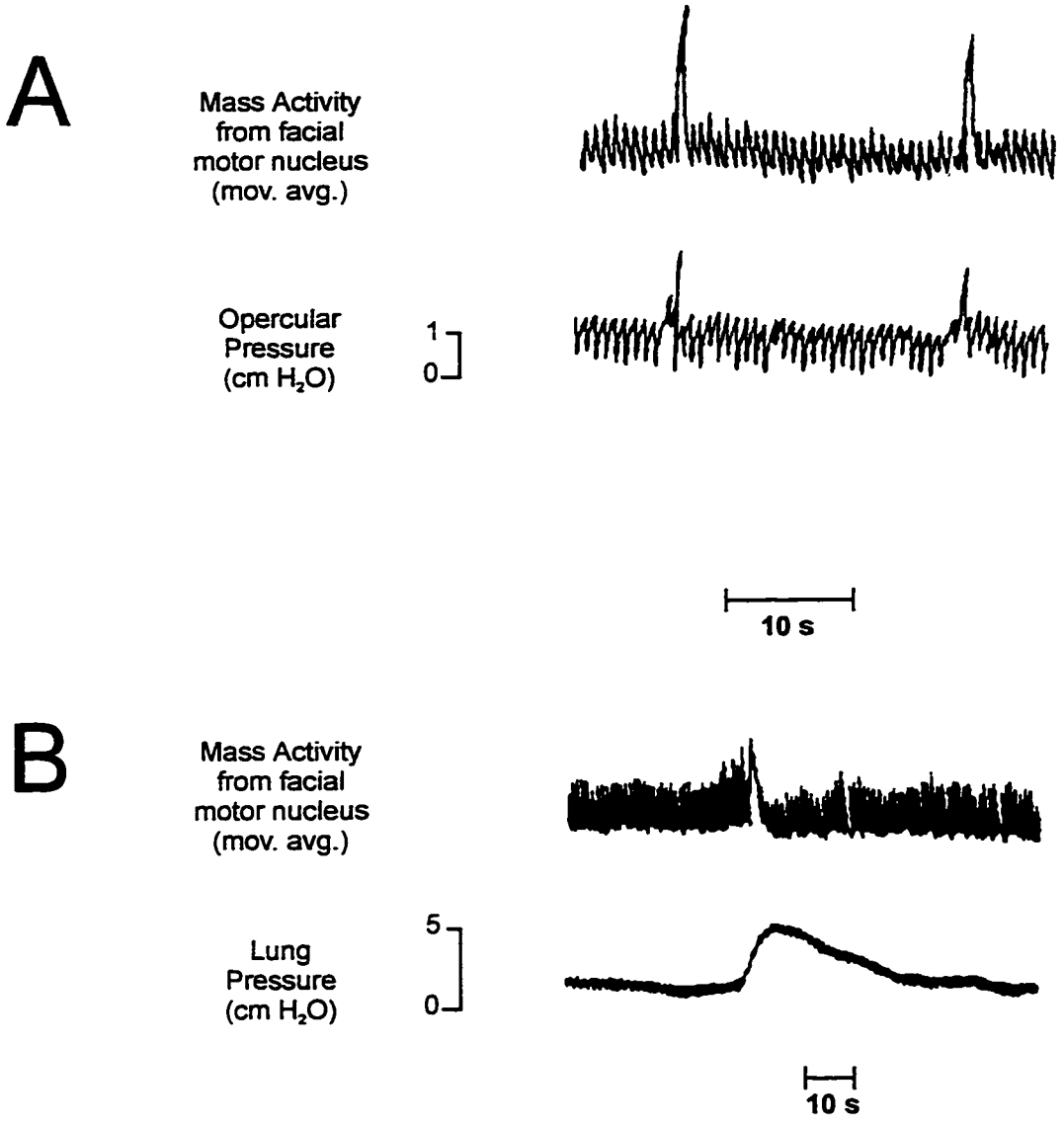


**Figure 4.1** (A) Simultaneous recording of the moving average of neuronal activity from the 7th motor nucleus and the opercular pressure. (B) Simultaneous recording of the moving average of neural activity from the same nucleus and the intrapulmonary pressure. (Adapted from Pack et al., 1983).

## 4.2 METHODS

### 4.2.1 Animals and surgical preparation

Experiments were performed on 16 metamorphic *Rana catesbeiana* larvae of either sex that possessed functional gills and lungs (stages 15-19). The tadpoles were purchased from a commercial supplier and maintained as formerly described in Chapter 2.

The animals were weighed then anesthetized via immersion in tricaine methanesulphonate (MS-222; 1:10,000) until unresponsive to touch. Rhythmic gill ventilation was consistently observed following anesthesia. Fine wire electrodes (100 μm diameter) were implanted through a ventral incision into the left buccal levator muscle (interhyoideus). This muscle is innervated by CN VII (Gradwell, 1971b). To record oropharyngeal pressure ($P_{OP}$), a cannula of polyethylene (PE) 50 tubing was introduced through the naris into the buccal cavity. This end of the cannula was led out through the mouth, heat flared to form a flange and retracted back into the buccal cavity. The flared end of the tubing was secured to the interior narial opening forming a tight seal. The external end of the tubing was connected to a differential pressure transducer (Statham P23 AA) and the oropharyngeal pressure signal amplified (11-4307-04, Gould Inc.). To measure intrapulmonary pressure ($P_{IP}$), an incision was performed on the dorsolateral surface of the body wall and the base of the lung

was exposed. A catheter-tipped transducer (Millar TC-500, Millar Instruments Inc.) was ligated (surgical silk, 5-0, Ethicon) directly in the lung via a lateral incision and the intrapulmonary pressure signal was amplified (11-4307-00, Gould Inc.).

Through a dorsal incision, the cranium was opened and the forebrain rostral to the optic lobes transected, referred to as pre-tectal decerebration. Further removal of the cartilaginous skull, exposing the anterior part of the spinal cord, allowed for transection of the spinal cord caudal to the SN 2. With the aid of a dissecting microscope, CN VII, X and SN II on the side of the tadpole opposite the EMG wire insertion was transected and freed from the surrounding tissue. A separate superfusion well was created around the craniotomy using an elastomer (Silly Putty®, Binney and Smith, Ontario) and filled with aCSF (described in Methods Section 2.1.2) saturated with 98% $O_2$, 2% $CO_2$ (pH 7.8).

### 4.2.2 Recording Chamber

The tadpole was transferred to a whole body superfusion-recording chamber (Fig. 4.2) and submersed in dechlorinated tap water equilibrated with 100% oxygen. In the experimental recording chamber, the tadpole was oriented dorsal surface up in the trough and held in place with small pins. Water was delivered at room temperature into the chamber at a rate of 10-12 ml/minute through an inflow aperture near the head of the tadpole. The level of the water

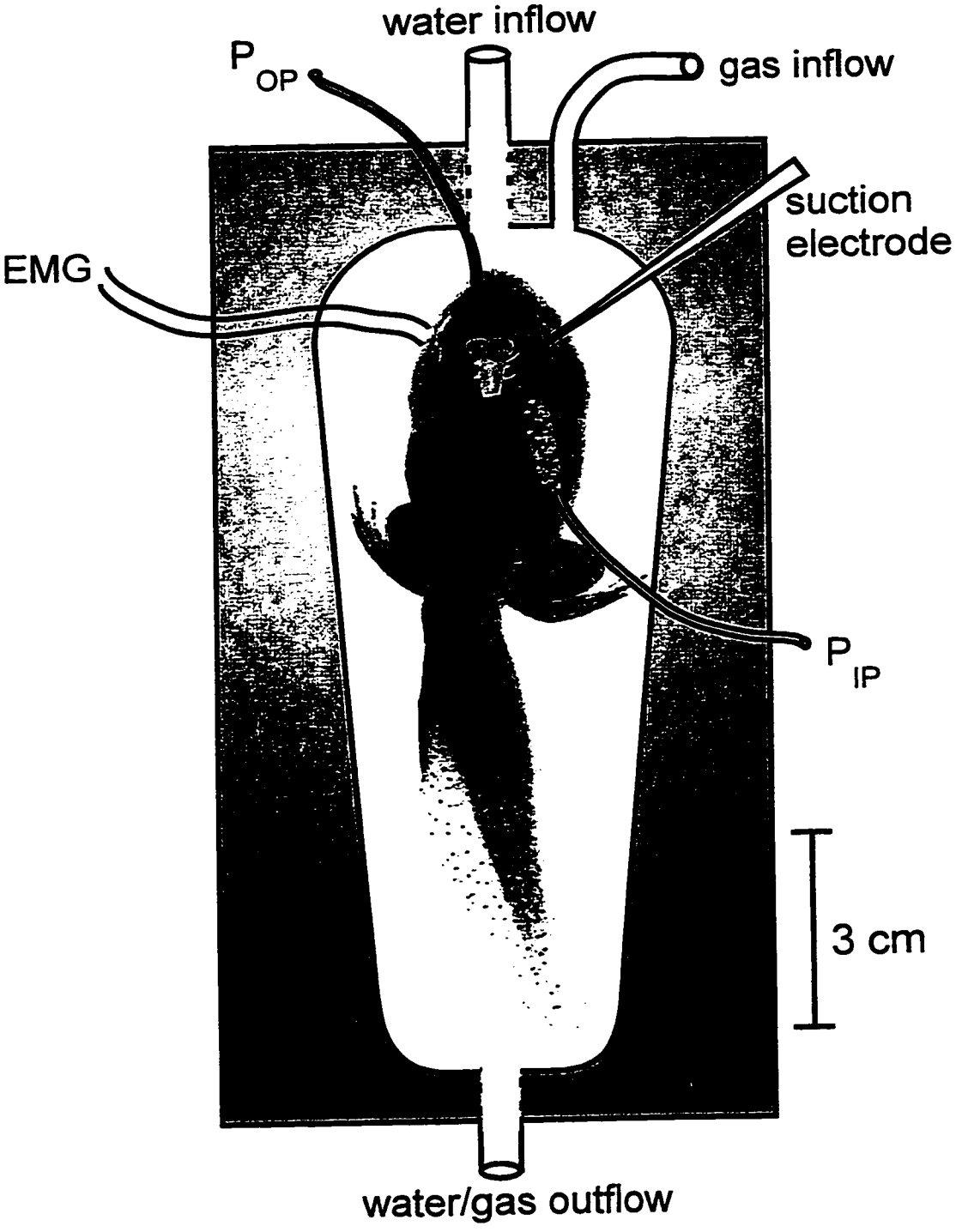


**Figure 4.2** Diagram showing the position of the tadpole in the recording chamber. Oropharyngeal pressure ($P_{OP}$) and intrapulmonary pressure ($P_{IP}$) were measured along with EMG of buccal levator muscle (interhyoideus) and CN efferent motor activity (via a suction electrode).

was adjusted to completely submerge the tadpole, depending on its size. This solution was drawn out the recording chamber from an outflow aperture near the tail. The gaseous atmosphere overlying the superfusate was purged with the same gas as was equilibrated with the superfusate.

### 4.2.3 Neural recordings

Efferent neural activity was recorded, as previously detailed in Chapter 2, from the central cut-end of CN V, VII, X and SN II using suction electrodes.

### 4.2.4 Experimental protocol

The study used three experimental groups: Group A, in which CN V (n=2) or VII (n=6) activities, contralateral EMG, $P_{OP}$, and $P_{IP}$ were simultaneously recorded; Group B, where CN V and VII, $P_{OP}$, and $P_{IP}$ (n=4) were simultaneously recorded to describe the phase relation of neural activities of two cranial nerves; and Group C, where SN II, $P_{OP}$, and $P_{IP}$ activities were recorded (n=4) to characterize further respiratory related activity in SN II.

Following instrumentation, tadpoles recovered for a one-hour period while submersed with water saturated with room air (21% oxygen). Oropharyngeal pressure, EMG and neural activity were then recorded for 15 minutes. The fluid in the chamber was drained via the outflow port and replaced with normoxic gas

(21% oxygen). After a 15 min equilibration period, intrapulmonary and oropharyngeal pressure, EMG and neural activity was recorded for 15 minutes.

### 4.2.5 Data analysis

Gill breaths were defined by the rhythmic oscillations in oropharyngeal pressure with no changes in intrapulmonary pressure, whereas lung breaths were identified by increases in both intrapulmonary and oropharyngeal pressures. In order to characterize neural gill and lung ventilation, the neural bursting activities of CN V, VII and SN II, EMG, and $P_{OP}$ and $P_{IP}$ recordings were analyzed to identify: 1) the relationship between lung burst onset with respect to the ongoing gill cycle; 2) recruitment of an additional population of motor neurons during lung bursts; 3) CN VII minimal peak amplitude associated with lung bursts; 4) phase relationships (latency of onset and duration) between neural, muscular, and mechanical components of gill and lung ventilation.

Burst duration was defined as the time from the onset of activity to peak amplitude. The latency of onset of each variable was calculated with respect to the onset of CN VII activity with the exception of SN II, which was calculated with respect to $P_{OP}$. In plotting these data, however, mean burst onset time were normalized to CN V for gill ventilation and CN VII for lung ventilation, as these

neural activities marked the primary event within each type of ventilation. Mean SN II onset time was normalized to the onset of $P_{OP}$ activity.

The onset of lung ventilation with respect to gill ventilation during normoxia was determined in a subset of animals (n= 6). Relative timing variables were defined for the gill cycle as follows: $T_B$, the time from the onset of neural bursting activity to the maximum amplitude of bursting activity; $T_{IB}$, the interburst time from the maximum amplitude to the onset of the next neural burst; and $T_C$, the total gill ventilatory cycle time ($T_B + T_{IB}$). Mean $T_B$, $T_{IB}$, and $T_C$ were calculated for at least 15 control gill breaths prior to each lung breath. For the lung cycles, relative timing variables were defined as follows: $T_I$, the time from the onset of neural bursting activity to the maximum amplitude of bursting activity; $T_E$, the time from the maximum amplitude to the onset of the next neural burst; $T_{TOT}$, the total respiratory time ($T_I + T_E$). In calculations of lung breath frequency, series or bouts of lung inflation were counted as one lung breath ventilation episode. In order to determine the timing of lung burst activity with respect to the ongoing gill cycle, $T_I$, $T_E$ and $T_{TOT}$ were calculated for CN VII lung activity for the first burst of a lung episode and $T_B$, $T_{IB}$, and $T_C$ were calculated for the gill breath just prior to the lung burst. These data were expressed as a percentage of the control gill breaths prior to lung burst episode.

Statistical analysis included one-way analysis of variance with repeated measures and both Student Newman-Keuls and Tukey tests for multiple pairwise

comparisons. $P<0.05$ was the criterion for significance. Unless otherwise stated, values reported are mean ± 1 SEM.

## 4.3 RESULTS

### *4.3.1 Mechanical and EMG correlation with cranial nerve activity*

Simultaneous recordings of CN (V or VII) neurograms, interhyoideus EMG, $P_{OP}$, and $P_{IP}$, demonstrated a coordination of mechanical, EMG, and neural activities during spontaneous breathing. Two distinct and consistent patterns of activity in cranial nerve recordings were observed in Fig. 4.3. One was a low-amplitude, high-frequency bursting pattern in phase with EMG bursts and low-level oscillations in oropharyngeal pressure. Since these activities occurred at a constant lung pressure, they are classified as gill ventilation. The other pattern consisted of high-amplitude, low-frequency bursts in CN V or VII in phase with a larger EMG burst and a sharp increase in intrapulmonary pressure, indicating that they constitute lung bursts.

Lung ventilation occurred either as isolated large bursts or a series of large bursts of CN and SN activity (illustrated in Figs. 4.3, 4.4 and 4.5). The amplitude of gill $P_{OP}$ waves and gill bursts in CN and EMG was reduced following spontaneous lung inflation (Fig. 4.3). This reduction was also observed following passive inflation of the lung with room air, which was performed occasionally in order to check the patency of the lung catheter.

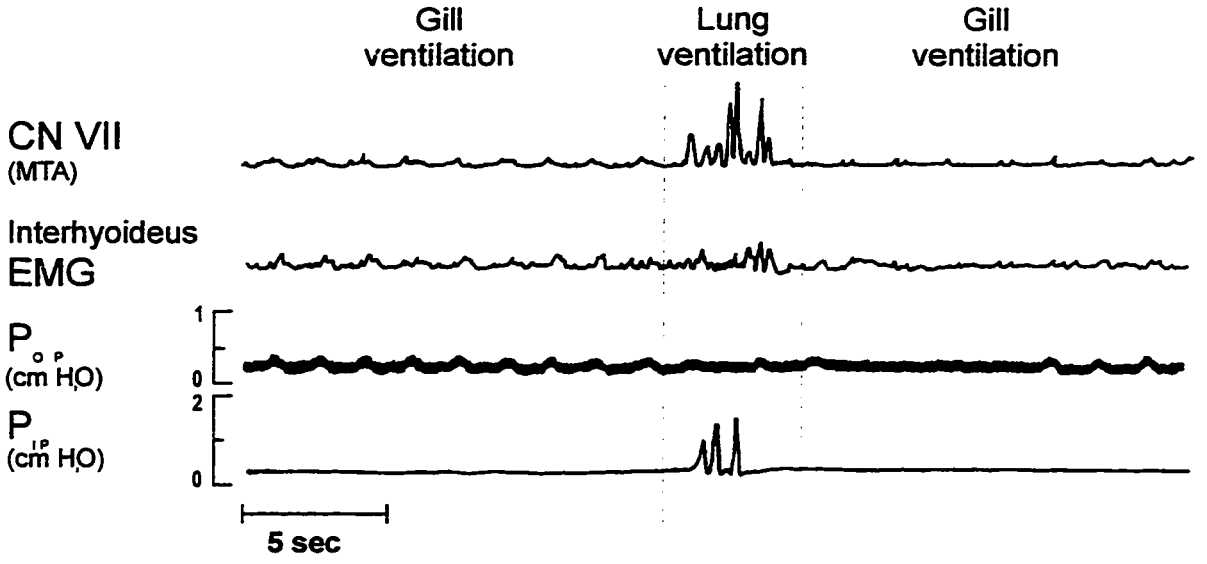


**Figure 4.3** Simultaneous recordings of the moving time average (MTA) of CN VII, interhyoideus EMG, oropharyngeal pressure ($P_{OP}$) and intrapulmonary pressure ($P_{IP}$) during gill ventilation and lung ventilation. Note the concomitant increases in CN VII and EMG activities and $P_{IP}$ during lung ventilation, and the reduction of gill amplitude and frequency following lung inflation.

### 4.3.2 Spinal nerve II bursting activity

Efferent activity of SN II consisted of relatively large amplitude burst that consistently occurred during lung breaths, i.e., the bursts coincided with increases in $P_{IP}$ (Fig. 4.4). All lung breaths were associated with an SN II burst, and an SN II burst was never observed without a lung breath. Unlike CN V and VII, SN II recordings did not exhibit rhythmic bursting activity during gill ventilation, as shown in Fig. 4.4. SN II activity occurred as single bursts or as a series of bursts similar to the patterns observed in CN V and VII. Because each burst of SN II occurred exclusively during increases in $P_{IP}$, these bursts represent a component of lung ventilation and not gill ventilation. The frequency of lung bursting activity of SN II (0.54 ± 0.21 $min^{-1}$) observed in Group C was not different ($P$ >0.05) from CN VII lung frequency (0.29 ± 0.10 $min^{-1}$, see Table 4.1) observed in Group A. $P_{OP}$ increased with SN II bursts in some instances, whereas in other cases negative pressures in the buccal cavity occurred during the SN II burst.

### 4.3.3 Quantification of neural gill and lung bursting activities

Mean values of gill and lung burst amplitude and frequency are listed in Table 4.1.

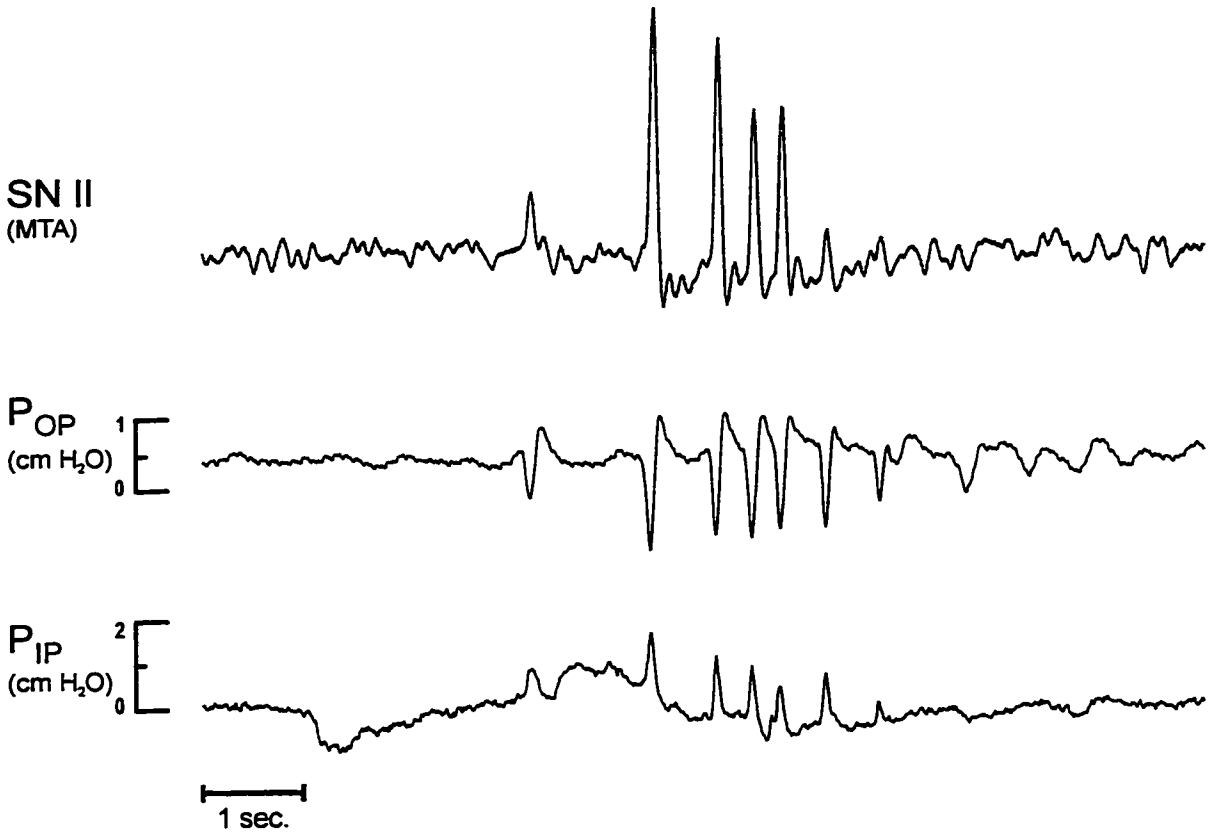


**Figure 4.4** SN II moving time average (MTA), oropharyngeal pressure ($P_{OP}$) and intrapulmonary pressure ($P_{IP}$) during gill ventilation and lung ventilation. Note the absence of rhythmic SN II activity during gill ventilation (denoted by oscillations in $P_{OP}$).

Table 4.1. CN VII gill and lung burst amplitude (% of gill amplitude) and frequency ($min^{-1}$)

| CN VII Ventilatory Activity | |
|---|---|
| Gill burst amplitude (% of gill) | 100 |
| Gill burst frequency ($min^{-1}$) | 49.3±6.1 |
| Lung burst amplitude (% of gill) | 250±65 |
| Lung burst frequency (min-1) | 0.3±0.10 |

*4.3.3.1 Lung burst onset with respect to gill burst*

Lung burst $T_I$ (76.55 ± 13.59% of gill), $T_E$ (90.22 ± 7.53% of gill) or $T_{TOT}$ (92.41 ± 5.21% of gill) did not differ ($P>0.05$) with respect to gill burst values of $T_B$, $T_{IB}$, and $T_C$, respectively. Mean $T_B$ and $T_{IB}$ for gill bursts prior to lung episodes were not significantly different from gill bursts (91.23 ± 9.78 and 80.78 ± 12.34% of gill, respectively), however, mean $T_C$ for gill breaths prior to lung breaths was significantly lower than control (80.68 ± 9.31% of gill). Although mean $T_{IB}$ of the gill breath prior to the lung burst was not significantly different from control, significant decreases in $T_{IB}$ were found in five of six animals, while the remaining animal possessed increases in $T_{IB}$ for the gill breath prior to the lung episode.

*4.3.3.2 Action potential recruitment during lung bursts*

Because nerve activities were fed to a moving average circuit (see Methods), the increases in CN VII amplitude with lung bursts (Fig. 4.3) may be due to an increase in action potential frequency and or amplitude, the latter indicating the recruitment of additional populations of motor neurons. Examination of action potentials in the unprocessed nerve recording reveal the appearance during lung breaths of action potentials with considerably greater amplitude than those observed during gill ventilation (Fig. 4.5).

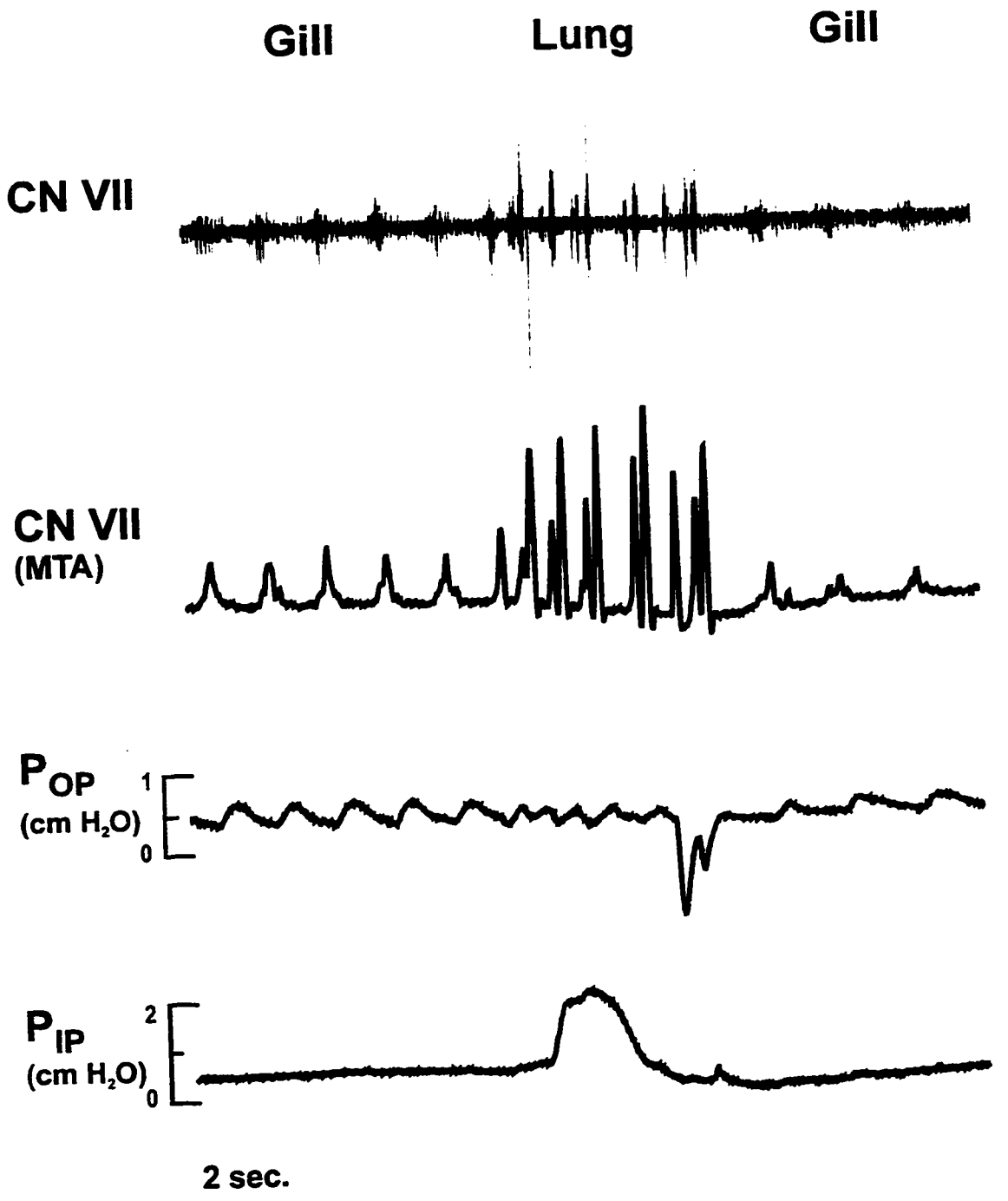


**Figure 4.5** Unprocessed and moving time average (MTA) CN VII activities, oropharyngeal pressure ($P_{OP}$) and intrapulmonary pressure ($P_{IP}$) during gill and lung ventilation.

Such high amplitude action potentials were not a result of the summation of smaller amplitude activity, indicating recruitment of motor units during lung ventilation not active during gill ventilation. Action potentials of similar amplitude as those occurring during gill ventilation could also be observed during lung bursting activity, and their contribution to changes in increases in the amplitude of the moving average neurogram is uncertain.

*4.3.3.3 CN VII peak amplitude associated with lung bursts*

In order to establish criteria for the relative cranial nerve activity associated with a lung breath, neurogram amplitude was examined during single lung breaths and within a series of lung breaths. The minimal amplitude of CN VII activity during a lung breath was 115% of gill amplitude when the breath was part of a series of lung breaths. During single lung breaths, mean CN VII amplitude was 248 ± 38% of gill breath amplitude, with a minimum amplitude of 136%.

*4.3.3.4 Latency of onset and duration of neural, muscular, and mechanical components of gill and lung ventilation*

Latency of onset and duration were calculated for neural burst discharge, interhyoideus EMG, $P_{OP}$ and $P_{IP}$ activities for both gill and lung ventilation. These data are listed in Table 4.2 and displayed in Fig. 4.6. The onset of activity during

**Table 4.2.** Mean latency and duration of CN V, CN VII, interhyoideus EMG, $P_{OP}$, SN II, and $P_{IP}$ during gill and lung ventilation.

| | Gill ventilation | | Lung ventilation | |
|---|---|---|---|---|
| **Respiratory Variables** | Latency (msec) | Duration (msec) | Latency (msec) | Duration (msec) |
| CN V | -370 ± 73* | 718 ± 204* | 41 ± 30 | 181 ± 59 |
| CN VII | 0† | 396 ± 101† | 0 | 328 ± 182 |
| Interhyoideus EMG | 132 ± 33† | 230 ± 183*,† | 74 ± 22 | 245 ± 156 |
| POP | 462 ± 68*,† | 409 ± 130† | 254 ± 112*,† | 261 ± 106 |
| SN II | N/A | N/A | 342 ± 25*,† | 155 ± 25 |
| PIP | N/A | N/A | 457 ± 99*,† | 146 ± 44 |

Data are shown as mean ± SEM. Latency of onset for each variable was calculated with respect to CN VII bursting activity defined as time zero. SN II and $P_L$ did not exhibit bursting activity during gill ventilation which is noted by N/A (no activity). * = significantly different from CN VII mean values within gill or lung ventilation; †= significantly different from CN V mean values within gill or lung ventilation ($P < 0.05$).

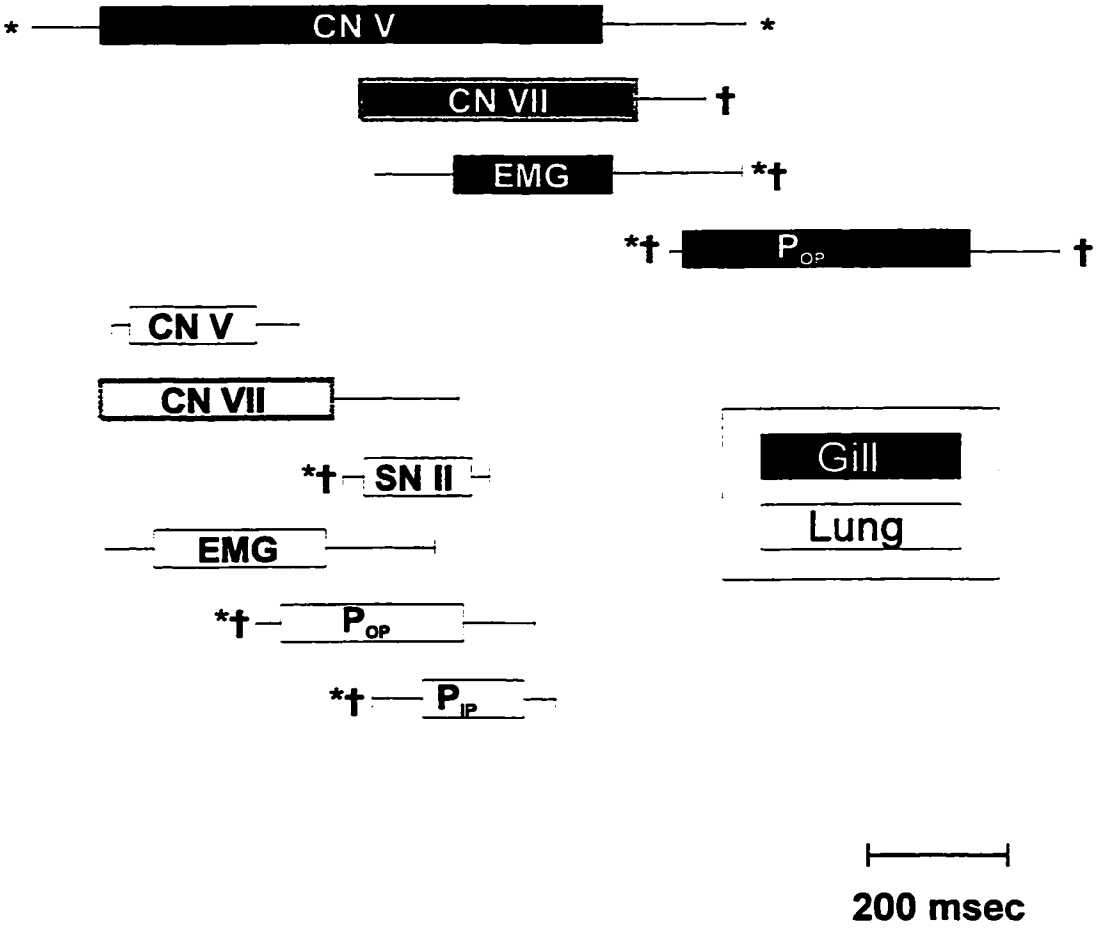


**Figure 4.6** Phase relations and durations of CN V, VII, interhyoideus EMG, $P_{OP}$, $P_{IP}$, and SN II during gill and lung ventilation. The mean latency of the onset of activities (normalized as described in Methods) and their associated standard errors are indicated by the left-hand side of the horizontal bars. The lengths of the bars indicate mean duration and the error bars on the right-hand indicate standard error of the duration. *significantly different from CN VII ($P<0.05$); †significantly different from CN V ($P<0.05$).

gill ventilation displayed a sequential neural-to-muscular-to-mechanical pattern. Specifically, the onset of CN V burst activity preceded that of CN VII, EMG activities, and $P_{OP}$ wave ($P<0.05$) during gill ventilation. CN VII and EMG gill burst activities occurred nearly simultaneously ($P>0.05$), and prior to the onset of the $P_{OP}$ wave ($P<0.05$). No significant differences in gill duration were observed between CN V, VII, EMG, and $P_{OP}$, with the exception of the CN VII-$P_{OP}$ interaction (Table 4.2).

Unlike the pattern observed in gill ventilation, CN V, VII, and EMG burst in synchrony during lung ventilation ($P<0.05$). SN II, $P_{OP}$, and $P_{IP}$ activities occurred synchronously as well, however their onset of activation occurred significantly later than CN V, VII and EMG ($P<0.05$). No significant differences were observed in the duration of all variables recorded during lung ventilation. The latency and duration of oscillation were compared in gill and lung ventilation. CN V gill burst duration (718 ± 204 msec) was significantly greater ($P<0.05$) than lung burst duration (181 ± 59). In addition, CN V latency of onset was shorter in gill (-370 ± 73 msec) than in lung (41 ± 30) ventilation.

## 4.4 DISCUSSION

The present study has demonstrated that the spontaneously breathing, decerebrate, metamorphic tadpole displays two distinct patterns of efferent cranial and spinal nerve motor output associated with mechanically defined gill and lung ventilations: the former was associated with high-frequency, low-amplitude bursts and the latter with low-frequency, high-amplitude burst. These findings confirm the preliminary report by Pack *et al.* (1993) and support the amplitude criterion for gill and lung bursts in the *in vitro* brainstem used by Liao *et al.* (1996) and Galante *et al.* (1996). Nonetheless, the amplitude criterion alone does not allow the unequivocal identification of lung versus gill fictive ventilation. The observation that CN V and VII burst sequentially during gill ventilation and synchronously during lung ventilation, and the discovery that an SN II burst occurs only during the lung breath provide new criteria for distinguishing lung and gill ventilation. When used together with an amplitude criterion, these allow separate and specific identification of lung and gill bursts.

Even though the tadpole preparation employed in this study was decerebrate and the efficiency of gas exchange unknown, the lung and gill ventilation observed resembled in many respects that reported for intact, free-swimming tadpoles. First, gill frequency for decerebrate (49 ± 6 $min^{-1}$) animals approximated that for intact animals (60 ± 4 $min^{-1}$, West and Burggren 1982). Second, in larval bullfrogs, lung ventilation occurs either in single breaths or as a

series of consecutive breaths (Burggren and West 1982; Infantino 1992; West and Burggren 1982; West and Burggren 1983). Both single bursts and series of bursting activity were observed in cranial and spinal nerve motor output, as well as in oropharyngeal and intrapulmonary pressures, and buccal elevator muscle EMG activity in the tadpole. Lung inflation series patterns of cranial nerve activity were occasionally observed in the *in vitro* tadpole brainstem preparation described in Chapter 5, and Liao *et al.* (1996) reported observing "complex lung burst-like activity" in CN VII in the *in vitro* tadpole brainstem preparation. The lack of a 1:1 correlation between CN VII burst activity and $P_{IP}$, as shown in Figs. 4.3 and 4.5, does not negate the role of this pattern of bursting activity in lung inflation. Similar lung burst patterns can be observed in data reported by Pack *et al.* (1993), in which several larger amplitude bursts of facial nucleus activity occur several seconds before any increase in lung pressure. This finding may reflect buccal oscillations associated with air breathing that occur while the glottis remains closed. While it is not certain if the pattern of CN lung burst activity observed in this study is a phenomenon of the decerebrate preparation, due to the technical difficulty associated with these experiments, the possibility that some leakage occurred at either the narial or lung catheter cannot be excluded.

A third similarity between intact and decerebrate preparations relates to the observed reduction of gill ventilation (amplitude and frequency) following

lung inflation, as illustrated in Figs. 4.3 and 4.5. This interaction in the tadpole has been described by West and Burggren (1983) who observed marked reductions in gill frequency following both spontaneous lung inflation in free-swimming tadpoles subjected to aquatic hypoxia and in simulated lung inflations of cannulated lungs regardless of the $P_{O_2}$. These workers suggested that this inhibition may be due to input from both pulmonary stretch receptors and/or an increase in $P_{O_2}$ following a normoxic lung breath. Although both chemoreceptor and pulmonary stretch receptor activation may play a role in reducing gill ventilation, the reductions in gill ventilation following lung inflation observed in this study were due primarily to pulmonary stretch receptor activation and less likely due to changes in alveolar $P_{O_2}$, as $O_2$ levels were held constant prior to and during lung breaths. A central inhibitory pathway between gill and lung central pattern generators, however, cannot be excluded.

Pack *et al.* (1993), in a preliminary report, described an association between facial nucleus multiunit activity and opercular or intrapulmonary pressures in the decerebrate tadpole. The results reported here confirm the results of Pack *et al.* (1993) and provide a more useful and more complete characterization of neural gill and neural lung ventilation by recording $P_{OP}$ and $P_{IP}$ simultaneously, and by recording efferent activity of CN V, CN VII, and SN II as well as interhyoideus EMG. The appearance of neural lung burst activity during

the ongoing gill ventilatory cycle demonstrates coordination between the timing of these two neural ventilatory discharge patterns. The present study demonstrates that an additional population of motor neurons discharge during lung ventilation, as illustrated in Fig. 4.5. This confirms the results of Liao *et al.* (1996), who described modulation of respiratory-related facial nucleus motor neuron membrane potentials.

Efferent bursting activity of SN II, which gives rise to the hypoglossal in the adult frog, coincident with increases in intrapulmonary pressure and not during gill ventilation contrasts the neural discharge patterns of CN V and VII. This unique behavior of SN II thereby provides a consistent neural marker for lung ventilation in the metamorphic tadpole. Similarly, SN II activity of the *in vitro* superfused premetamorphic tadpole brainstem preparation described in Chapter 5 also lacks the "fictive" gill ventilatory bursting pattern. However, Chapter 5 reports high-frequency, low-amplitude SN II activity in phase with neural "fictive" gill ventilation in the postmetamorphic larvae. This behavior resembles that reported by Kogo *et al.* (1994) in adult frogs showing low-amplitude, high-frequency bursts in both the main and sternohyoid branches of the hypoglossus during buccal ventilation.

The pattern of activation of respiratory-related neural, muscular, and mechanical components measured in this study reveal distinct differences between gill and lung ventilation. Significant differences in the latency of onset for these components were observed during gill ventilation, however these differences were not observed during lung ventilation. During gill ventilation these activities consist of a sequential, relatively slow augmenting pattern and contrasts with the more rapid, simultaneous onset pattern of activation seen during lung ventilation. The rapid and synchronous onset of these activities observed during lung ventilation may be necessary to produce and maintain sufficient pressure to inflate the lungs. The existence of distinct gill and lung respiratory central pattern generators (CPG) has been proposed for both the tadpole (Galante *et al.* 1996; Liao *et al.* 1996; Pack *et al.* 1993) and frog (Kogo *et al.* 1994; Kogo and Remmers 1994; McLean *et al.* 1995a, b). The characterization of these two distinct respiratory-related neural discharge patterns suggest the possibility that two highly coordinated respiratory central pattern generators are present in the tadpole.

The primary goal of this study was to characterize and quantify the neural bursting patterns of several cranial and spinal nerve motor pools of the semi-intact tadpole during mechanically defined gill and lung ventilation. Simultaneous recordings of interhyoideus EMG, $P_{OP}$ and/or $P_{IP}$ and nerve burst activity have permitted unequivocal discrimination of these neural activities as gill

or lung ventilation. More importantly, the two distinct bursting patterns reported here corresponded to the appropriate mechanical events that have been documented for gill and lung ventilation in the tadpole. Quantification of the magnitude of neural lung breaths as well as the pattern of neural efferent activities is essential for interpretation of cranial and spinal nerve activities recorded in the *in vitro* tadpole brainstem preparation (Chapter 5). Finally, the identification of SN II efferent activity exclusively during lung ventilation in the metamorphic tadpole will further facilitate the validation and classification of fictive gill and lung ventilation *in vitro*.

# *CHAPTER FIVE*

## *Characterization of Spontaneous Bursting Activity in the Tadpole Brainstem*

## 5.1 INTRODUCTION

Investigation of the neural mechanisms responsible for respiratory neuromuscular activity in amphibians has been facilitated by the development of superfused *in vitro* brainstem-spinal cord preparations (McLean *et al.* 1995a, b; Galante *et al.*, 1996; Liao *et al.*, 1996). The functional significance of the patterns of spontaneous bursting activity observed in cranial nerve (CN) roots of the completely isolated adult frog brainstem preparations (McLean *et al.* 1995a, b) has been elucidated by correlating CN root activity with activity of nerves to respiratory muscles in an *in situ* preparation (Kimura *et al.* 1997) and with neurograms, electromyograms and mechanical events related to oropharyngeal

and pulmonary ventilatory cycles from *in vivo* preparations (deJongh and Gans, 1969; Ito *et al.*, 1962; Kogo *et al.*, 1994; Kogo and Remmers, 1994; Sakakibara, 1984a, b; West and Jones, 1975). Similarly, recent studies of *in vitro* tadpole brainstem preparations have begun to characterize the patterns of respiratory activity related to gill and lung ventilation (Galante *et al.*, 1996; Liao *et al.*, 1996; Pack *et al.*, 1993). However, the separate identification of lung and gill ventilatory activities in these studies must be considered tentative, as an arbitrary CN amplitude criterion alone was used to identify putative gill and lung bursts in CN roots, i.e. large amplitude bursts were assumed to be fictive lung breaths and small amplitude bursts were assumed to be fictive gill bursts. This distinction, in practice, is difficult to draw since the difference between the peak amplitudes of small and large bursts in cranial nerves are often modest (see Fig. 5.3). If the isolated tadpole brainstem preparation is to be utilized as a tool to investigate fundamental questions of rhythmogenesis and central chemoreception, fictive gill and lung ventilatory activity must be separately identified.

The primary purpose of the present study is to describe the spatial and temporal patterns of spontaneous bursting activity characteristic of fictive gill and lung ventilation in the *in vitro* tadpole brainstem in order to provide data that can be correlated with comparable observations from the spontaneously breathing, decerebrate tadpole in which lung and gill ventilation are mechanically identified.

A second purpose is to describe the spatio-temporal features of gill and lung ventilatory motor output with development. To achieve these two goals, efferent activity from CN roots, the second spinal nerve (SN II) root and the laryngeal branch of the vagus (X*ℓ*) was recorded in pre- and post-metamorphic tadpoles. SN II innervates the hypoglossal muscles and has been shown to be a marker of a lung breath in the metamorphic tadpole *in vivo* (Chapter 4). X*ℓ* can be considered a peripheral respiratory nerve since its efferent activity controls the precise opening and closing of the glottal valve during lung ventilation.

## 5.2 MATERIALS AND METHODS

### 5.2.1 Animals and surgical preparation

Experiments were performed on 17 larval bullfrog tadpoles (*Rana catesbeiana*), of either sex, weighing between 8-13 grams. Animals were purchased from a commercial supplier and cared for by methods previously detailed (Chapter 2). Specimens were assigned to one of two groups based on the criteria of Taylor and Köllros (1946): pre-metamorphic (stages 4-14, n=10,) and post-metamorphic (stages 20-22, n=7).

Surgical procedures for brainstem removal were performed according to the protocol previously described in Chapter 2. In a subset of pre-metamorphic tadpoles (n=3), the peripheral nerve, X*ℓ*, which innervates glottal constrictors and dilators, was dissected over its entire length on one side and left attached to the brainstem. In these animals, the main trunk of the vagus was exposed and dissected free using a dorsal approach after resecting the cartilage surrounding the postotic foramen and by careful excision of the dorso-lateral margin of the semicircular canal. Using a ventral approach, the entire length of X*ℓ* was exposed and dissected free by excising the overlying tissue, thereby isolating the entire nerve. The brainstem was then removed as described previously (Chapter 2) with the main trunk of the vagus and the X*ℓ* on one side attached

### 5.2.2 Recording chamber and neural recordings

The brainstem was transferred to a superfusion recording chamber where spontaneous rhythmic motor output was recorded from the roots of CN V, VII, CN X, SN II and X$\ell$ using suction electrodes according to the protocol detailed in Chapter 2. Bursting activities from the root of CN X and X$\ell$ were recorded from opposite sides of the brainstem.

### 5.2.3 Experimental protocol

Equilibration of the superfusate with gas having a $P_{CO_2}$ of 45 and 17 Torr (balance $O_2$) produced pH values of 7.4 and 7.8. After the brainstem had been superfused in the recording chamber for at least 60 min (pH 7.8), stable nerve activities were recorded for 10 min at pH 7.8 and 7.4. Between each 10 min recording, a 5 min equilibration period ensued to allow equalization of tonometer and recording chamber pH and stabilization of the brainstem response to the new superfusate pH.

### 5.2.4 Data analysis

As described in Results, gill and lung bursts were identified using SN II amplitude criteria and by correlations with the SN II recordings from the decerebrate tadpole described in Chapter 4. Burst frequency was defined as the number of bursts per unit time. To evaluate developmental differences in

respiratory bursting patterns from CN V, VII, X, SN II and X*ℓ*, the time to peak and relative time of onset of fictive gill and lung ventilatory bursts was measured for each 10 min recording at pH 7.4. Mean time to peak was calculated from the onset of the burst to the time of peak amplitude and mean latency of fictive gill and lung ventilation was determined for each nerve with respect to the onset of the CN VII burst. Mean values of gill and lung motor output for each animal were then used to calculate group means ± S.E.M. Significant differences in the latency and time to peak of fictive gill and lung ventilation within and between each developmental group were examined using a one-way ANOVA for repeated measures, with the criterion of statistical significance at $P<0.05$. A Student-Newman-Keuls test of pairwise multiple comparisons was used to test significant differences between nerves within treatment groups when ANOVA revealed significant treatment effects.

## 5.3 RESULTS

Rhythmic, coordinated bursting patterns were recorded from CN V, VII, X, SN II and Xℓ in pre-metamorphic (n=10) and post-metamorphic (n=6) larvae when superfused with aCSF of pH 7.8 and 7.4. Although simultaneous recordings of all nerves were not successful in all animals, rhythmic bursts were recorded in two or more of the nerves in each experiment. Table 5.1 provides the number of animals in which each nerve was successfully recorded.

### 5.3.1 Bursting patterns

As illustrated in Fig. 5.1, integrated neurograms of CN V, VII and X from a pre-metamorphic tadpole revealed two different patterns of rhythmic activity: high burst frequency, low-amplitude bursts (Pattern 1) and low burst frequency, high-amplitude bursts (Pattern 2). Fig. 5.2 shows both unprocessed and integrated neurograms of CN V, VII and X in a pre-metamorphic (stage 4) tadpole, demonstrating Patterns 1 and 2. Examination of action potentials in all three nerve records indicates the recruitment of new motor units during Pattern 2 as described in the spontaneously breathing, decerebrate tadpole (Chapter 4), further substantiating the distinction between the two motor output patterns.

Commonly, Patterns 1 and 2 were not clearly distinguishable from the amplitude of bursts of CN roots. An example of such is illustrated in Fig. 5.3, where differences between the peak amplitude of Patterns 1 and 2 in CN VII

**Table 5.1** Mean latency and time to peak of Pattern 1 and 2 bursts from CN V, VII, X, SN II and Xℓ.

| Nerve | PREMETAMORPHIC STAGES | | | | | POSTMETAMORPHIC STAGES | | | | |
|---|---|---|---|---|---|---|---|---|---|---|
| | n | Pattern 1 | | Pattern 2 | | n | Pattern 1 | | Pattern 2 | |
| | | Latency | Time to Peak | Latency | Time to Peak | | Latency | Time to Peak | Latency | Time to Peak |
| CN V | 5 | -481.4 ±73.7* | 367.7 ±39.9 | 232.3 ±79.5* | 547.00 ±127.3 | 5 | -416.1 ±81.3* | 324.20 ±24.3* | 394.2 ±50.6* | 444.5 ±61.3* |
| CN VII | 10 | 0.0† | 473.1 ±45.5 | 0.0 | 603.90 ±98.1 | 6 | 0† | 628.00 ±41.8 | 0.0 | 755.8 ±36.2 |
| CN X | 6 | 454.3 ±53.8*† | 472.5 ±91.6 | 286.5 ±16.1* | 503.10 ±91.5 | 5 | 388.60 ±19.8*† | 360.40 ±31.6* | 320.7 ±38.7* | 404.1 ±39.1* |
| SN II | 7 | N.A. | N.A. | 324.3 ±59.5* | 378.40 ±88.8 | 5 | 541.90 ±35.4*† | 471.50 ±28.8* | 246.1 ±34.1*† | 549.5 ±30.3* |
| CN Xℓ | 3 | -90.4 ±42.5 | 496.9 ±142.0 | 231.8 ±124.7* | 209.10 ±58.4 | – | – | – | – | – |

Data are shown as mean (msec) ± S.E.M. Onset latency of Pattern 1 and 2 bursts calculated with respect to CN VII. SN II displayed no activity (N.A.) during fictive gill ventilation in premetamorphic tadpoles. Bursting activity of Xℓ was measured in premetamorphic tadpoles only. (* significantly different from CN VII mean values within both developmental group and type of ventilation ($P < 0.05$), † significantly different from CN V mean values within both developmental group and type of ventilation ($P < 0.05$)).

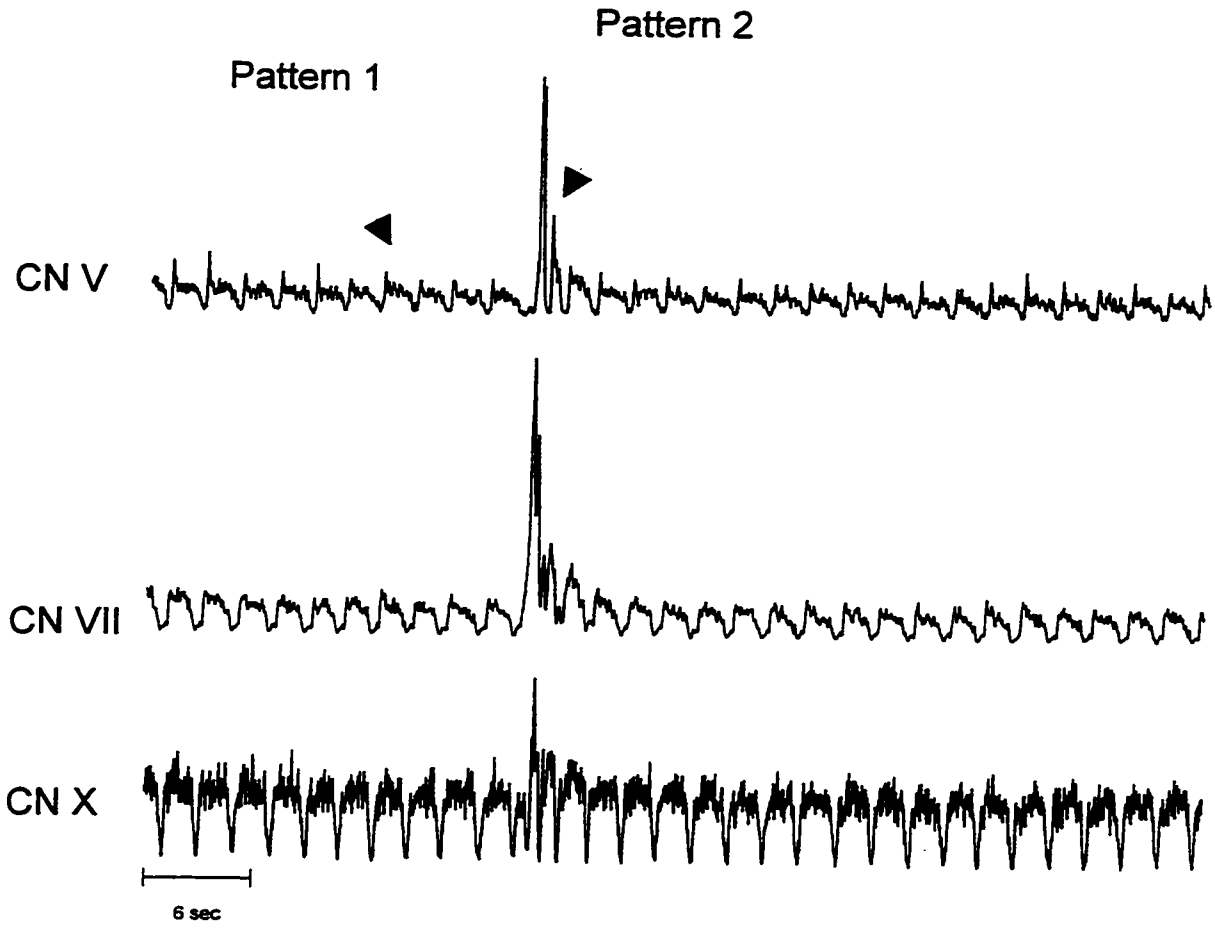


**Figure 5.1** Moving time average of CN V, VII and X showing Patterns 1 and 2 from the isolated brainstem preparation of a stage 11 Rana catesbeiana tadpole superfusate with aCSF having a $P_{CO_2}$ of 45 Torr and pH of 7.4. The height of the respiratory bursts was measured as arbitrary units.

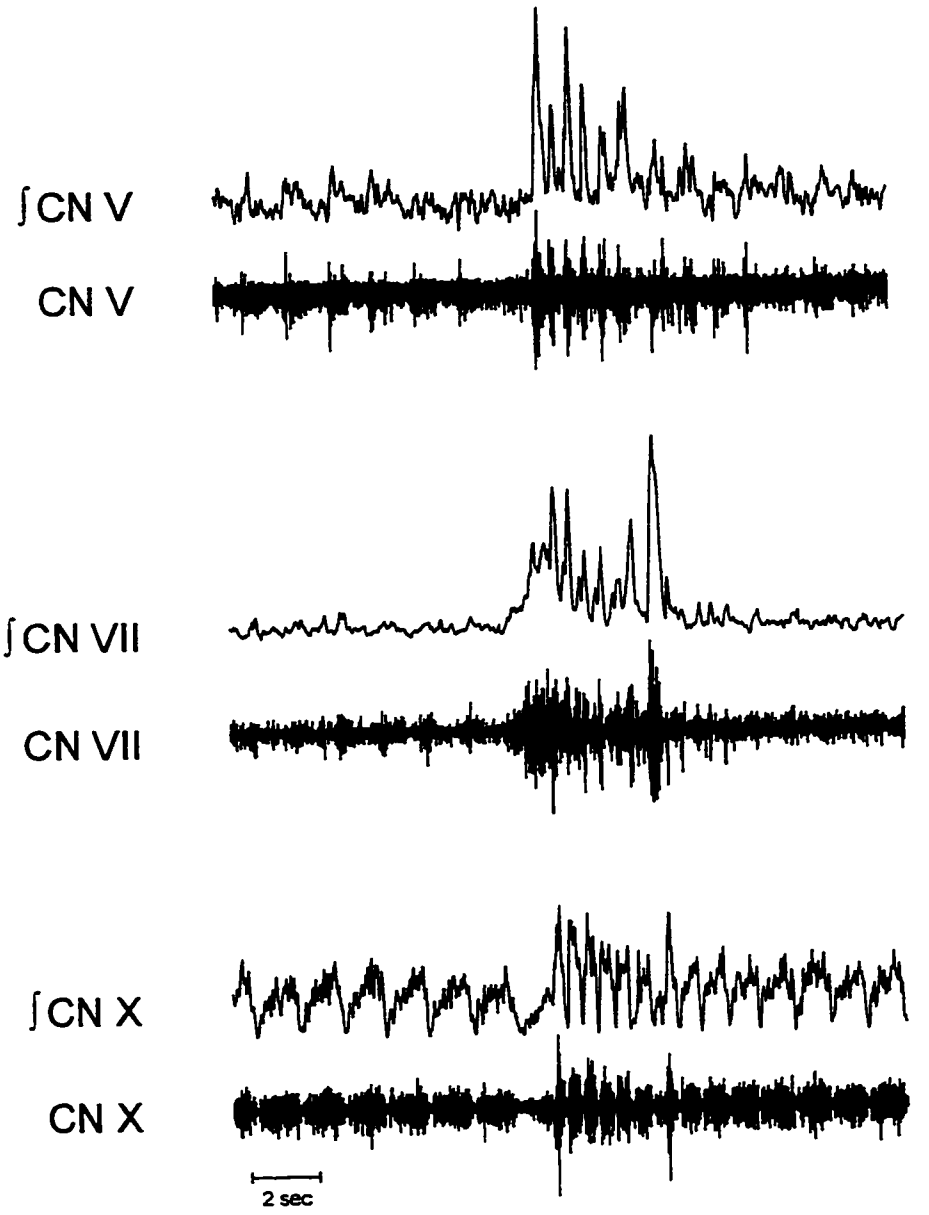


**Figure 5.2** Unprocessed and integrated neurograms of CN V, VII and X recorded from a pre-metamorphic (stage 4) tadpole brainstem preparation superfused with aCSF having a $P_{CO_2}$ of 45 Torr and pH of 7.4. In raw neurograms, the recruitment of new motor units during Pattern 2 is clearly distinguishable. The height of the respiratory bursts was measured using arbitrary units.

were minimal. However, the large amplitude SN II burst during Pattern 2 provided a marker for this pattern and allowed ready distinction between the two fictive ventilatory patterns. Because of the high signal to noise ratio of SN II bursts and their direct correlation to lung ventilation, as reported in Chapter 4, SN II was used as the marker of Pattern 2, whenever possible, in analysis. Similarly, the X$\ell$ neurogram demonstrated pronounced bursting during Pattern 2 but only modest activity during Pattern 1, as shown in Fig. 5.4. This distinctive behavior of SN II and X$\ell$ neurograms during Pattern 2 was consistently observed in all recordings. In 3 of 10 pre-metamorphic animals and 1 of 6 post-metamorphic larvae, adequate recordings were not available from SN II. In these animals, an amplitude criterion was used to identify Pattern 2 bursts in the analysis shown in Table 5.1.

The pattern of respiratory motor output was dependent upon developmental stage. Fig. 5.5 shows typical simultaneous integrated neurograms of CN VII, X and SN II from pre-metamorphic (stage 12) and post-metamorphic (stage 22) tadpole larvae. Pre-metamorphic fictive ventilation was characterized by Pattern 1 bursts observed in CN VII and X, punctuated by sporadic, usually isolated, Pattern 2 bursts appearing in all three nerve recordings. Post-metamorphic fictive ventilation, by contrast, was distinguished by an increase in the frequency of Pattern 2 bursts in CN VII, X and SN II,

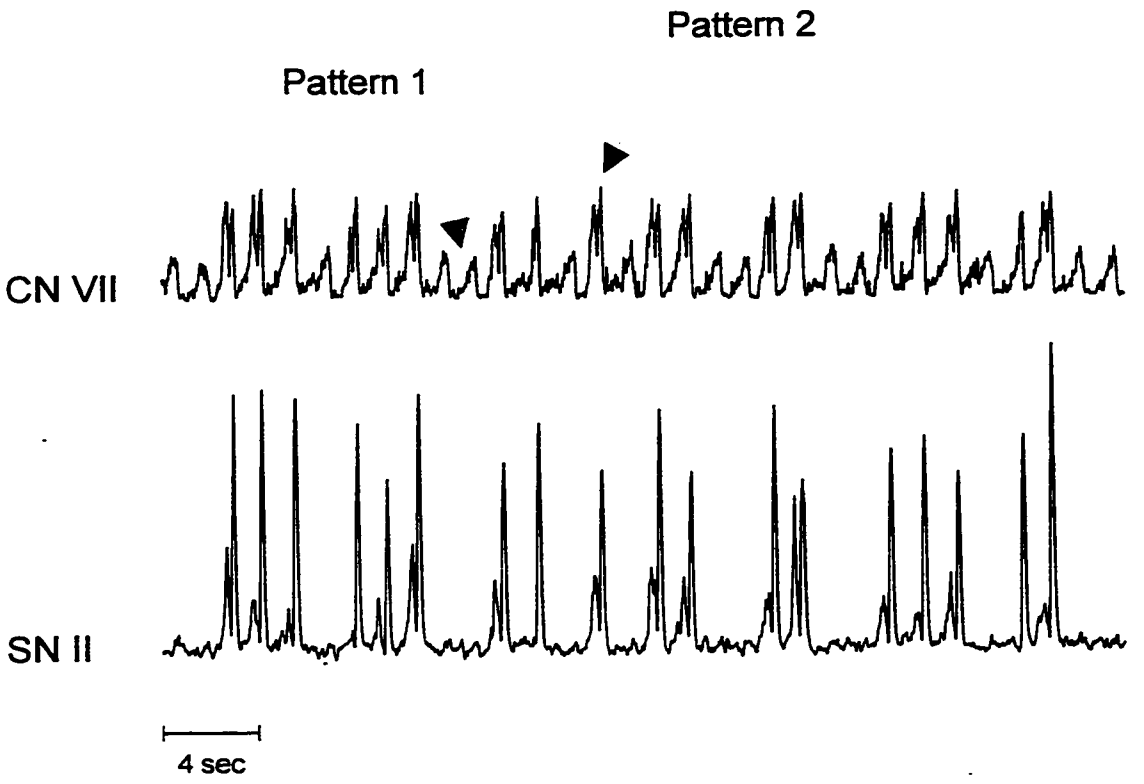


**Figure 5.3** Integrated neurograms of CN VII and SN II showing Patterns 1 and 2 recorded from a post-metamorphic (stage 21) tadpole brainstem preparation superfused with aCSF having a $P_{CO_2}$ of 45 Torr and pH of 7.4. The height of the respiratory bursts was measured using arbitrary units.

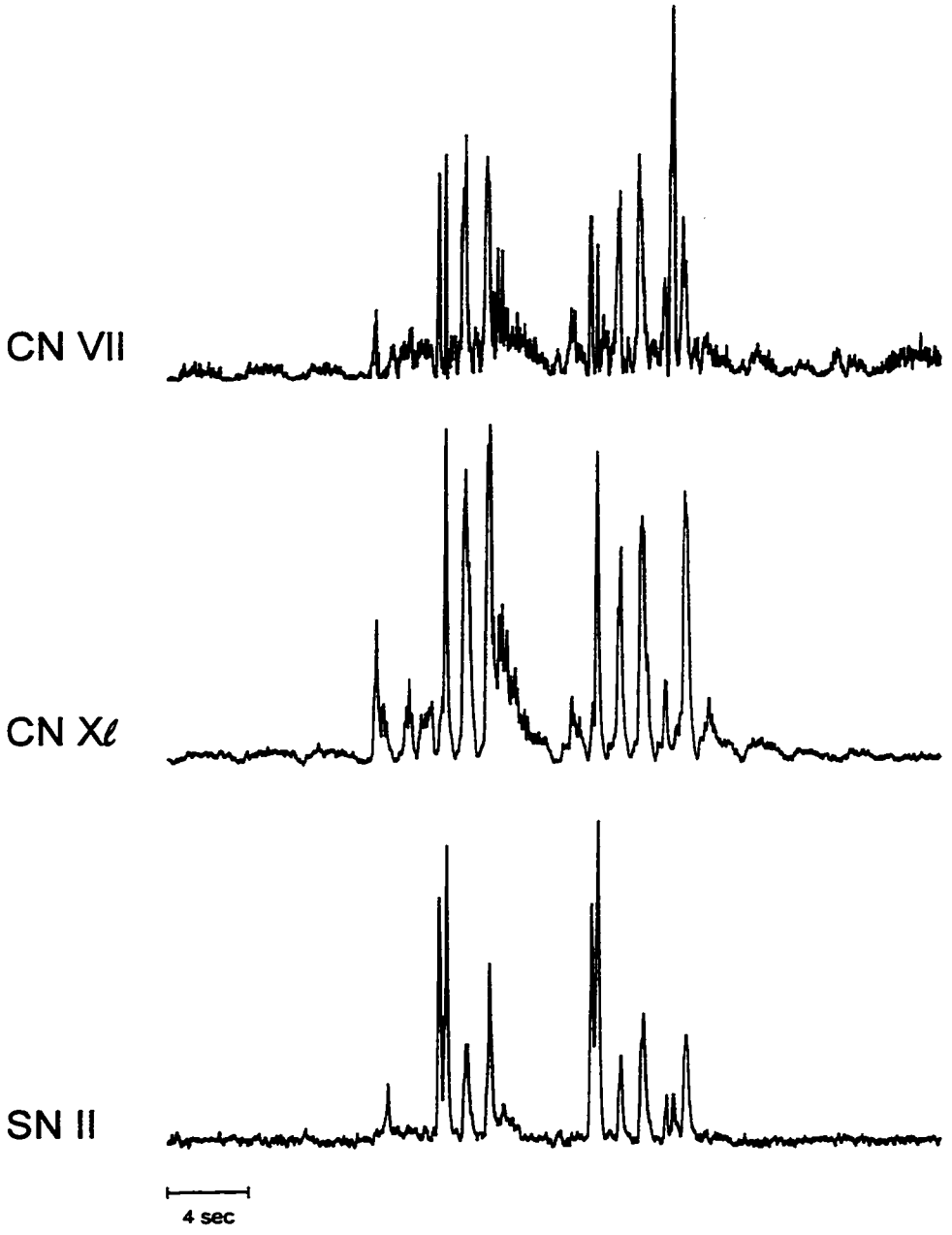


**Figure 5.4** Integrated neurograms of CN VII, Xℓ and SN II showing Patterns 1 and 2 recorded from a pre-metamorphic (stage13) tadpole brainstem preparation superfused with aCSF having a $P_{CO_2}$ of 45 Torr and pH of 7.4. The height of the respiratory bursts was measured using arbitrary units.

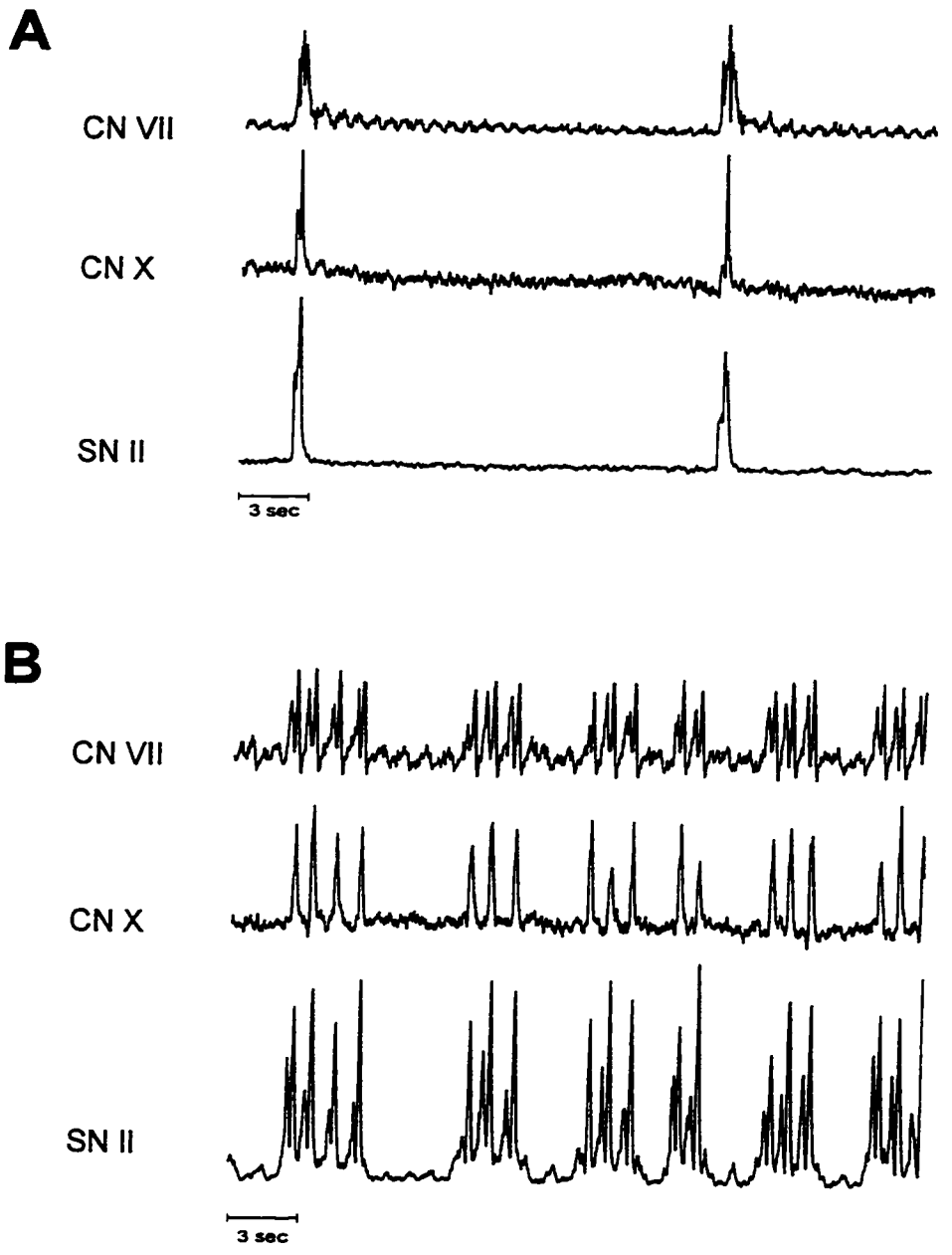


**Figure 5.5** Integrated neurograms of CN VII X and SN II recorded from pre-metamorphic (stage 12) (Panel A) and post-metamorphic (stage 22) (Panel B) tadpole brainstem preparations superfused with aCSF having a $P_{CO_2}$ of 45 Torr and pH of 7.4, showing transition in the pattern of fictive ventilation with development. The height of the respiratory bursts was measured using arbitrary units.

occurring predominantly in clusters, and by the emergence of a Pattern 1 in SN II neurograms.

### 5.3.2 Burst latency and time to peak: pre-metamorphic

Mean time to peak and latency values of Patterns 1 and 2 are displayed in Fig. 5.6 and listed in Table 5.1. The Pattern 1 ventilatory cycle of pre-metamorphic tadpoles was characterized by sequential bursts in CN V, VII and X roots, with activity in X$\ell$ occurring in phase with CN VII (Fig. 5.6A, filled bars). Onset latency of CN V, VII and X differed significantly ($P<0.05$) from each other, as well as the onset of X$\ell$ in comparison to CN V and CN X. By contrast, Pattern 2 cycles in pre-metamorphic tadpoles began with slowly augmenting CN VII discharge that burst synchronously with CN V, X, SN II and X$\ell$ (Fig. 5.6A, open bars). The onset of the Pattern 2 bursts in CN V, X, X$\ell$ and SN II significantly lagged ($P<0.05$) the onset of lung activity in CN VII. Pre-metamorphic tadpoles showed no significant difference ($P>0.05$) in the time to peak of cranial and spinal nerve bursts when comparisons were made within Pattern 1 and 2 ventilatory cycles.

### 5.3.3 Burst latency and time to peak: post-metamorphic

Pattern 1 in post-metamorphic larvae was distinguished by the emergence of SN II discharge that burst following sequential activation of CN V, VII, and X

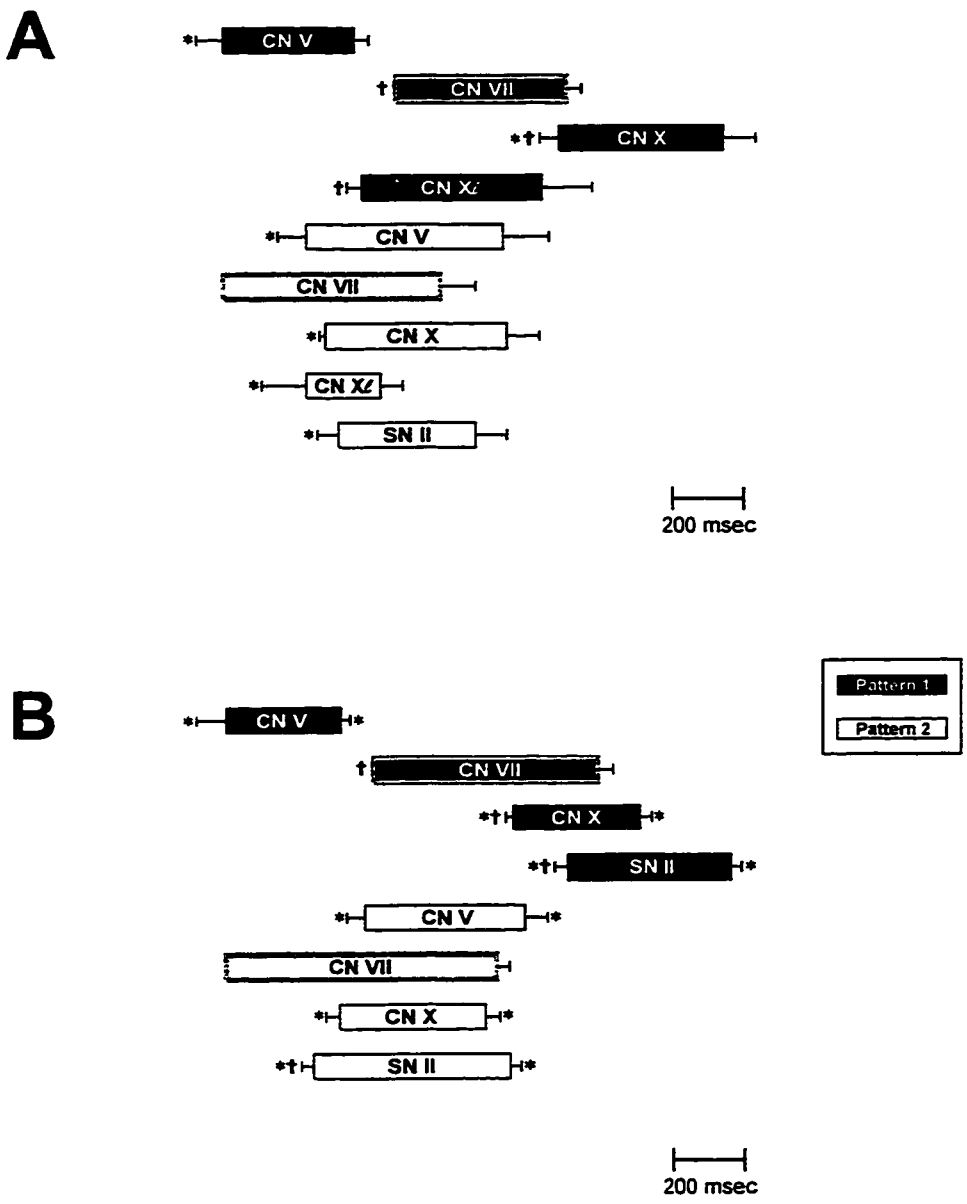


**Figure 5.6** Onset latency and time to peak profiles of Pattern 1 and 2 bursts in pre- (A) and post-metamorphic (B) tadpole larvae. Mean time to peak represented by the relative length of the bars with standard errors plotted on the right. Mean onset burst latency determined with respect to CN VII (outlined by gray) and indicated by the relative horizontal position of bars with standard errors shown on the left. (* significantly different from CN VII mean values within both developmental group and type of ventilation ($P < 0.05$), † significantly different from CN V mean values within both developmental group and type of ventilation ($P < 0.05$)).

(Fig. 5.6B, filled bars). The relative mean onset latency of CN V, VII, X and SN II bursts all differed significantly ($P<0.05$) with respect to each other. The time to peak for CN VII bursts was significantly greater ($P<0.05$) than for CN V, X, and SN II bursts, and the time to peak of SN II burst activity significantly greater ($P<0.05$) than CN V and X. Further, the time to peak of CN VII Pattern 1 bursts of post-metamorphic larvae was significantly greater ($P<0.05$) than that of pre-metamorphic tadpoles.

Like pre-metamorphic patterns, Pattern 2 in post-metamorphic tadpoles was initiated by augmenting activity in CN VII. However, following preliminary CN VII onset, post-metamorphic Pattern 2 cycles were characterized by sequential bursting of SN II, followed by simultaneous onset of CN V and X activities (Fig. 5.6B, open bars). With respect to the mean latency of burst onset, CN VII led CN V, X and SN II by a significant interval ($P<0.05$), and the onset of SN II bursts significantly preceded ($P<0.05$) that for CN V bursts. The time to peak of Pattern 2 in CN VII was significantly longer ($P<0.05$) than that observed in CN V, CN X and SN II of post-metamorphic larvae.

## 5.4 DISCUSSION

Recordings of efferent activity from the roots of CN V, VII, X, SN II, and from the respiratory nerve, X*l*, in the isolated brainstem preparation of larval *Rana catesbeiana* displayed two types of rhythmic bursting: Pattern 1, a high-frequency, low-amplitude oscillation in a rostral-to-caudal sequence; and Pattern 2, a low-frequency, high-amplitude rhythm initiated by CN VII and lacking the rostral-to-caudal progression (Figs 5.1-5.5). Pattern 1 was virtually identical in pre- and post-metamorphic animals with the exception that the latter included an oscillation in SN II. Pattern 2 was similar in pre- and post-metamorphic larvae but exhibited distinct differences in the burst latency between nerves as noted below. These patterns bear a striking resemblance to those recorded from CN V, VII and SN II in the spontaneously breathing decerebrate tadpole, where gill and lung ventilation were mechanically defined (Chapter 4). Because of their close correspondence to the *in vivo* patterns, Pattern 1 was classified as fictive gill ventilation and Pattern 2 as fictive lung ventilation.

Previous studies have used an arbitrary CN amplitude criterion for identifying gill and lung bursts (Galante *et al.*, 1996; Liao *et al.*, 1996; Pack *et al.*, 1993). The use of such criterion has not been validated, and its sensitivity and specificity are suspect. The present study enlarges on the work of Pack *et al.* (1993) by describing the use of high amplitude SN II bursts as a sensitive marker of fictive lung ventilation. The present study also describes correlates of

fictive gill and lung ventilation such as the spatio-temporal characteristics as well as recruitment of X$\ell$ bursts during fictive lung ventilation. From experience, CN burst amplitude is not adequate to identify fictive gill and lung bursts in many cases, but, when used in combination with SN II, any particular burst can be unequivocally identified as Pattern 1 or Pattern 2.

The overall burst frequency and rostral-to-caudal sequence of Pattern 1 observed in the present study closely resembles those reported for gill ventilation in the decerebrate tadpole preparation (Chapter 4). Comparison of Fig. 4.6 from Chapter 4 and Fig. 5.6 from the present chapter show both fictive gill cycles were initiated by bursts in CN V followed by activity in CN VII. Further, the frequency of gill bursts in decerebrate metamorphic tadpoles ($49.3 \pm 6.1$ min$^{-1}$) correlates with gill burst frequency ($43.0 \pm 2.7$ min$^{-1}$) measured in the isolated pre-metamorphic tadpole brainstem preparation of the present study when superfused with aCSF of pH 7.8. This evidence supplements the recruitment and amplitude data discussed above and leads to the conclusion that low-amplitude, high-frequency bursts *in vitro* represent fictive gill ventilation.

In the decerebrate tadpole (Chapter 4), lung ventilation was characterized by synchronous burst activity in CN VII and V, and by the recruitment of SN II. Similarly, the *in vitro* preparation displayed simultaneous bursting in CN V, VII and the appearance of SN II bursts during Pattern 2, suggesting that high-amplitude, low-frequency bursts represent fictive lung activity. Further, fictive

lung ventilation frequency, in the isolated pre-metamorphic brainstem, (0.2 ±0.1 $min^{-1}$, aCSF pH 7.8) matched measurements reported in Chapter 4 for the decerebrate metamorphic tadpole (0.3 ± 0.1 $min^{-1}$). Although the time to peak of gill and lung bursts recorded *in vitro* ranged between 10 to 100% of *in vivo* burst time to peak measurements, correlation between both preparations were close, in view of *in vitro* peripheral deafferentation and gas/pH tissue status (Chapter 3).

Although the spatio-temporal characteristics of Pattern 1 and 2 bursts appear similar in pre- and post-metamorphic larvae, several important distinctions can be made. In pre-metamorphic larvae (< stage 16), respiratory neural output consisted predominantly of gill activity interrupted occasionally by isolated lung bursts. This finding corresponds with respiratory patterns described in intact pre-metamorphic tadpoles (Burggren and Doyle, 1986; Infantino, 1992) and confirms previous results from isolated pre-metamorphic tadpole brainstem preparations (Liao *et al.,* 1996).

Pre-metamorphic gill motor output cycles, *in vitro,* were initiated by CN V activity and followed by sequential bursts of equal time to peak in CN VII and X. This finding agrees with Gradwell's (1972a, b) description of gill irrigation mechanics in pre-metamorphic tadpoles, showing coordination of mouth opener and closer muscles (innervated by CN V), buccal floor elevators and constrictors (innervated by CN VII) and pharyngeal cavity constrictors and dilators

(innervated by CN X). In the isolated pre-metamorphic tadpole brainstem preparation no bursting activity in SN II during fictive gill ventilation was detected. Although Gradwell (1972a, b) attributed the activation of mouth opener and pharyngeal constrictor muscles to spinal nerve motor output, the contribution of these muscles to gill ventilation was minimal based upon electromyographic and pressure recordings. Further, these results agree with Taylor (1985) who reported a similar rostral to caudal bursting sequence in CN output during gill ventilation in studies of dogfish. Finally, rhythmic activity in Xℓ was observed during fictive gill ventilation that burst in phase with CN VII. Xℓ innervates dilator and constrictor muscles of the glottis (Sakakibara, 1984) and has been previously shown to display bursting activity during fictive oropharyngeal ventilation in *in vivo* (Kogo *et al.*, 1994; Kogo and Remmers, 1994) and *in situ* (Kimura *et al.*, 1997) adult bullfrog preparations. Xℓ activity in pre-metamorphic larvae during fictive gill ventilation may represent fictive glottal closure, ensuring that no water enters the lungs before being forced over the gills.

Fictive lung ventilatory cycles in pre-metamorphic tadpoles were led by CN VII, demonstrating biphasic activity, with a preliminary slowly augmenting discharge followed by an abrupt increase in activity synchronous with CN V, X, Xℓ and SN II. Recordings of Xℓ activity, showing a burst of activity coincident with

synchronous lung bursts in CN V, X, and SN II, suggest that laryngeal muscle activity is modulated during gill and lung bursts. This agrees with results reported by Kogo *et al.* (1994), Kogo and Remmers (1994) and Kimura *et al.* (1997) in the adult frog. In both *in vivo* (Kogo *et al.*, 1994; Kogo and Remmers, 1994) and *in situ* (Kimura *et al.*, 1997) preparations, fictive lung ventilation was characterized by synchronous bursting of Xℓ, CN V and the hypoglossal nerve. Further, exclusive lung burst activity in SN II provides a specific and sensitive marker of fictive lung activity in pre-metamorphic tadpole, allowing clear differentiation from gill motor output.

While no study has systematically described the mechanics of lung ventilation in larval amphibians, the basic mechanism, coordinated by buccal and pharyngeal musculature normally used to propel water through the branchial chambers, is thought to resemble lung ventilation described in lung fish (McMahon 1969) and adult frogs (DeJongh & Gans, 1969; MacIntyre & Toews, 1976; West & Jones, 1975). In the adult frog, McLean *et al.* (1995a, b), Kogo *et al.* (1994), Kogo and Remmers (1994) and Kimura *et al.* (1997) recorded efferent activity from specific branches of CN V, X and SN II innervating buccal and laryngeal muscles, and characterized the fictive lung ventilatory cycle by augmenting activity in the sternohyoid branch of SN II followed by synchronous bursting in CN V, X and the main branch of SN II. This sequential pattern resembles that observed in the post-metamorphic tadpole but contrasts with

fictive lung bursts of pre-metamorphic animals, showing simultaneous activation of CN V, X, Xℓ and SN II.

In the pre-metamorphic tadpole brainstem preparation, Galante *et al.* (1996) established that fictive lung bursts, defined without using SN II, persisted in chloride-free superfusate and suggested that post-synaptic inhibition is not essential for fictive lung rhythmogenesis. Accordingly, fictive lung breathing in the pre-metamorphic tadpole may be generated from a primitive lung CPG not requiring post-synaptic inhibition, while fictive lung bursts in the adult frog arise from a CPG containing well developed network properties with inhibitory post-synaptic pathways. Interestingly, Kimura *et al.* (1997) showed, in the *in vitro* adult frog brainstem, the dependency of fictive lung ventilation on post-synaptic inhibition; superfusion of the adult brainstem preparation with aCSF containing the glycine-receptor blocker, strychnine, induced a sudden change in the timing and shape of fictive lung bursts from a sequential, augmenting pattern to a synchronous onset burst with decrementing trajectory.

Post-metamorphic (>stage 20) fictive ventilation featured increased frequency lung burst activity interspersed with rhythmic gill output. While clusters of neural lung activity appeared in pre-metamorphic larvae, they were more frequently observed in post-metamorphic ventilatory patterns (Fig. 5.5B) and may be correlated with episodes of uniform lung ventilations or lung inflation cycles described in intact adult frogs (DeJongh and Gans, 1969; Kogo *et al.*,

1994; Kogo and Remmers, 1994). This pattern agrees with previous descriptions of post-metamorphic tadpole ventilation in the intact, freely swimming animal (Burggren and Doyle, 1986; West and Burggren, 1982; Infantino, 1992).

Fictive gill burst cycles in post-metamorphic larvae were distinguished from pre-metamorphic patterns by sequential, unequal time to peak bursts in CN V, VII, X, and SN II. Differences in the time to peak of cranial and spinal nerve respiratory motor output may be attributed to the shift in respiratory muscle activation with development. In the pre-metamorphic tadpole, gill irrigation is achieved by the coordination of buccal and pharyngeal muscles innervated primarily by CN VII and X (Gradwell, 1972a, b), while in the adult frog, oropharyngeal cavity ventilation is performed by activation of elevator and depressors muscles innervated by branches of CN V and SN II (Sakakibara, 1984a, b). The emergence of gill motor output in SN II of post-metamorphic larvae corresponds with spontaneous oropharyngeal bursting in specific branches of SN II observed in the *in vitro* adult frog brainstem preparation (Kogo *et al.*, 1994; Kogo and Remmers, 1994; McLean *et al.*, 1995a, b), demonstrating that, as metamorphosis proceeds, the pattern of gill motor output takes on adult characteristics.

Like pre-metamorphic patterns, fictive lung ventilatory cycles in post-metamorphic tadpoles were initiated by augmenting CN VII activity that burst simultaneously with CN V and X. By contrast, the onset of post-metamorphic

lung burst activity in SN II preceded burst onset in CN V and X, shifting towards CN VII. This pattern resembles the phase relations of lung burst activity reported by Kogo *et al.* (1994), Kogo and Remmers (1994), McLean *et al.* (1995a, b) and Kimura *et al.* (1997) in the adult frog, demonstrating similarity between post-metamorphic and adult lung ventilatory cycles.

Overall, cranial and spinal nerve activity from the isolated brainstem of larval *Rana catesbeiana* closely resembles the pattern of neural activity during gill and lung ventilation in the spontaneously breathing decerebrate tadpole. Recordings of SN II bursts improve the accuracy of distinguishing fictive lung from gill ventilation, and in many cases, are essential for separating these two types of ventilatory motor outputs. Fictive gill and lung ventilatory patterns in post-metamorphic tadpoles differ in burst onset latency from pre-metamorphic tadpole patterns and resembles fictive oropharyngeal and pulmonary burst cycles in adult frogs. Thus, in addition to establishing an experimental model for investigating the ontogeny of neural-respiratory control *in vitro*, this study demonstrates a shift in the pattern of gill and lung motor output which accompanies the transition from water to air breathing and provides new insight into the origin and development of the amphibian respiratory CPG.

# *CHAPTER SIX*

## *Ontogeny of Central Respiratory Chemoreception in the Isolated Tadpole Brainstem*

## 6.1 INTRODUCTION

The complex development of the structure and function of amphibian respiratory gas-exchange organs necessitates the simultaneous development and coordination of respiratory controllers. In early anuran larvae (stages 5-15), aquatic hypoxia stimulates gill and lung ventilation, hyperoxia induces apnea and hypercapnic challenge evokes no ventilatory response (Burggren and Doyle, 1986; Infantino, 1992). During metamorphosis (stages 16-19), the gill and lung hypoxic responses persist, and a response to changes in $CO_2$ levels appears in both gill and lung ventilation (Infantino, 1992). Postmetamorphic larvae (stages 20-25) display lung, but not gill, responses to hypoxia (Burggren and Doyle,

1986) and hypercapnia (Infantino, 1992). Such responses are apparently mediated reflexly by peripheral mechano- and chemoreceptors intimately associated with lung and gill function (West and Burggren, 1983), and further, by central medullary chemoreceptors in the adult (Smatresk and Smits, 1991; McLean *et al.*, 1995a, b). Collectively, these data indicate that progressive larval development is associated with a shift in the site of ventilatory responses from the gills to the lungs and is accompanied by the emergence of $CO_2$ as a source of respiratory drive.

Despite recent advances, the mechanisms of neurorespiratory control are not fully understood. Although most investigations of respiratory rhythmogenesis have been carried out in isolated mammalian preparations (Feldman and Smith, 1989; Onimaru *et al.*, 1989; Feldman *et al.*, 1990; Issa and Remmers, 1992; Kawai *et al.*, 1996), their neural complexity in addition to their temperature and oxygen demands makes amphibian models of respiratory control an attractive alternative. By elucidating the neural mechanisms of central chemoreception and respiratory rhythm generation in the amphibian, it may be possible to gain new insights in to the origin, maturation and properties of a respiratory rhythm generator. Recent studies of adult frogs have explored the central neuronal substrate of respiratory rhythm generation by relating global changes in the execution of respiratory motor acts to brainstem neural phenomena (Kogo *et al.*, 1994; Kogo and Remmers, 1994; McLean *et al.*, 1995a,

b; Kimura *et al.,* 1997). While such studies have begun to define the basic mechanisms of central chemoreception and respiratory rhythm generation, they have not shed light on the development of such processes as the animals undergo transformation from aquatic breathing using their gills to air breathing, using pulmonary gas exchange. No systematic study has yet described the developmental transitions of central respiratory chemoreception and rhythm generation in amphibians.

The aim of the present investigation was to examine the ontogeny of central respiratory chemoreception in tadpoles during the transition from gill to lung ventilation. In order to compare central mechanisms controlling breathing during successive stages of development, fictive gill and lung ventilation was investigated in an isolated *in vitro* brainstem preparation from *Rana catesbeiana* tadpoles. Studies outlined in Chapters 2, 3 and 4 have established that the isolated brainstem is well-oxygenated, moderately hypercapnic and retains the necessary neural circuitry to generate the complex rhythmic neural output responsible for gill and lung ventilation. These results were pivotal in enabling the further investigation of central respiratory chemoreception during ontogeny. In light of studies in the intact tadpole (Infantino, 1992), showing progressive ventilatory responsiveness to hypercapnia, and in the *in vitro* tadpole brainstem (Chapter 5), establishing a developmental shift in respiratory motor output from

gill to lung ventilation, I hypothesize that the isolated tadpole brainstem will transfer central chemoreceptive influence from gill to lung regulation.

## 6.2 MATERIALS AND METHODS

### 6.2.1 Animals and surgical preparation

Experiments were performed on 30 *Rana catesbeiana* male or female tadpoles, 8-13 grams body weight. Animals were obtained and cared for as described in Chapter 2. Tadpoles were assigned to four groups according to the staging of Taylor and Köllros (1946) as follows: stages 3-9, (n=8); stages 10-14, (n=9); stages 15-19, (n=7); and stages 20-25, (n=6). The brainstem was removed from the cranium, transected, and superfused within the recording chamber as previously described in Chapter 2.

### 6.2.1 Recording chamber and neural recordings

After the brainstem was transferred to a superfusion chamber, fictive gill and lung ventilation were recorded from the roots of CN V, VII and X using suction electrodes according to the protocol detailed in Chapter 2. SN II recordings were not obtained in the present study. As a result, distinction between gill and lung activity was made using CN amplitude and frequency criteria.

### 6.2.3 Experimental protocol

The central respiratory chemoresponsiveness of each of the four groups was evaluated by varying the pH/$P_{CO_2}$ of the superfusate. The experimental protocol began after the brainstem had been superfused in the recording chamber for at least 60 min at pH 7.8 and when recordings of nerve activities exhibited rhythmic bursting. Stable nerve activities were recorded for 10 min during randomly administered test solutions of pH 7.4, 7.6, 8.0 and 8.4 interspersed with 10 min baseline recordings at pH 7.8. After each 10 min recording, a 5 min equilibration period ensued to allow equalization of tonometer and recording chamber pH and stabilization of the brainstem response to the new target pH.

### 6.2.4 Data analysis

For each of the four developmental groups, the effects of superfusate pH on gill and lung ventilatory motor output from CN V, VII and X were analyzed. The mean burst frequency and peak integrated amplitude for gills and lungs were measured for each 10 min recording period (pH 7.4, 7.6, 7.8, 8.0 and 8.4) with baseline recordings (pH 7.8) further averaged within each animal. Baseline recordings were made between each test period in order to quantify any drift that may have occurred during the course of the experiment. Mean values of fictive gill burst amplitude, frequency and respiratory output (frequency x

amplitude) at pH 7.4, 7.6, 7.8 and 8.4 were then expressed as the % change from pH 8.0 and group means ± S.E.M. were calculated. A reference value of pH 8.0 was chosen since preliminary inspection of the data revealed linear increases in frequency, amplitude and respiratory output with reductions in pH from this point. The mean gill and lung frequency motor output values for each animal were used to calculate group means ± S.E.M. for each pH level. A two-way analysis of variance (ANOVA) was used to test for the significance of pH effects at different developmental stages. A Tukey test of pairwise multiple comparisons was utilized to test significant differences between individuals within treatment groups when statistically significant ($P<0.05$) interaction between pH and developmental stage occurred. The significance of pH effects within each developmental group was examined using a one-way ANOVA with repeated measures, with the criterion of statistical significance at $P<0.05$. When ANOVA revealed significant treatment effects, differences between individuals means within a developmental group were assessed for significance using the Dunnett's method of multiple comparisons.

## 6.3 RESULTS

### 6.3.1 Patterns of respiratory motor output

All animals (n=30) displayed rhythmic bursts of action potentials in CN V, VII and X when superfused with aCSF having a $P_{CO_2}$ of 17 Torr and a pH of 7.8. While simultaneous recordings of all nerves were not successful in all animals, rhythmic bursts were observed in one or more of the nerves. All four developmental groups displayed two distinct patterns of cranial nerve activity. As shown in Fig. 6.1, typical integrated neurograms from CN VII and CN X of a stage 16 tadpole, oscillating slightly out of phase, demonstrate a high-frequency, low-amplitude bursting rhythm punctuated by low-frequency, high-amplitude bursts (at pH 7.37). Because significant correlation was demonstrated between neural activity and respiratory mechanical events of the spontaneously breathing decerebrate tadpole (Chapter 4) and spontaneous bursting activity of the *in vitro* brainstem (Chapter 5), high-frequency, low-amplitude bursts were classified as fictive gill ventilation and low-frequency, high-amplitude bursts as fictive lung ventilation

The prevalence of fictive gill and lung respiratory activity under baseline conditions (pH 7.8) was contingent upon the developmental stage of the tadpole. As shown in Table 6.1, stages 3-9, 10-14 and 15-19 displayed rhythmic neural

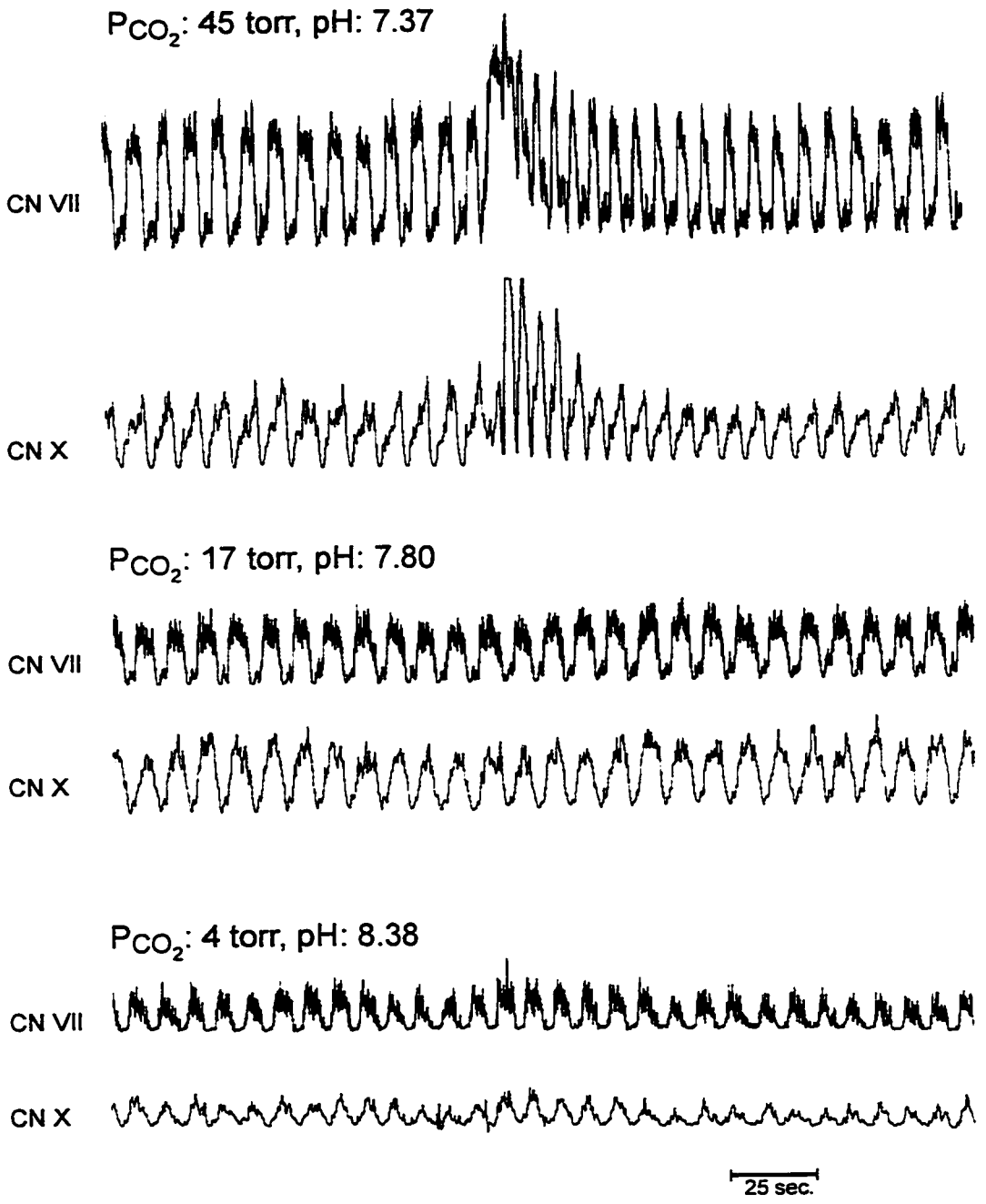


**Figure 6.1** Moving time average of CN VII and X gill and lung ventilatory motor output from a stage 16 Rana catesbeiana tadpole in response to changes in superfusate pH and $P_{CO_2}$.

**Table 6.1** Gill and lung ventilatory motor output frequency from CN VII and X in response to superfusate pH as a function of development.

| pH | Developmental Stage | | | | | | | |
|---|---|---|---|---|---|---|---|---|
| | 3-9 | 10-14 | 15-19 | 20-25 | 3-9 | 10-14 | 15-19 | 20-25 |
| | Fictive Gill Frequency ($min^{-1}$) | | | | Fictive Lung Frequency ($min^{-1}$) | | | |
| 8.4 | 45.15 ± 3.14 | 30.31 ± 5.47 | 37.64 ± 3.92 | 41.85 ± 10.65 | 0.20 ± 0.09 | 0.18 ± 0.07 | 0.03 ± 0.03 | 0.03 ± 0.03 |
| 8.0 | 43.04 ± 3.37 | 29.04 ± 6.32 | 34.67 ± 2.63 | 38.40 ± 10.92 | 0.30 ± 0.14 | 0.16 ± 0.06 | 0.06 ± 0.04 | 0.03 ± 0.03 |
| 7.8 | 46.50 ± 3.29 | 33.94 ± 6.21 | 42.97 ± 2.74 | 38.46 ± 9.79 | 0.31 ± 0.11 | 0.17 ± 0.06 | 0.10 ± 0.06 | 1.69 ± 1.17 |
| 7.6 | 48.68 ± 3.54 | 39.84 ± 7.59* | 46.80 ± 3.60* | 42.95 ± 9.04 | 0.28 ± 0.13 | 0.18 ± 0.08 | 0.31 ± 0.22 | 5.13 ± 2.79*† |
| 7.4 | 45.21 ± 4.58 | 39.44 ± 8.00* | 45.29 ± 3.90* | 36.36 ± 7.69 | 0.38 ± 0.14 | 0.69 ± 0.23 | 0.71 ± 0.17* | 8.23 ± 2.92*† |

Data are shown as mean ± S.E.M., n = 6-9 (* significantly different from values at pH 8.0 ($P < 0.05$), † significantly different from all other stages at the same pH level ($P < 0.05$)).

gill bursts with infrequent lung bursts occurring at irregular intervals. However, neural lung respiratory activity increased significantly ($P<0.05$) in tadpoles of stage 20-25 at lower pH values. Fictive lung ventilation commonly occurred in stages 3-9 and 10-14 as isolated bursts, whereas in older larvae (stages 15-19, 20-25) clusters of lung bursts appeared.

### 6.3.2 Effects of pH/$P_{CO_2}$ on fictive gill ventilation

The response of fictive gill ventilation to increases in $CO_2$ varied with developmental stage. Figs 6.2, 6.3 and 6.4 plot, respectively, the amplitude, frequency and respiratory output (amplitude x frequency) of CN VII and X gill ventilatory activity as a function of superfusate pH in four developmental groups. In early developmental stages (3-9) (n=8), fictive gill ventilation showed no response in any output variable to reductions in pH when compared with pH 8.0 with one exception: fictive gill amplitude in CN X increased slightly, but significantly ($P<0.05$), at pH 7.6 and 7.4 (Fig. 6.2). In contrast, fictive gill ventilation in larvae of stage 10-14 (n=9) responded significantly in amplitude, frequency and respiratory output to hypercapnic superfusion, as illustrated in Figs 6.2, 6.3 and 6.4. All these output variables in CN VII and X increased significantly ($P<0.05$) with reductions in pH to 7.6 and 7.4. Furthermore, CN X gill amplitude and respiratory output in stage 10-14 tadpoles increased significantly ($P<0.05$) at pH 7.4 and 7.6 compared with all other stages.

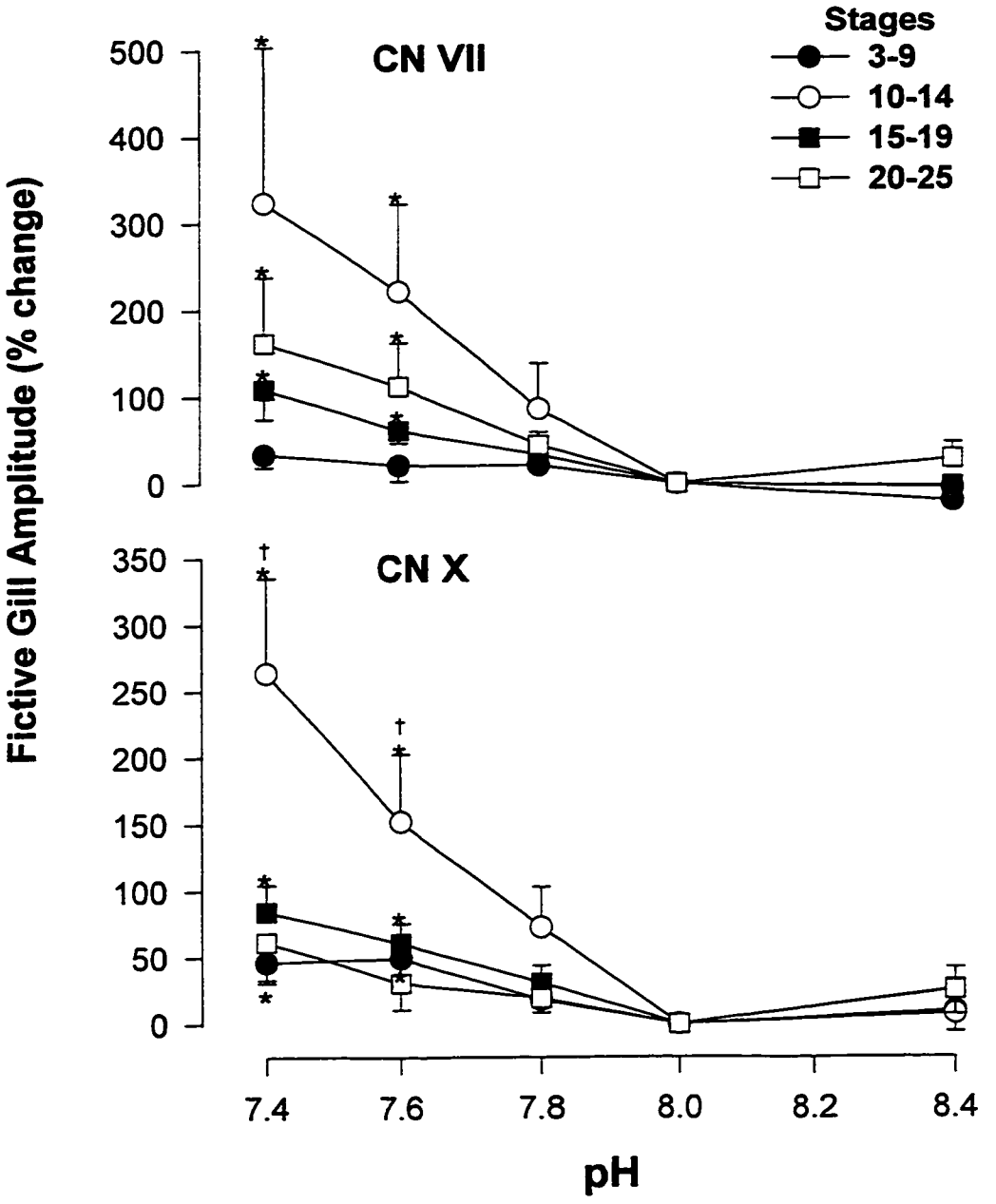


**Figure 6.2** Fictive gill amplitude of CN VII and X in response to changes in superfusate pH as a function of developmental stage. Values are expressed as mean relative change (%) from the value at pH 8.0. Data are shown as mean ± S.E.M., n = 6-9 (* significantly different from values at pH 8.0 ($P < 0.05$), † significantly different from all other stages at the same pH level ($P < 0.05$)).

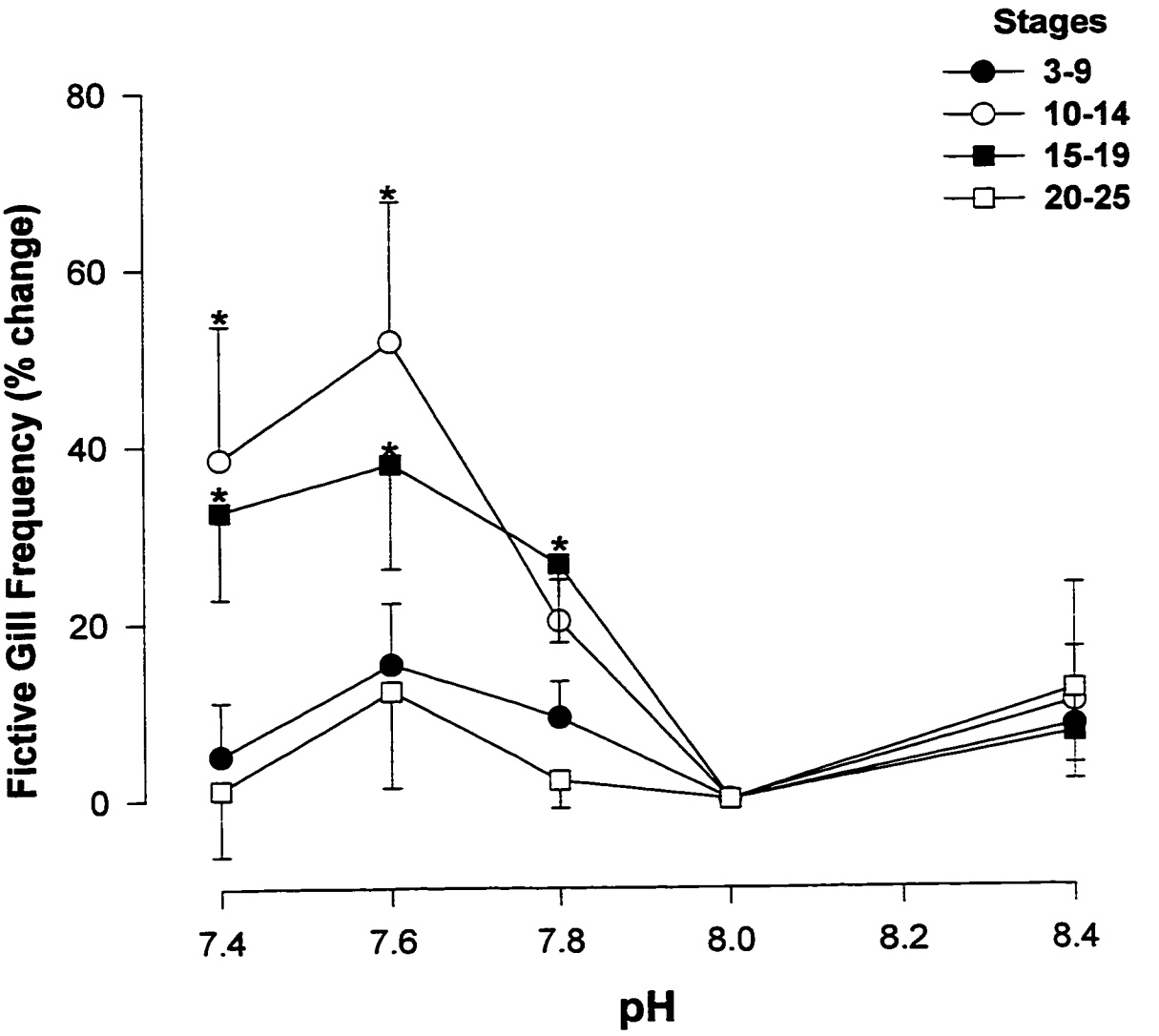


**Figure 6.3** Fictive gill frequency of both CN VII and X in response to changes in superfusate pH as a function of developmental stage. Values are expressed as mean relative change (%) from the value at pH 8.0. Data are shown as mean ± S.E.M., n = 6-9 (* significantly different from values at pH 8.0 ($P<0.05$)).

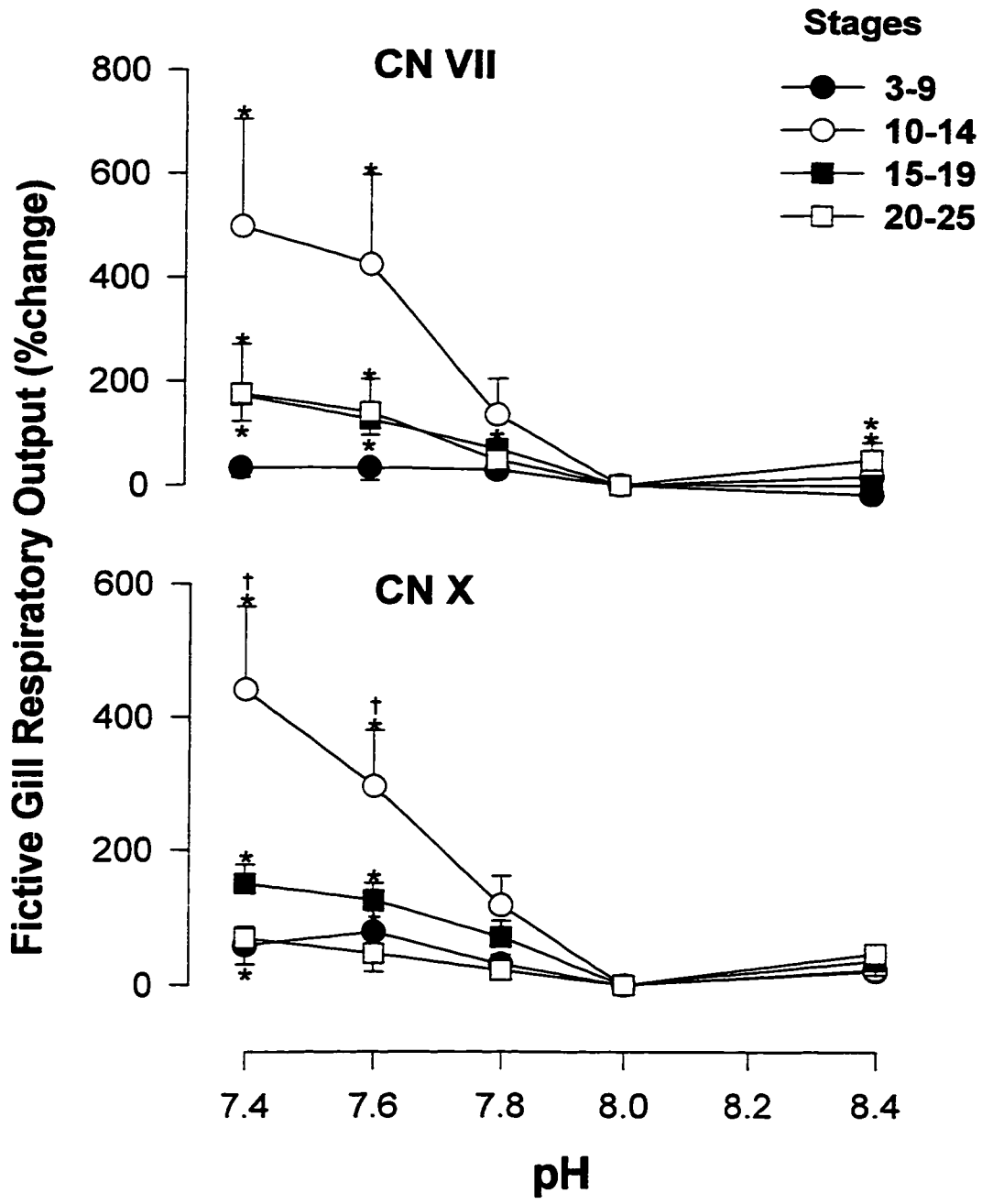


**Figure 6.4** Fictive gill respiratory output of CN VII and X showing the combined response of frequency and amplitude to changes in superfusate pH. Values are expressed as mean relative change (%) from the value at pH 8.0. Data are shown as mean ± S.E.M., n = 6-9 (* significantly different from values at pH 8.0 ($P < 0.05$), † significantly different from all other stages at the same pH level ($P < 0.05$)).

Fictive gill ventilation in metamorphic larvae, stages 15-19 (n=7), also responded significantly to hypercapnic stimulation. As illustrated in Fig. 6.1, reduction of pH from 7.8 ($P_{CO_2}$= 17 Torr) to 7.37 ($P_{CO_2}$= 45 Torr) increased the amplitude of fictive gill respiration and induced the appearance of fictive lung bursting, while increasing pH to 8.38 ($P_{CO_2}$= 4 Torr) decreased gill amplitude. Figs 6.2 and 6.3 demonstrate significant increases ($P<0.05$) in gill burst amplitude and frequency in both CN VII and X when pH was reduced to pH 7.6 and 7.4 and compared with pH 8.0. At pH 7.8, significant increases ($P<0.05$) in both CN VII and X were observed in fictive gill ventilation frequency only (Fig. 6.3). Correspondingly, fictive gill respiratory output increased significantly ($P<0.05$) at pH 7.8, 7.6 and 7.4 in CN VII and at pH 7.6 and 7.4 in CN X. Despite this stimulatory effect, however, fictive gill amplitude and respiratory output from CN X were significantly smaller ($P<0.05$) than that those observed in stages 10-14 at pH 7.4 and 7.6.

Stage 20-25 tadpole larvae (n=6) showed no fictive gill ventilatory response of any output variable to central hypercapnic challenge in CN X (Figs 6.2, 6.3, 6.4). By contrast, CN VII demonstrated small, but significant, increases ($P<0.05$) in amplitude and respiratory output at pH 7.6 and 7.4 compared with pH 8.0. The values for gill burst frequency of CN VII and X, listed in Table 6.1, further reflected developmental shifts in chemosensitivity, increasing significantly

($P$<0.05) at pH 7.6 and 7.4 in stages 10-14 and 15-19 as compared with values at pH 8.0.

### 6.3.3 Effects of pH/$P_{CO_2}$ on fictive lung ventilation

Fictive lung respiration, like fictive gill ventilation, exhibited a developmentally dependent response to decreases in superfusate pH. Fig. 6.5 and Table 6.1 illustrate the effect of pH variation (7.4-8.4) on the frequency of fictive lung ventilation in all four developmental stage groupings. Fictive lung frequency in stage 3-9 and 10-14 tadpoles was insensitive ($P$<0.05) to hypercapnia, while fictive lung burst frequency in stages 15-19 demonstrated a significant increase ($P$<0.05) at pH 7.4. Fictive lung frequency in stages 20-25 responded significantly ($P$<0.05) to pH reduction at pH 7.6 and 7.4 and was significantly ($P$<0.05) greater than fictive lung burst frequency in all other stages at these pH levels. In contrast, fictive lung amplitude remained relatively constant during development and appeared insensitive to pH reduction.

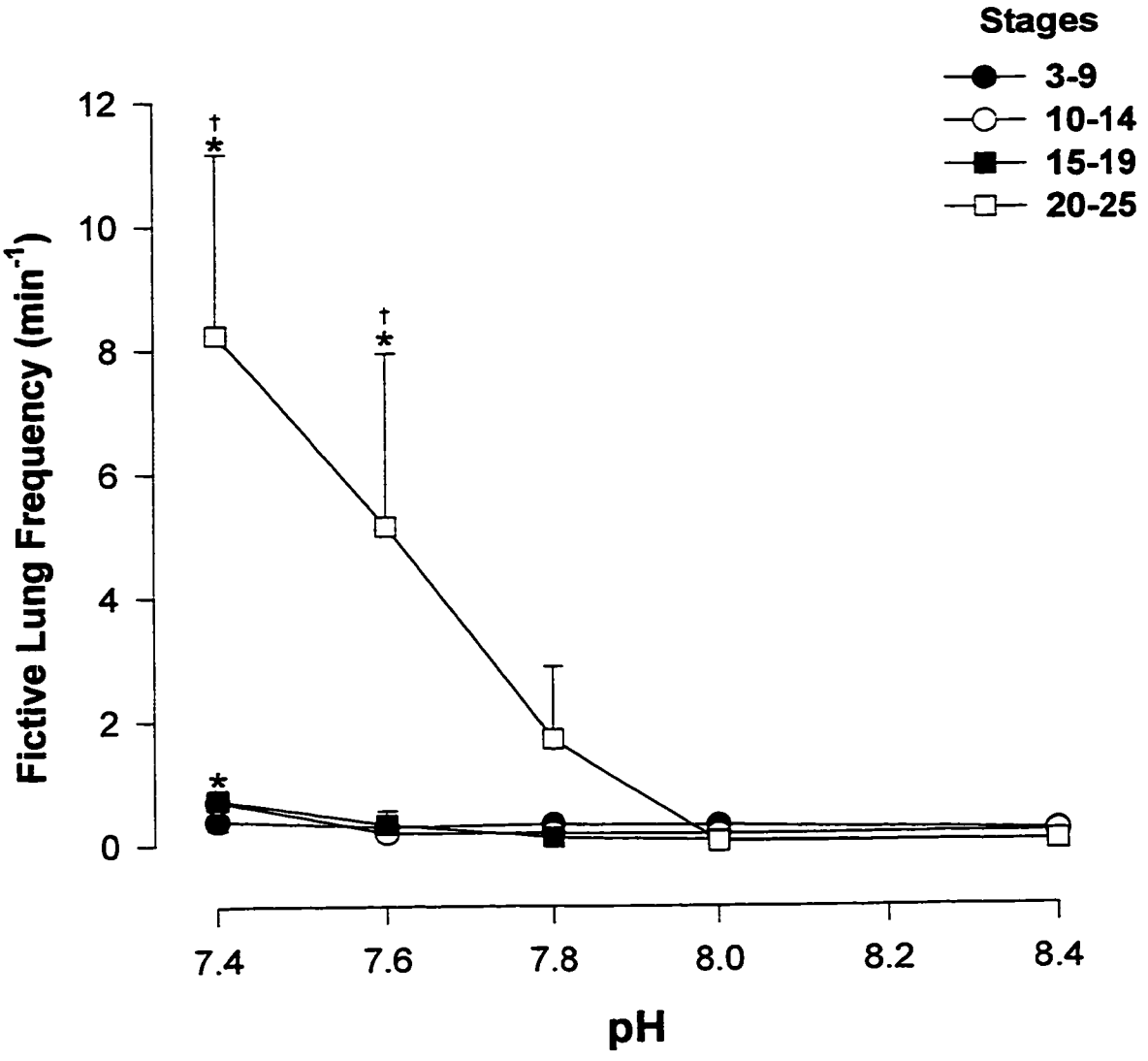


**Figure 6.5** Fictive lung frequency of CN VII and X in response to changes in superfusate pH as a function of developmental stage. Data are shown as mean ± S.E.M., n = 6-9 (* significantly different from values at pH 8.0 ($P < 0.05$), † significantly different from all other stages at the same pH level ($P < 0.05$)).

## 6.4 DISCUSSION

In the phylogenetic progression from fish to birds and mammals, central respiratory chemosensitivity has been clearly established in amphibians (for reviews, see Smatresk, 1990; Milsom, 1995; Shelton *et al.*, 1986). Comparative studies have documented the regulation of lung ventilation by central $CO_2$ chemoreceptor stimulation in adult frogs and toads (Branco *et al.*, 1992; Smatresk and Smits, 1991; Kogo *et al.*, 1994; Kogo and Remmers, 1994; McLean *et al.*, 1995a, b). The influence of central chemoreceptive function on gill ventilation, however, is largely unknown. The present investigation has demonstrated the existence of central respiratory chemoreception in the *in vitro* brainstem of anuran tadpoles that exert a developmentally dependent influence on fictive gill and lung ventilation. These results show that hypercapnia has a significant influence on fictive gill ventilation in tadpoles of intermediate developmental stages (10-14 and 15-19) and that significant hypercapnic stimulation of fictive lung ventilation occurs in older animals (stages 15-19 and 20-25).

### 6.4.1 Bursting Patterns

The overall pattern and burst frequency of fictive gill and lung ventilation observed in the present study closely mirrored previous results from *in vitro* brainstem preparations of pre- and post-metamorphic tadpole reported in

Chapter 5, indicating a development shift in the generation of respiratory motor output from the gills to the lung. In both *in vitro* studies, respiratory neural output from pre-metamorphic larvae (< stage 16) consisted predominantly of gill activity interrupted occasionally by isolated lung bursts. In the present study, the frequency of gill bursts in pre-metamorphic larvae (stage 3-9: 46.5±3.29 $min^{-1}$, stage 10-14: 33.94±6.21 $min^{-1}$; pH 7.8) compared with gill burst frequency previously measured in Chapter 5 (stages 4-14: 43.0±2.7 $min^{-1}$; pH 7.8), as did lung burst frequency (present study: stage 3-9, 0.31±0.11 $min^{-1}$, stage 10-14, 0.17±0.06 $min^{-1}$; previous study: stage 4-14, 0.20±0.10 $min^{-1}$; pH 7.8). Similarly, post-metamorphic patterns of respiratory motor output in the present study matched previous *in vitro* descriptions reported in Chapter 5 of similar stage animals as a prevalence of lung burst activity interspersed with rhythmic gill output. Further, post-metamorphic lung burst frequency in the present study (stage 20-25: 1.69±1.17 $min^{-1}$; pH 7.8) corresponded with values previously described in Chapter 5 from similar stage tadpoles (stage 20-22: 2.14±1.38 $min^{-1}$; pH 7.8).

### 6.4.2 Regulation of fictive gill ventilation

For the brainstems of immature larvae (stages 3-9), reductions in the pH of the superfusate had no general effect on gill ventilatory motor output; fictive gill burst frequency and amplitude of CN VII were statistically unresponsive to

hypercapnia. Gill amplitude recorded from CN X, however, showed small but significant increases to a fall in superfusate pH (7.6, 7.4). This finding agrees with the results of Infantino (1990, 1992), who showed that hypercapnia had no effect on gill frequency in freely swimming, stage 4-7 tadpoles. Thus, it appears that central or peripheral respiratory chemoreceptors in stages 3-9 play little role in driving gill ventilation output. This finding may be attributed to a sparse distribution of medullary respiratory chemoreceptors in early larvae, thereby decreasing the overall drive to respiratory pattern generators or reducing chemoreceptive synaptic connectivities. Despite the apparent lack of central or peripheral $CO_2$ regulation of gill ventilation in stage 3-9 larvae, previous studies by Burggren and Doyle (1986) and Infantino (1992) on intact larvae indicate strong hypoxic gill ventilatory drive during this period as well as apnea following hyperoxic exposure.

In pre-metamorphic larvae (stages 10-14), gill ventilation displayed a vigorous response to central hypercapnic stimulation. Gill frequency and amplitude increased significantly when the brainstem preparation was exposed to a superfusate pH of 7.6 and 7.4. Furthermore, gill amplitude and respiratory output at pH 7.4 and 7.6 in CN X was significantly greater than at all other stages. Ontogenetic studies of intact stage 9-14 tadpoles by Infantino (1992) showed that mild hypercapnia ($P_{CO_2}$= 12 Torr) produced no significant difference in the frequency of gill ventilation when compared with baseline $P_{CO_2}$ levels (< 2

Torr) before metamorphosis (stage 16) while the response of gill frequency to severe hypoxia ($P_{O_2}$ = 30 Torr) was maximal (Burggren and Doyle, 1986). However, the results of the present study agree with those from Infantino (1992) when ventilatory responses to equivalent hypercapnic challenge are compared; the *in vitro* preparation also showed no significant difference in fictive gill frequency when exposed to aCSF at a $P_{CO_2}$ of 17 Torr. During pre-metamorphic development, the gills are the second major site of oxygen uptake and $CO_2$ elimination (approximately 40%) next to the skin (Burggren and West, 1982), so it is not surprising that gill motor output, which ultimately produces ventilation of the gills, can be regulated in response to central chemoreceptor stimulation.

By stage 16 of development, tadpoles begin to undergo metamorphosis, reaching climax by stage 18-19. During this time, the gills, lung and skin all contribute to $O_2$ and $CO_2$ exchange and the pattern of ventilation shifts from gills to lungs as gill regression begins and pulmonary respiratory efforts become regular (Burggren and West, 1982). In metamorphic stages 15-19, significant increases in the amplitude and frequency of gill ventilation were observed. This response contrasts with the results generated in previous studies by Infantino (1992). Using intact metamorphic tadpoles, Infantino (1992) demonstrated that aquatic hypercapnia produced significant depression of gill ventilation frequency, concluding that such a response must serve to reduce the uptake of $CO_2$ across the gills. These discrepancies may reflect differences in the level of hypercapnic

stimulation, differences between intact and *in vitro* preparations or differences between central and peripheral $CO_2$ chemoreceptor influence on gill ventilation.

Although a significant hypercapnic influence on gill ventilation was observed in stage 15-19 brainstem preparations in the present study, gill amplitude and respiratory output in CN X responded significantly less than that observed in pre-metamorphic animals (stages 10-14). These results suggest a progressive decrease in central hypercapnic chemoreceptive regulation of gill ventilation prior to reabsorption of the gills. Similarly, Burggren and Doyle (1986) found gill frequency unresponsive to hypoxia after stage 16, indicating a reduction in hypoxic reflex regulation controlling gill ventilation as branchial regression was initiated. Together, these studies imply that as metamorphosis proceeds, reflexes regulating $CO_2$ and $O_2$ levels are shifted away from buccal pattern generators.

In stage 20-25 post-metamorphic tadpoles, fictive gill ventilatory output was insensitive to central hypercapnic challenge with one exception: the amplitude of gill motor output in CN VII showed small, significant increases during reductions in the pH of the superfusate. After stage 20, rapid regression of the internal gill and operculum occurs with complete regression by stage 24 (Taylor and Köllros, 1946; Atkinson and Just, 1975). Thus, the overall reductions in frequency and amplitude observed in the present study are not surprising and

agree with studies in intact tadpoles (Infantino, 1992), which concluded that post-metamorphic gill ventilatory reflexes are insignificant.

Although the response of gill ventilation to $CO_2$ has been previously described in water- and air-breathing fishes and larval amphibians, the role of central chemoreceptors has not been defined (Shelton *et al.*, 1986; Milsom, 1995). Gill ventilation of intact water- and air-breathing fishes has been shown to respond modestly to aquatic hypercapnia, although the specific site of action has not been identified (Johansen, 1970; Randall and Jones, 1973; Janssen and Randall 1975; Eddy, 1976; Hargis, 1976; Dively *et al.*, 1977; Cameron, 1978; Thomas and LeRuz, 1982; Thomas, 1983; Heisler *et al.*, 1988; Wood *et al.*, 1990; Aoto *et al.*, 1990; Kinkead and Perry, 1991). Acidic superfusion of the isolated brains of carp, lamprey and lungfish has also been shown to produce no significant change in gill ventilation (Hughes and Shelton, 1962; Rovainen, 1977; Burleson *et al.*, 1996). In an abbreviated report, Walker *et al.* (1990) showed in an *in vitro* tadpole brainstem-spinal cord preparation, displaying fictive gill and lung ventilation that gill frequency was insensitive to hypercapnic superfusion (pH 7.2-7.8), suggesting a lack of central chemoreceptors. Thus, the present study provides the first unequivocal demonstration of central $CO_2$ chemoreception influencing gill ventilation in fish or larval amphibians.

### 6.4.3 Regulation of fictive lung ventilation

Despite the presence of lungs by stage 3 of development (Atkinson and Just, 1975; Burggren and Mwalukoma, 1983; Burggren 1989), pulmonary ventilation in normoxic water at 25°C occurs irregularly until metamorphic stages are reached (Burggren, 1984; Helff, 1932; Infantino, 1992; Burggren and Doyle, 1986; Burggren and Infantino, 1994). Previous studies by Helff (1932) indicated that the lungs are not essential prior to metamorphosis in *Rana pipiens* and *Rana catesbeiana* (Just *et al.*, 1973). Significant stimulation of fictive lung frequency in the *in vitro* tadpole brainstem preparation by exposure to strong central hypercapnic challenge (pH 7.4) did not occur until developmental stages 15-19. These results contrast directly with those documented by Walker *et al.* (1990), who found, in an isolated metamorphic tadpole brainstem-spinal cord preparation, complete insensitivity of fictive lung ventilation to central hypercapnic stimulation. Since the tadpole developmental stage and $P_{CO_2}$ level were not reported in this study, the source of the discrepancy is not apparent. These results coincide with studies by Infantino (1992) that showed the frequency of lung ventilation in intact tadpoles was significantly increased by increases in $CO_2$ levels during metamorphosis. An investigation of amphibian pulmonary $O_2$ and $CO_2$ exchange by Burggren and West (1982) showed that during stages 16-19 the lungs account for 20% of total $O_2$ uptake, increasing to 70-80% after metamorphic climax. Metamorphosis, therefore, marks the

initiation of regular pulmonary ventilation, which becomes increasingly dominant with development (Burggren and Infantino, 1994).

During post-metamorphic stages (20-25), fictive lung frequency in the *in vitro* brainstem preparation increased significantly in response to hypercapnia and differed significantly from hypercapnic responses at all other stages. This response confirms previous studies by Infantino (1992) in intact tadpoles at a similar stage, as well as in adult bullfrogs (Smyth, 1939; Jackson and Braun, 1979; McLean *et al.*, 1995a). Overall, it appears that central chemoreceptive reflexes regulating $CO_2$ are shifted towards the regulation of fictive lung ventilation once metamorphosis begins.

### 6.4.4 Ontogenetic coordination of central gill and lung ventilatory regulation

The present study of *Rana catesbeiana* has shown that stimulation of central chemoreceptors initiate changes in reflexes modulating the amplitude and frequency of respiratory motor output and that these are transferred from the gill to the lungs as development proceeds. Stimulation of fictive gill ventilation during central hypercapnia peaks in the intermediate stages of larval development (stages 10-14), declining from this point as fictive lung ventilation becomes increasingly sensitive to central pH stimulation. Furthermore, stimulation of central chemoreceptors generate significant changes in both gill

and lung motor output only during a brief metamorphic period (stage 15-19). Hence, the emergence of central respiratory chemoreception of pulmonary function immediately precedes the disappearance of gill central respiratory chemoreceptor regulation. Such patterns have also been observed in ontogenetic studies of hypoxic sensitivity in intact tadpole larvae (Burggren and Doyle, 1986). A parsimonious model that may account for the complex developmental transitions of neural respiratory function in anuran larvae is shown in Fig. 6.6. This model is based on the parallel developmental changes in three functional entities: central respiratory chemoreception (CRC), the gill CPG and the lung CPG. Early in development, the gill CPG is highly functional and rhythmic branchial oscillations for gill ventilation dominate respiratory output while lung central CPG output is nascent. As development proceeds, lung CPG output gradually becomes more functional and gill CPG output is reduced. In later stages of neural ventilatory development, the lung CPG function dominates while the expression of gill CPG function is minimal. Concomitant with the ontogenetic modulation of ventilatory pattern generation, central respiratory chemoreceptive drive progressively increases. Therefore, central chemoreceptive reflexes modulating gill CPGs should be most sensitive at intermediate stages of development and those regulating lung CPGs should peak at later stages.

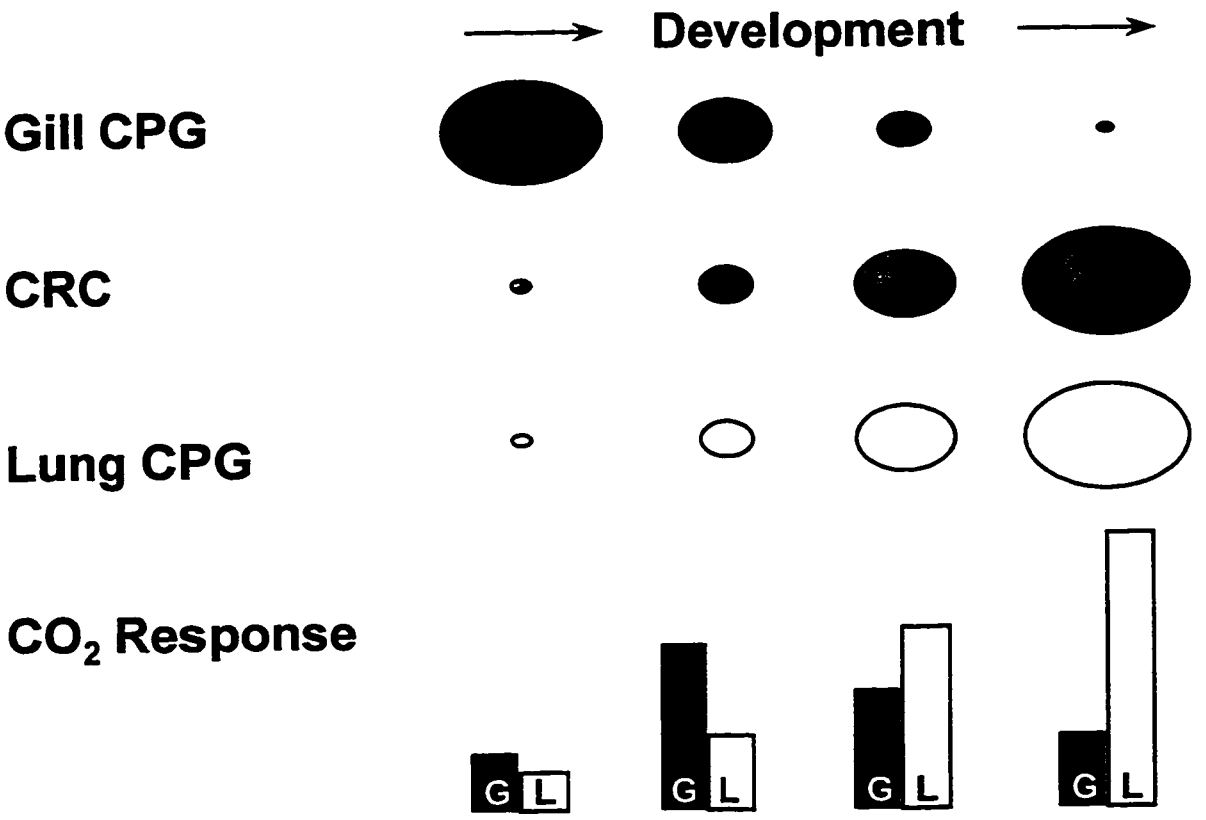


**Figure 6.6** A diagram of a possible model for the ontogeny of neural respiratory function. Concomitant with a developmental increase in the role of central respiratory chemoreceptors (CRCs), gill central pattern generator (CPG) functionality gradually decreases in strength while lung central pattern generator function increases. Differential responses of these ventilatory rhythmicities to $CO_2$ predict a maximal gill (G) response at intermediate stages and a peak response in lung (L) ventilatory output at the oldest stages.

Although clear evidence has been presented demonstrating the developmental role of central respiratory chemoreceptors in amphibian larvae, further studies are needed to determine the location, distribution, biophysiological characteristics and plasticity of such receptors during development. The *in vitro* tadpole brainstem may represent an ideal model for such studies as well as for those investigating other mechanisms of neurorespiratory control.

# *CHAPTER SEVEN*

## *Location of Central Respiratory Chemoreceptors in the Isolated Tadpole Brainstem during Development*

## 7.1 INTRODUCTION

Central respiratory chemosensitivity has been clearly established in amphibians (for reviews, see Smatresk, 1990; Milsom, 1995; Shelton *et al.*, 1986). In adult frogs (Kogo *et al.*, 1994; Kogo and Remmers, 1994; McLean *et al.*, 1995a, b; Kinkead and Milsom, 1997) and toads (Branco *et al.*, 1992; Smatresk and Smits, 1991), central $CO_2$ chemoreceptors have been shown to regulate lung ventilation. A preliminary report of studies of intact tadpoles by Infantino (1992) indicates that larval maturation is accompanied by the emergence of $CO_2$ chemoreception as a source of respiratory drive for both gill and lung ventilation and that this development is associated with a shift in the ventilatory responses from the gills to

the lungs. Results from Chapter 6 demonstrate the existence of central respiratory chemoreceptors in the tadpole brainstem that mediate fictive gill and lung ventilation in response to hypercapnia and confirm that chemoreceptive influence is transferred from gill to lung regulation. However, the precise location and mechanisms by which CRCs respond to such stimulation has not been resolved.

Central respiratory chemoreceptive sites in mammalian preparations have been traditionally described as being located in the superficial layers of the ventral surface of the medulla (Loeschcke *et al.*, 1970; Mitchell *et al.*, 1963). Recent *in vitro* and *in vivo* mammalian studies, however, indicate that central respiratory chemoreceptors are widely distributed within the brainstem (Issa and Remmers,1992; Coates *et al.*,1993; Bernard *et al.*,1996; Nattie and Li,1996; Li and Nattie, 1997). Issa and Remmers (1992) showed in the *in vitro* brainstem of the neonatal rat that tissue acidosis caused by microinjection of $CO_2$-enriched aCSF below the ventral medullary surface increased the frequency of fictive lung ventilation. Nevertheless, because the tissue pH in the region of focal acidification was not measured, the CRC fields could not be precisely delineated.

Coates *et al.* (1993) demonstrated in *in vivo* rats and cats that microinjection of acetazolimide (AZ), a carbonic anhydrase inhibitor, beneath the ventral medullary surface and in regions of the locus coeruleus and nucleus tractus

solitarii stimulated respiratory output. Similarly, in an *in vivo* rat preparation, Bernard *et al.* (1996) and Nattie and Li (1996) showed increases in ventilatory output in response to AZ microinjection in the caudal medullary raphe and ventral respiratory group. While focal tissue acidosis by AZ injection may be useful in the evaluation of CRC regions, examination of mechanism and sensitivity are limited since AZ-induced tissue pH changes are prolonged with fixed intensity. Using a $CO_2$-diffusion pipette to produce quickly reversible focal tissue acidosis, Li and Nattie (1997) recently established that reduction of tissue pH in the region of the retrotrapezoid nucleus increased respiratory motor output recorded from the phrenic nerve in an *in vivo* adult rat preparation.

The aim of the present study was to localize CRC regions sensitive to local changes in $P_{CO_2}$ in the developing tadpole brainstem *in vitro,* and to determine whether chemoreceptive regions maintain an exclusive association with the type of motor output that it stimulates, i.e., gill or lung. In order to elucidate the development of central respiratory chemoreceptive fields, the entire brainstem was systematically explored by microinjecting $CO_2$-enriched aCSF and monitoring the response of fictive gill and lung ventilation. I hypothesize that central respiratory chemoreceptive areas become more prevalent with development and that their location changes as the hypercapnic response shifts from gill to lung ventilation. Further, I hypothesize that CRCs have common functionality, driving both gill and lung motor output.

## 7.2 MATERIALS AND METHODS

### 7.2.1 Animals and surgical preparation

Experiments were performed on 24 larval bullfrog tadpoles (*Rana catesbeiana*), of either sex, obtained from a commercial supplier and maintained using the protocol described in Chapter 2. Specimens were assigned to one of two groups based on the criteria of Taylor and Köllros (1946): pre-metamorphic (stages 9-12, n=12,) and post-metamorphic (stages 23-25, n=12). Brainstem removal from the cranium was performed using the protocol previously described in Chapter 2.

### 7.2.2 Recording chamber and neural recordings

Following the transfer of the brainstem to the superfusion recording chamber, efferent recordings, representing global respiratory activity, were obtained from the roots of CN VII and SN II as formerly outlined in Chapter 2.

### 7.2.3 $CO_2$-injection pipette

Four-barrel borosilicate glass tubing (1 mm OD, 0.75 mm ID, WPI) was pulled with a vertical pipette puller (Narishige), fractured to produce an outer tip

diameter of 30 μm and forged. Because plugging of the pipette with neural tissue was not uncommon, two barrels were filled with hypercapnic aCSF equilibrated in a tonometer with a 100% $CO_2$, producing a pH of 6.0. Similarly, two barrels were filled with control aCSF, equilibrated with a $P_{CO_2}$ of 17 Torr to produce a pH of 7.8. Each barrel was separately connected to a 4-channel picosprizter (General Valve Corporation, model 2) for pressure ejection. Short duration pressure pulses (range: 5-300 msec, 125 psi) were delivered to individual barrels of the pipette, which were immediately vented upon cessation of the pressure pulse application. The volume injected was calculated from the measured radius of the pipette and the change in the position of the meniscus during a pressure pulse. The meniscus was viewed through a horizontally positioned microscope (Zeiss, 31.25X) equipped with a fine reticule that provided a maximal resolution of 5 nl.

To evaluate the $CO_2$ diffusional efflux from the tip of the four-barrel pipette, preliminary experiments were performed with the tip immersed in water for 4 hours, the typical duration of the full experiments. A pH microelectrode (see below) was positioned 25 μm from the tip of the 4-barrel injection pipette. At 30 min intervals, 150 nl of hypercapnic aCSF (pH 6.0) was injected into water and the pH of the water surrounding the tip of the injection pipette was simultaneously measured. Injection of acid decreased the pH of the water to 6.0, which gradually returned to baseline. The minimum pH produced by the test injection was virtually constant over the 4 hour period, rising from 6.0 to 6.15. This indicates

that over the time course of a typical experiment, diffusional $CO_2$ loss from the pipette was negligible.

### 7.2.4 Characterization of tissue acidification

Preliminary experiments were carried out to ascertain the minimum volume of hypercapnic aCSF required to produce global responses in respiratory motor output. Pilot mapping studies demonstrated that pressure injection in the region of CN X of 5.5-11 nl aCSF (0.5-1.0 reticule divisions) equilibrated with 100% $CO_2$ (pH 6.0) often evoked lung burst activity in both CN VII and SN II. However, because injection of 11 nl hypercapnic aCSF more consistently elicited changes in global respiratory motor output, this volume was used throughout all experiments. Evaluation of the reproducibility of the ventilatory response to injection of hypercapnic aCSF was also performed. In these tests, 11 nl of hypercapnic aCSF was repeatedly injected below the ventral brainstem surface at the same site every minute while respiratory activity was recorded from CN VII and SN II. These tests confirmed that consecutive hypercapnic injections at the same site repeatedly elicited lung burst activity with similar amplitude and shape.

In 5 animals the distribution of pH in brain tissue near the injection site was characterized using a pH microelectrode (#823, Diamond General, 90% response

time < 5 sec). To describe the spatio-temporal characteristics of acidification, tissue pH was measured at 0, 100, 200 and 300 μm, after 11 nl microinjection of hypercapnic aCSF 500 μm below the ventral surface at the level of CN X. These measurements indicated that injection of 11 nl hypercapnic aCSF, corresponding to a sphere with a radius of 140 μm, acidified a region within 250 μm of the pipette tip (see Results, Fig. 7.1A). Although the geometry of the region of acidification was not measured, I euphemistically refer to it as a "sphere". However, because the dorsal-ventral diffusional distance was roughly half of the lateral-lateral diffusion distance, it was suspected that while the convective component of tissue acidification is spherical, the diffusional component is more likely elliptical.

### 7.2.5 Experimental protocol

Once positioned in the recording chamber, the brainstem was superfused with oxygenated aCSF for at least 60 min prior to recording to allow stabilization. Compound neural activity was recorded in CN VII and SN II roots. The isolated tadpole brainstem was systematically explored in 500x500x500 μm volume segments, corresponding to diameter of the tissue acidification sphere. Using the basilar artery to demarcate the midline and CN/SN roots as rostral-caudal markers,

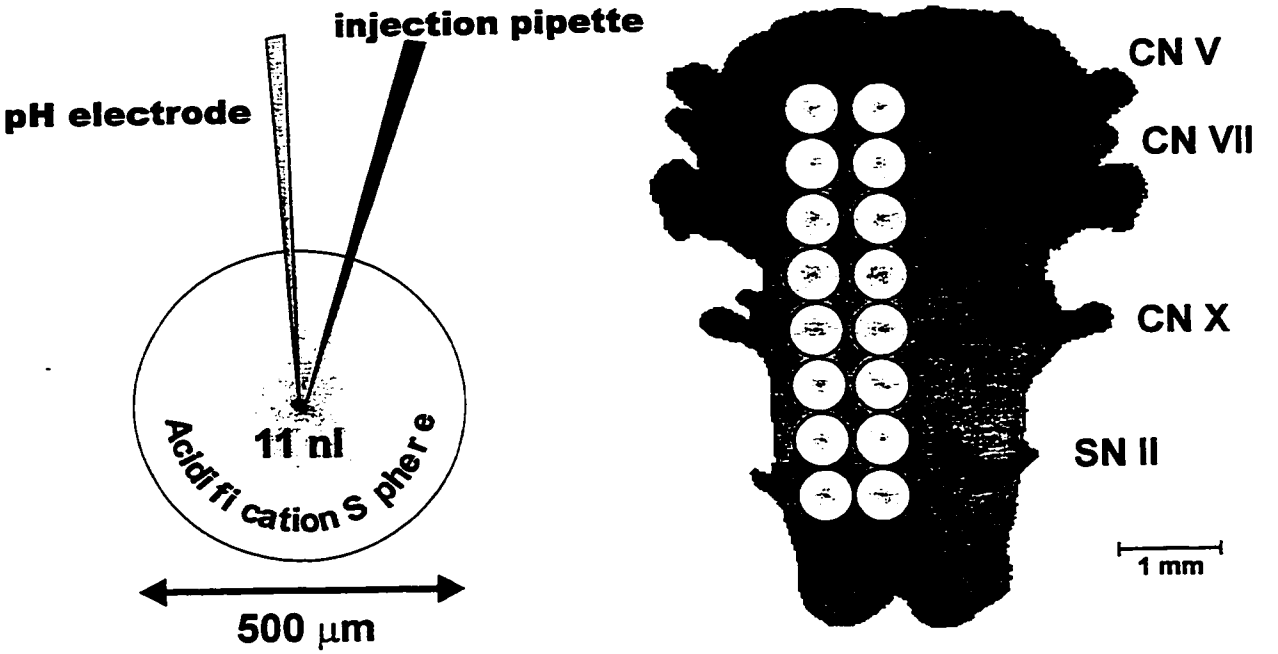


**Figure 7.1** Schema of the acidification sphere and microinjection sites in the isolated tadpole brainstem

8 medial and 8 lateral penetration sites were defined, each 500 μm apart, ranging from 500 μm rostral to the level of CN V to 500 μm caudal to the level of SN II (Fig. 7.1B). Because minimal changes in the rostral-caudal dimension of the brainstem occurred with development, equivalent penetration sites in pre- and post-metamorphic brainstems were obtained in constant relation to the nerve roots. By contrast, substantial increases in brainstem dorsal-ventral thickness were observed with development. Dorsal-ventral medullary thickness in pre-metamorphic animals measured 600-1600 μm compared with 1200-1800 μm in post-metamorphic larvae. As a result, we did not frequently microinject at depths 1000 and 1500 μm below the ventral surface in pre-metamorphic tadpoles.

The 4-barrel injection pipette was attached to a vertical motorized micro-manipulator (Nanostepper, Type B, WPI), providing positioning resolution of < 1 μm. The positioner was mounted vertically on a two-dimensional slide mechanism, which was manipulated by two manual micrometers (Newport Corp., Fountain Valley, CA) with a resolution of 5 μm. Contact of the $CO_2$-injection pipette with the surface of the tissue (zero depth) was determined visually with the aid of a dissecting microscope (x 313 magnification). The $CO_2$-injection pipette was then advanced in steps of 50 μm to depths of 500, 1000 and 1500 μm below the ventral surface. An injection trial was conducted in each of these strata. Each injection trial consisted of an 11 nl injection of hypercapnic aCSF (pH 6.0)

followed by an injection of 11 nl control aCSF (pH 7.8) at the same site 5 min later. Rhythmic respiratory activity in CN VII and SN II was continuously observed during each trial. In order to maintain brainstem viability, a maximum of 8 penetration sites were explored in each brainstem.

### 7.2.6 Data analysis

Individual injection trials generated positive or negative chemoreceptive responses. A positive chemoreceptive response consisted of a lung burst in CN VII and SN II occurring within 2 sec of hypercapnic aCSF injection together with no lung burst activity within 2 sec following injection of control aCSF injection. A negative response consisted of either failure of hypercapnic aCSF injection to evoke a fictive lung breath, or any response to hypercapnic aCSF together with the stimulation of a lung burst by control aCSF injection. Use of a brief time discrimination window (2 sec), minimized the chance that a positive chemoreceptive response might be the result of the random occurrence of lung burst.

Within pre- or post-metamorphic groups, chemoreceptive responses at the same rostro-caudal level from medial and lateral penetration sites were combined by stratum and analyzed using McNemar's Test for repeated observations on the

same individuals. A stratum in which the proportion of positive responses was significantly greater than expected from chance alone was identified as chemoreceptive site. Each developmental group had a total of 24 possible chemoreceptive sites. To compare chemoreceptive responses between pre- and post-metamorphic groups at each rostral-caudal level, all data from medial and lateral penetration sites at the same rostro-caudal level were grouped, independent of dorsal-ventral strata, and significant differences between response rates were assessed using the Fisher Exact Test. Differences in the overall frequency of positive chemoreceptive responses, between pre- and post-metamorphic larvae, regardless of location, were determined using the Chi-Square Test.

## 7.3 RESULTS

Two patterns of coordinated rhythmic activity were recorded from CN VII and SN II in all pre- (n=12) and post-metamorphic (n=12) larvae: high-frequency, low-amplitude bursts and low-frequency, high-amplitude bursts. Based on correlative studies of spontaneously breathing decerebrate tadpoles previously described in Chapter 4, these bursts have been shown to represent fictive gill and lung ventilation, respectively (Chapter 5). Distinction between gill and lung bursts was made clear by recording SN II activity.

Fig. 7.2 demonstrates the spatio-temporal distribution of pH after injection of hypercapnic aCSF, 500 μm below the ventral surface. Panel A shows the mean tissue pH change for 5 animals as a function of time following injection of 11 nl of hypercapnic aCSF. Tissue pH at 0, 100, 200 and 300 μm from the site of injection fell to minimal levels 7-12 seconds after acidic microinjection and returned to baseline (dashed line) after 60 sec. Minimum tissue pH was recorded at the site of injection (0 μm). The magnitude of pH change progressively decreased at 100 μm and 200 μm from the site of injection, with little or no tissue pH changes observed after acid injection 300 μm from the site of injection. Panel B plots mean tissue pH change for the 5 animals as a function of distance from the microinjection site at 10, 30 and 60 sec after hypercapnic injection. Ten seconds after hypercapnic aCSF injection, tissue pH at the site of injection decreased 0.23

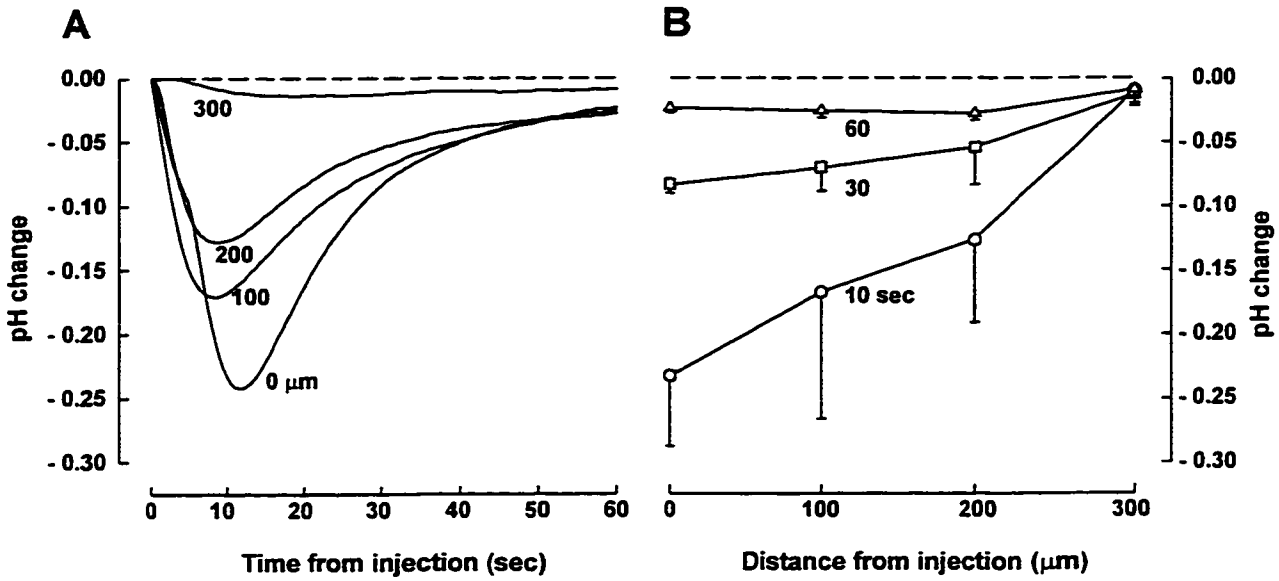


**Figure 7.2** Spatio-temporal pH distribution in isolated brainstem of a pre-metamorphic (stage 11) tadpole during 11 nl microinjection of $CO_2$-enriched aCSF. Hypercapnic aCSF was injected 500 µm below the ventral brainstem surface at the level of the CN IX root. The dashed line indicates tissue pH, 500 µm below the ventral surface, prior to injection. Panel A: tissue pH change as a function of time from injection measured at 0, 100, 200 and 300 µm from the microinjection site. Panel B: tissue pH change as a function of distance from injection at 10, 30 and 60 sec after microinjection. Plotted are mean values (± SEM), n = 3.

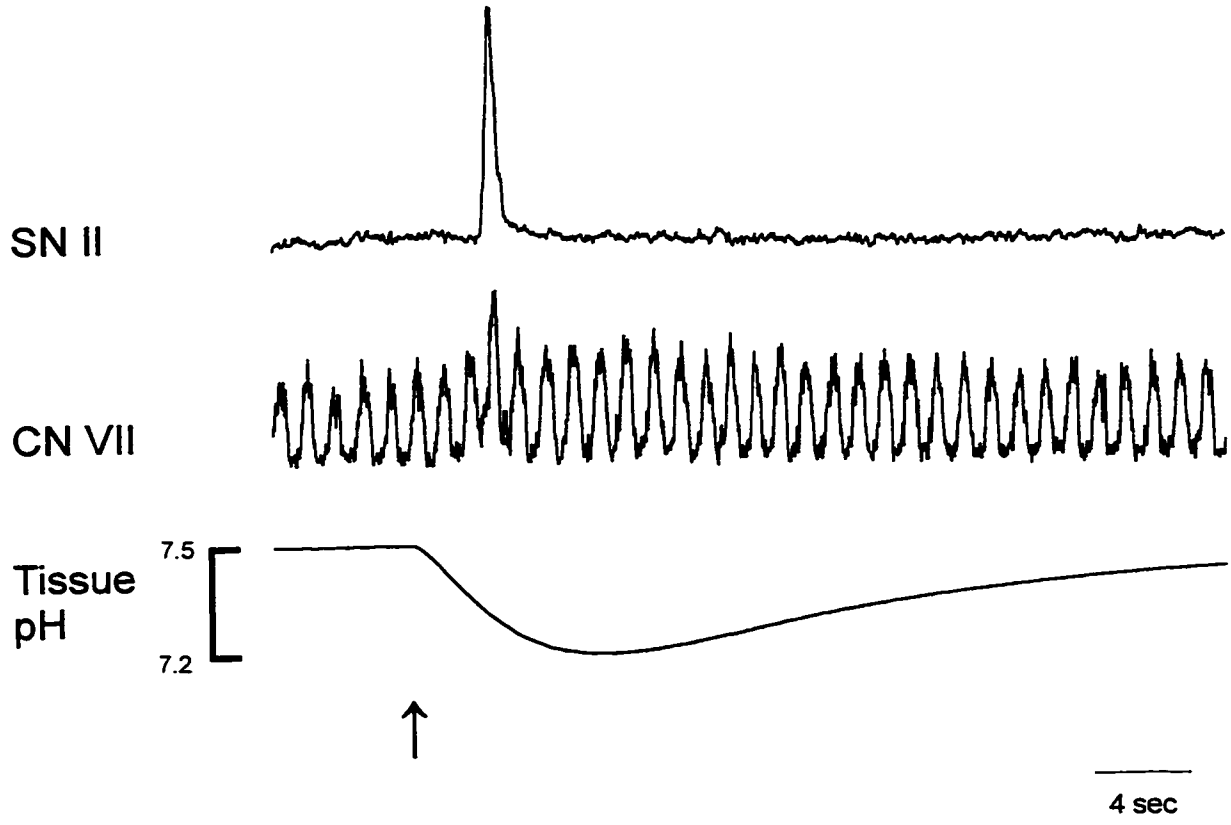


**Figure 7.3** Stimulation of respiratory motor output during hypercapnic microinjection. Simultaneous recordings of CN VII and SN II neurograms showing gill and lung ventilatory motor output and tissue pH from the isolated brainstem of a pre-metamorphic (stage 14) Rana catesbeiana tadpole superfused with artificial CSF ($PCO_2$ 17 Torr; pH 7.8) during 11 nl pressure injection of hypercapnic aCSF (pH 6.0) (indicated by the arrow). Hypercapnic aCSF was injected 500 μm below the ventral brainstem surface at the level of CN IX root and pH was recorded within 25 μm of the injection site. The height of the respiratory bursts was measured using arbitrary units.

± 0.06 pH units (from 7.34 to 7.10) and a steep pH gradient was evident. This pH gradient decreased 30 sec following acid injection and was virtually absent after 60 sec. This indicates a 500 μm sphere of acidification and provides the rational for separating injections by 500 μm.

Fig. 7.3 illustrates a recording of tissue pH at the site of injection together with an evoked fictive lung ventilatory response. Injection of 11 nl hypercapnic aCSF produced a transient (60 sec) decrease (pH 7.5 to 7.2) that reached a minimum in 7 sec and elicited lung burst activity in CN VII and SN II. Lung burst responses occurred 2 sec after hypercapnic aCSF microinjection, well before minimum tissue pH was reached, suggesting that CRC responses were followed by a refractory period.

A typical positive chemosensitive response of a pre- and a post-metamorphic tadpole is displayed in Fig. 7.4. Hypercapnic aCSF (11 nl) was injected 500 μm below the ventral surface at the level of SN II in the pre-metamorphic tadpole and 500 μm rostral to the root of CN V in the post-metamorphic tadpole. In pre-metamorphic larvae, fictive ventilation prior to injection was characterized by fictive gill bursts in CN VII punctuated by sporadic, usually isolated, lung bursts in both CN VII and SN II (Fig. 7.4A). By contrast, fictive ventilation in post-metamorphic tadpoles prior to injection was distinguished

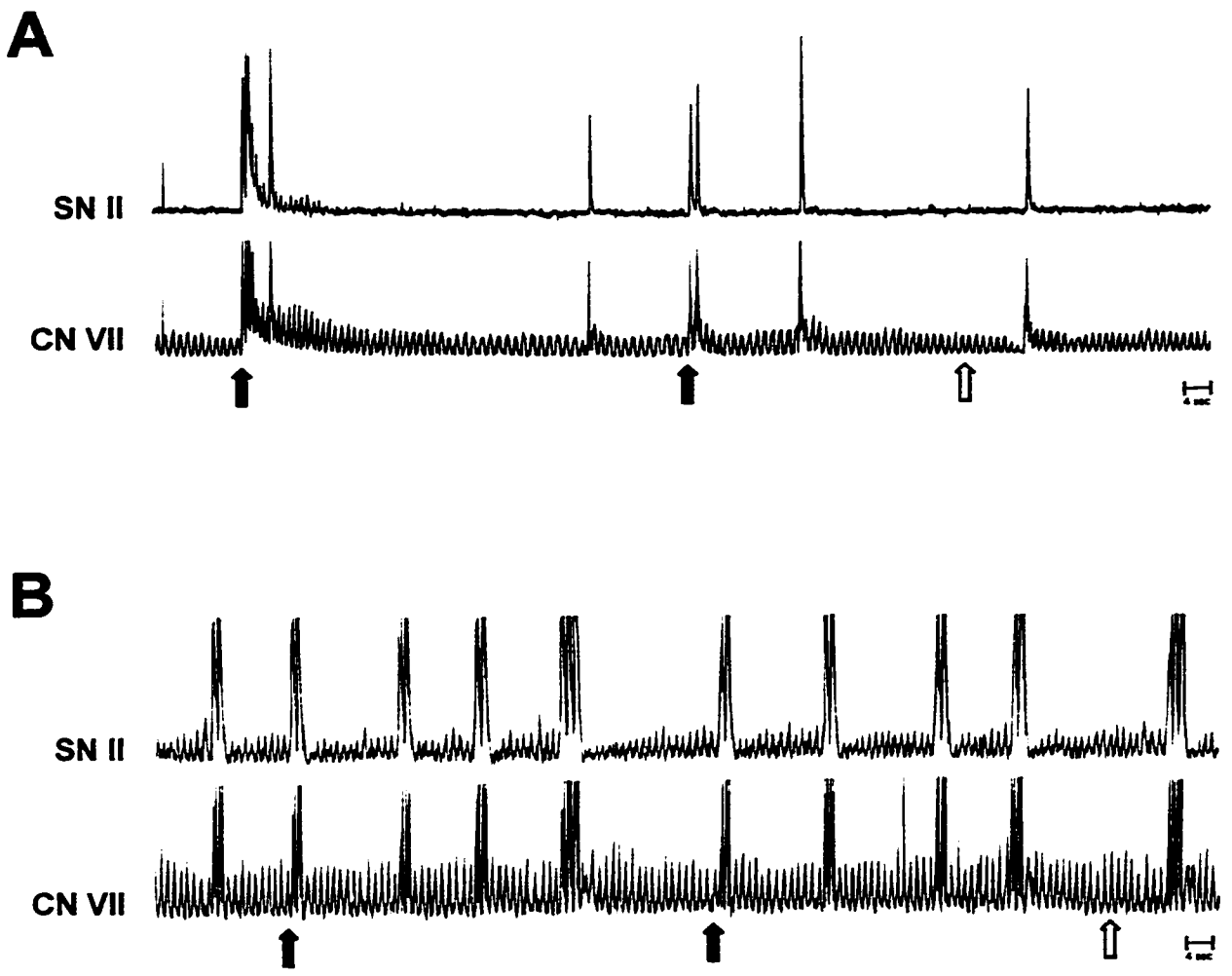


**Figure 7.4** Typical positive CRC responses to 11 nl injection of acidic (filled arrow) and control (open arrow) aCSF in pre- (Panel A) and post-metamorphic (Panel B) brainstem preparations. Ejection of hypercapnic aCSF evoked lung burst activity in both CN VII and SN II 500 μm below the ventral surface at the level of SN II in pre-metamorphic tadpole and 500 μm below the ventral surface at a level 500 μm rostral the CN V in post-metamorphic tadpoles. Ejection of control aCSF in these regions failed to change lung burst frequency in CN VII and SN II.

by frequent lung bursts in CN VII and SN II and by the emergence of gill bursts in SN II neurograms. Injection of 11 nl of hypercapnic aCSF (pH 6.0) evoked both gill and lung burst activity in CN VII and SN II of pre-metamorphic tadpoles within 2 sec and elicited lung bursts only from post-metamorphic larvae in this time (Fig. 7.4B). Five min after injection of hypercapnic aCSF, 11 nl of control aCSF (pH 7.8) injected into the same site elicited no change in respiratory output (Fig. 7.4C). Although changes in fictive gill motor output were frequently observed during hypercapnic aCSF injection, they were always associated with positive lung burst responses. Because of the difficulty in distinguishing between high amplitude gill bursts and low amplitude lung bursts, no analysis of the response of fictive gill ventilation was attempted.

Fig. 7.5 summarizes the results of 375 injection trails (each trial = acid + control aCSF injection) in the 8 medial and 8 lateral penetration sites of pre- and post-metamorphic tadpoles. In pre-metamorphic larvae, 31 of 131 injection trials produced positive responses (filled circles), and 27 of these lay caudal to CN IX and SN II. In post-metamorphic brainstems, 104 of 244 injection trails produced positive chemoreceptive responses, with 82 of these clustered in areas rostral to CN IX. The positive response occurrence rate in post-metamorphic brainstems (42%) was significantly greater ($P<0.001$) than that in pre-metamorphic preparations (27.3%). In pre-metamorphic tadpoles, the brainstem was not more

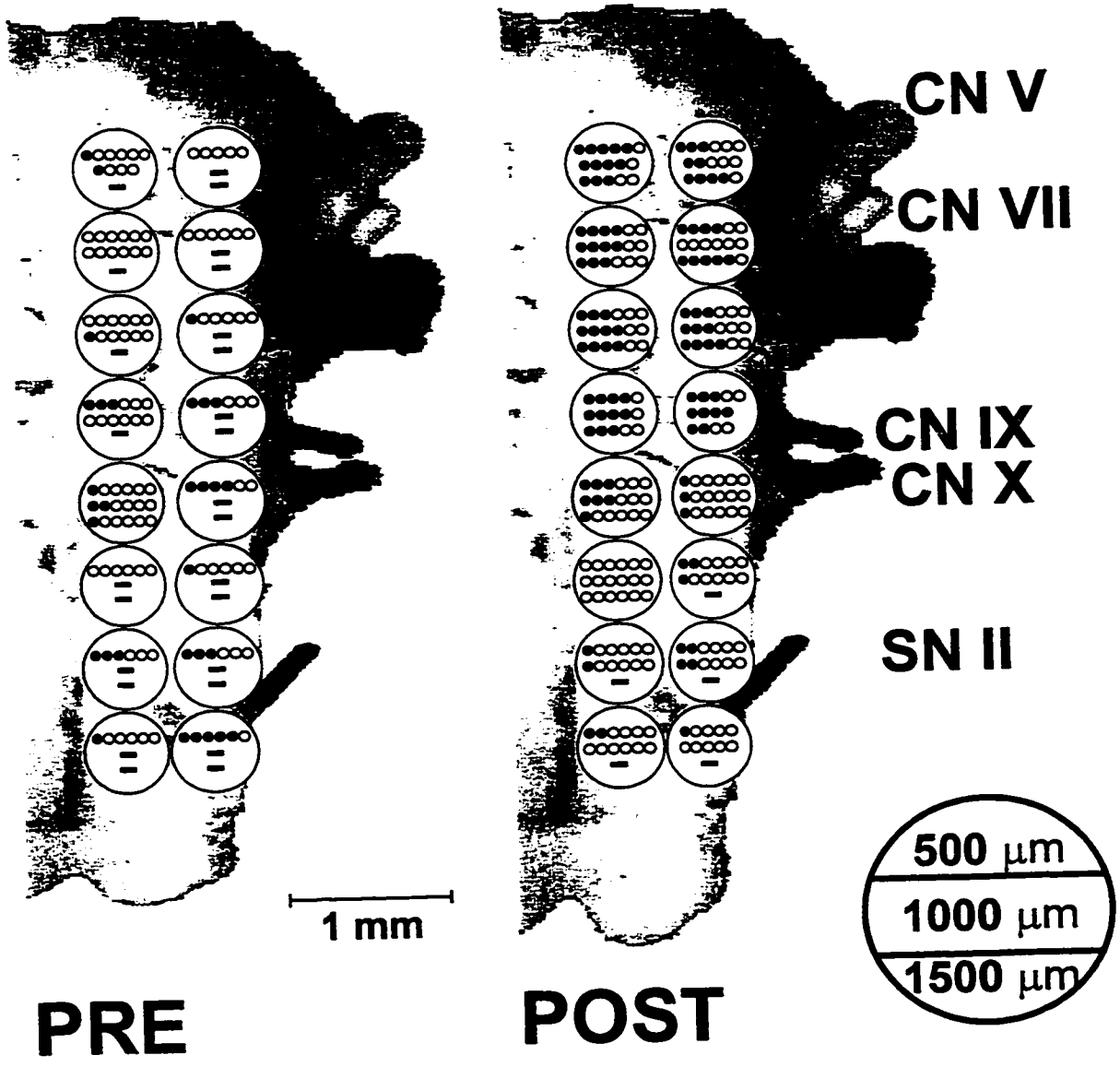


**Figure 7.5** Anatomic surface markings in pre- and post- metamorphic tadpole brainstems showing the 16 medial and lateral penetration sites (large open circles) and the distribution of positive (filled circles) and negative (small open circles) chemoreceptive responses. Within each penetration site, the top strata shows the number of chemoreceptive responses 500 μm below the ventral surface, the middle 1000 μm below and the bottom 1500 μm below. The black bar indicates no microinjection occurred.

than 600 μm thick at 11 of the 16 penetration sites and, accordingly, most chemoreceptive responses were localized in the most ventral strata. In thicker post-metamorphic brainstems, positive chemoreceptive responses appeared throughout all strata.

Fig. 7.6 summarizes the distribution of chemosensitive brainstem regions within each penetration site in pre- and post-metamorphic tadpoles. In pre-metamorphic tadpoles, chemosensitive brainstem regions lay 500 μm below the ventral surface in caudal brainstem regions at the level of CN IX and SN II. Here, the proportion of positive chemoreceptive responses from the most ventral strata of grouped medial and lateral penetration sites differed significantly ($P<0.05$: yellow) from random occurrence. Chemosensitive brainstem regions in post-metamorphic tadpoles were observed in all strata in rostral brainstem areas from the level of CN IX to a region 500 μm rostral to CN V ($P<0.02$: red, $P<0.03$: orange, $P<0.05$: yellow) with the exception of sites at the level of the root of CN V, 500 μm below the surface ($P>0.05$: blue) and those parallel to the root CN IX, 1500 μm below the surface ($P>0.05$: blue). Further, the prevalence of positive chemoreceptive responses at the same rostral-caudal level in post-metamorphic tadpoles significantly increased ($P<0.05$) compared to those observed in analogous areas of pre-metamorphic animals from the level of CN IX to a region 500 μm rostral to CN V. In pre-metamorphic tadpoles, the prevalence of positive chemoreceptive responses of corresponding medial and lateral penetration sites at

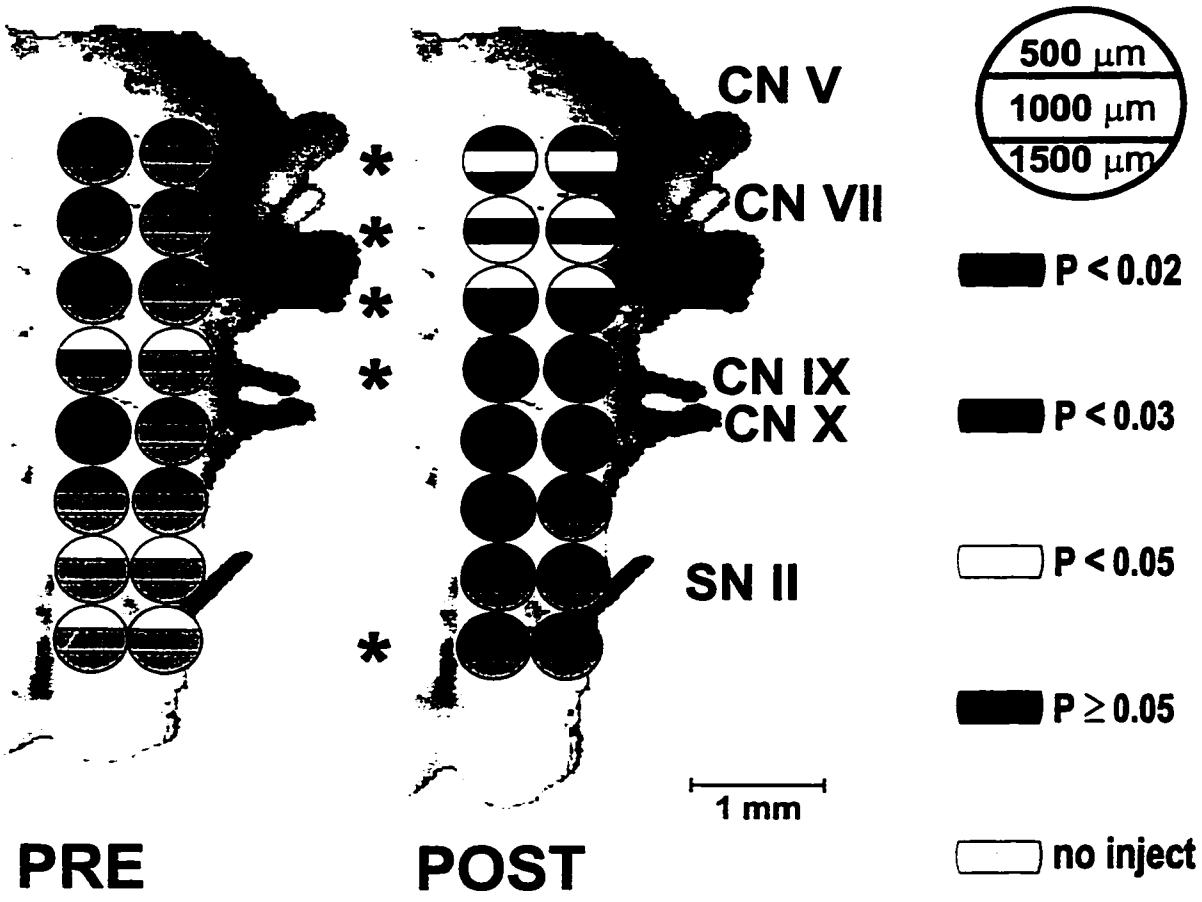


**Figure 7.6** Anatomic surface markings in pre- and post- metamorphic tadpole brainstems showing the distribution of chemoreceptive sites within medial and lateral penetration sites (large circles). Each penetration site is divided into 3 strata indicating microinjection depth below the ventral surface (500, 1000 and 1500 μm). The prevalence of positive chemoreceptive responses of corresponding medial and lateral penetration sites at the same depth beneath the ventral surface that differed from random occurrence are indicated by color: red, $P<0.02$; orange, $P<0.03$; yellow, $P<0.05$; blue, $P\geq0.05$. Gray circles indicate no microinjection occurred. * Significant differences between the responses in corresponding medial and lateral penetration sites of pre- and post-metamorphic tadpoles ($P < 0.05$).

the level of SN II were significantly greater ($P<0.05$) than those observed in analogous areas of post metamorphic animals.

## *7.4 DISCUSSION*

Systematic exploration of the tadpole brainstem demonstrates that local activation of respiratory chemoreceptive elements sensitive to $CO_2$ or pH can transiently activate both gill and lung ventilatory responses. The prevalence of CRC regions significantly increases with development and central respiratory chemoreceptive function translocates during development. In pre-metamorphic tadpoles the rate of positive lung chemoreceptive responses was significantly greater than predicted by chance alone near CN IX and SN II. In post-metamorphic animals, chemoreceptive regions producing a lung ventilatory response were located between CN IX and an area 500 μm rostral to CN V.

The microinjection strategy utilized in the present experiments produced rapid and transient tissue acidification through the convective and diffusive transport of $CO_2$ from the pipette tip. Measurements of tissue pH indicate that this transport of $CO_2$ established a "spherical" region of tissue acidosis, 500 μm in diameter, in which tissue pH transiently fell and then returned to baseline. Although these findings are consistent with calculations reported by Nicholson (1985) for pressure-injection of 10 nl of a solution into the extracellular space of brain tissue which forms a cavity and solute diffuses away from the cavitation site, the geometry of the acidification region *in vitro* is more likely elliptical, resulting from the establishment of steady-state diffusive $CO_2$ gradients (see Chapter 3). In the present study, microinjection of 11 nl aCSF equilibrated with 100% $CO_2$ (pH

6.0) decreased tissue pH from 7.34 to its minimum value of 7.10 ten seconds after microinjection. That the tissue pH decreased to 7.10, rather than 6.0, at the site of injection reflects buffering of the extracellular fluid, inasmuch as injection into unbuffered media (water) reduced the pH to 6.0. Tissue pH returned to baseline within 60 sec of hypercapnic aCSF injection as $CO_2$ diffused out into the surrounding tissue. Results show that such acidification of a "sphere" 500 μm in diameter stimulates a sufficient population of chemoreceptors to evoke a measurable global respiratory output. Accordingly, positive responses indicate the presence of chemosensitive areas that directly influence respiratory motor output of gill and lung CPGs.

### 7.4.1 Chemosensitive regions in pre-metamorphic tadpoles

In pre-metamorphic larvae, two $CO_2$-sensitive chemoreceptive regions were identified within 750 μm of the ventral surface, one lying at the level of CN IX and the other near the root of SN II. These results indicate CRC sites in young tadpoles are located in 2 locations within the medulla. However, compared to post-metamorphic animals, fewer CRC response regions were observed in pre-metamorphic tadpoles. This finding may correspond to the results of Chapter 6, demonstrating a developmental increase of central chemoreceptive influence on fictive lung ventilation in the isolated tadpole

brainstem, and confirms my hypothesis that CRCs are comparatively inactive in pre-metamorphic larvae.

The present study offers the first evidence of central $CO_2$ chemoreceptor influence on fictive lung ventilation in pre-metamorphic larvae (stages 9-12). Previous results from Chapter 6 demonstrated that in pre-metamorphic animals global hypercapnic superfusion (pH 7.4) stimulated fictive gill but not lung ventilation. Why lung burst activity in pre-metamorphic tadpoles is evoked by a focal but not a global hypercapnic stimulus is unclear. One possible explanation is that global hypercapnic superfusion might stimulate CRC elements and depress lung motor control systems. Stimulation of the total population of chemoreceptive elements, like that produced by global hypercapnic superfusion, might suppress the summation of CRC activity that selectively evokes lung bursts. As a result, no net ventilatory response would be observed with global hypercapnia even though discrete chemoreceptor stimulation would trigger a global response. Another possibility is that the chemoreceptor mechanism or the respiratory control system in the pre-metamorphic tadpole might show accommodation during sustained acidosis. Slow acidification of the brainstem that occurs with global hypercapnic superfusion may cause the chemoreceptive elements to adapt and thereby raise the threshold for lung responses. Hence, during hypercapnic aCSF injection, the sudden drop in tissue pH may have elicited both gill and lung responses well before the chemoreceptors had chance

to adapt. As shown in Fig 7.2, lung responses were evoked during the steepest part of the pH slope, well before the minimum tissue pH was established. This suggests that chemoreceptors were triggered not in response to an absolute drop in tissue pH, but rather in response to the rate of pH change.

Further, all gill responses observed in pre-metamorphic tadpoles were associated with lung responses. This observation suggests that there is no specialization of chemoreceptive elements that specifically drive gill and lung burst activity in early tadpoles, providing evidence for the existence of a common respiratory chemoreceptor.

### 7.4.2 Chemosensitive regions in post-metamorphic tadpoles

$CO_2$-sensitive chemoreceptive fields that influenced lung pattern generation in post-metamorphic tadpoles were distributed in rostral brainstem areas from CN IX to a region 500 μm rostral to the level of CN V throughout all tissue layers. The prevalence of CRC regions in post-metamorphic tadpoles was significantly greater than that in pre-metamorphic larvae. These results not only confirm previous *in vitro* brainstem studies of post-metamorphic tadpoles demonstrating progressive central chemoreceptive influence driving fictive lung ventilation (Chapter 6) but also reflect a functional developmental shift in the distribution of central chemoreceptors regulating fictive lung ventilation. In both

studies, hypercapnic stimulation (global or discrete) of post-metamorphic tadpoles stimulated lung burst activity and never gill motor output.

Rostral chemoreceptive areas described in post-metamorphic tadpoles lay within brainstem regions previously shown to contain structures essential for lung burst generation in the adult frog (Langendorff, 1887; Schmidt, 1992). Studies involving brainstem transection in the adult frog have identified critical areas for central respiratory-related activity lying between CN VIII and the caudal border of CN X (Langendorff, 1887; Schmidt, 1992). McLean *et al.* (1995b) recently demonstrated in the isolated frog brainstem that injection of excitatory and inhibitory amino acids between CN X and CN VIII influenced both the frequency and amplitude of lung burst activity. While the present study was not designed to investigate the type of cells sensitive to changes in $P_{CO_2}/H^+$ or the mechanisms of central $CO_2$-chemosensitivity, the results of the present study lead to the hypothesis that respiratory rhythmogenesis and central chemoreception are co-localized. Onimaru *et al.* (1989) reported that synaptically isolated Pre-I neurons below the ventral medullary surface of the in *vitro* neonatal rat were involved in both respiratory rhythm generation and $CO_2$ chemoreception. Issa and Remmers (1992) demonstrated similar co-localization of chemoreceptive areas sensitive to local changes in $P_{CO_2}$ in the ventral medulla of the *in vitro* neonatal rat. Further, using an *in vivo* cat preparation, Coates *et al.* (1993) localized chemoreceptors in the rostral ventrolateral medulla by

application of AZ beneath the surface. If respiratory rhythmogenesis and central chemoreception are indeed co-localized and their functions intimately associated, one possibility may be that brainstem respiratory neurons are intrinsically chemosensitive. Recently, Kawai *et al.* (1996) showed in the *in vitro* brainstem of the neonatal rat that "synaptically isolated" respiratory neurons in the VRG depolarized in response to acid challenge.

Overall, the results suggest that, with development, CRCs responding to $CO_2$ exert progressively greater influence on fictive lung ventilation and are functionally translocated from caudal to rostral brainstem areas. Accompanying this transition is a developmental shift in chemoreceptive function, from a non-differentiated form in which fictive gill and lung ventilation are influenced together to a form that influences lung bursts only. Further investigation is clearly needed to determine the correlation between central $CO_2$ chemosensitivity and respiratory central pattern generation in the developing amphibian. Elucidation of the biophysical characteristics and plasticity of central respiratory chemoreceptors and the mechanisms by which they respond to $CO_2$ has also yet to be resolved. Because more reduced preparations permit the use of cellular and molecular approaches, the *in vitro* tadpole brainstem may represent an excellent model for such studies.

# *CHAPTER EIGHT*

## *Location of Lung Rhythmogenic Regions in the Isolated Tadpole Brainstem during Development*

## 8.1 INTRODUCTION

Insight into the neural mechanisms controlling amphibian respiration has been facilitated by the development of *in vitro* tadpole brainstem preparations (Galante *et al.,* 1996). Extensive correlative studies described in Chapters 4 and 5 have demonstrated that the two patterns of rhythmic bursting activity recorded from the cranial nerve (CN) roots V, VII and X, and the spinal nerve (SN) root II, constitute fictive gill and lung ventilation; the pattern and profile of these bursts resemble the neural correlates of ventilation from decerebrate, spontaneously breathing tadpoles. Respiratory motor output in the tadpole has been clearly characterized with ontogeny (Chapter 5). The pre-metamorphic tadpole

brainstem displays predominantly fictive gill ventilatory activity that is stimulated by hypercapnia (Chapter 6). Brainstems from post-metamorphic animals, by contrast, generate fictive lung bursts as the principle form of respiratory motor output and these are stimulated by central chemoreceptive input (Chapter 6).

Galante *et al.* (1996) showed in the isolated brainstem of pre-metamorphic tadpoles that rhythmic bursting activities for lung and gill ventilation were generated by functionally separable neural systems, since fictive lung bursts, but not fictive gill bursts persist in chloride-free superfusate. These workers further suggested that, as was the case for lung bursts in the *in vitro* neonatal rat brainstem preparation, post-synaptic inhibition is not essential for fictive lung rhythmogenesis in the pre-metamorphic tadpole.

While both gill and lung oscillators lie within the tadpole brainstem, the exact location and distribution of neurons responsible for the generation of gill and lung motor output is unknown. Early studies in the adult frog by Langendorff (1887) demonstrated that breathing continued following medullary transections at the level of CN V and the caudal root of the CN X. Schmidt (1973) reported persistence of rhythmic movements of the glottis in the adult frog following transections at CN VIII and the rostral boarder of SN II. More recently, McLean *et al.* (1995) demonstrated in the isolated adult frog brainstem that injection of excitatory and inhibitory amino acids between CN VIII and CN X influenced both the frequency and amplitude of lung burst activity. Together,

these studies suggest that neurons generating lung ventilatory activity in the adult frog lie between CN VIII and CN X.

The goal of the present study was to identify brainstem regions critical for lung rhythmogenesis in the developing tadpole. I have progressively transected the *in vitro* tadpole brainstem and monitored efferent neural activity in CN VII, X and SN II. In Chapter 7, I describe a developmental translocation in the function of central respiratory chemoreceptive elements from caudal to rostral brainstem regions. I hypothesize that neuronal regions essential for lung rhythm generation anatomically tract central respiratory chemoreceptive areas and translocate rostrally with development. I further hypothesize that the rostral brainstem of the post-metamorphic tadpole contains neural elements sufficient for the generation of a lung ventilatory rhythm.

## 8.2 MATERIALS AND METHODS

### 8.2.1 Animals and surgical preparation

The study was performed on 27 larval bullfrog tadpoles (*Rana catesbeiana*) of either sex, weighing between 8-14 g (mean weight, 9.86 g). Animals were acquired from a commercial supplier and maintained according to the methods described in Chapter 2. Specimens were separated into two groups: pre-metamorphic (stages 9-14, n=14,) and post-metamorphic (stages 24-25, n=13).

Tadpoles were anaesthetized in tricaine methane sulphonate (1:10,000) and, once unresponsive, decerebrated by transection just rostral to the eyes (Transection x). This was followed by a caudal transection of the body: in pre-metamorphic animals just caudal to the level of the opercular slit and in post-metamorphic larva just behind the forelimbs (Transection y). The dorsal cranium was removed and a laminectomy performed at the first and second vertebrae. With the aid of a dissecting microscope, cranial nerves V, VII, IX, X and spinal nerve II were severed at their ostia, and the dura and arachnoid surrounding the brainstem carefully removed. Following surgery, the brainstem remained loosely attached to the ventral cranium by the unsevered cranial and spinal nerves. This arrangement allowed the ventral cranium to serve as a supportive bed during transection while facilitating the flow of superfusate between the ventral surface

of the brain and the cranium. Throughout the dissection, the brainstem was superfused with aCSF as previously described in Chapter 2.

### 8.2.2 Superfusion-recording chamber

The brainstem, loosely attached to the ventral cranium, was transferred to a superfusion-recording chamber. The cranium was pinned to the Sylgard-coated base (Dow Corning) so that the dorsal surface of the brainstem was facing upward. During the experiments, the brainstem was superfused with aCSF equilibrated with a 2% $CO_2$, 98% $O_2$ gas mixture in a room temperature tonometer (pH 7.8). Superfusate was delivered at a rate of 10 ml/min through an inflow stylus positioned at the rostral end of the brainstem and was conducted from the opposite end of the chamber via a paper wick.

### 8.2.3 Neural recordings

Compound neural activity was simultaneously recorded from the roots of CN VII, X and SN II by methods previously described (Chapter 2). In some experiments, the nerve was detached from the suction electrode during the transection process. This raised the possibility that rhythmic nerve activity may be altered by such an event. To evaluate the importance of a possible artifact introduced by such detachment/reattachment, preliminary experiments were performed to establish that multiple reattachment of the suction electrode to the same nerve

root did not affect the frequency or amplitude of the respiratory motor output. In these tests, 11 sequential electrode reattachments to CN VII caused no changes in the burst amplitude of the rhythmic lung respiratory activity.

### 8.2.4 Transection procedures

The brainstem was sectioned serially in the transverse plane using a fine-edged razor blade (Feather-S-Blade) fractured to a width of 3 mm. The blade was attached to a vertical motorized micro-manipulator (Nanostepper, Type B, WPI), providing positioning resolution of < 1 μm. The positioner was mounted vertically on a two-dimensional slide mechanism, which was manipulated by two manual micrometers (Newport Corp., Fountain Valley, CA) with a resolution of 5 μm. Fig. 8.1 shows a sagittal projection of the tadpole brainstem and the location of transection sites x, A, B, C, D and y that create brainstem segments 0, 1, 2, 3 and 4. The initial section of the cranium behind the eyes (described above) transected the brain just rostral to the optic tectum (Transection x, Fig. 8.1), while the caudal section of the body transected the brain 1 mm caudal to SN II (Transection y, Fig. 8.1). This pre-tectally transected brain provided baseline data, after which three sequential rostral-to-caudal transections were performed in each brainstem: 1) Transection A, located at the rostral margin of the cerebellar bar; 2) Transection B, positioned 500 μm rostral to the rostral root of CN IX or Transection C, immediately juxtaposed to the rostral root of

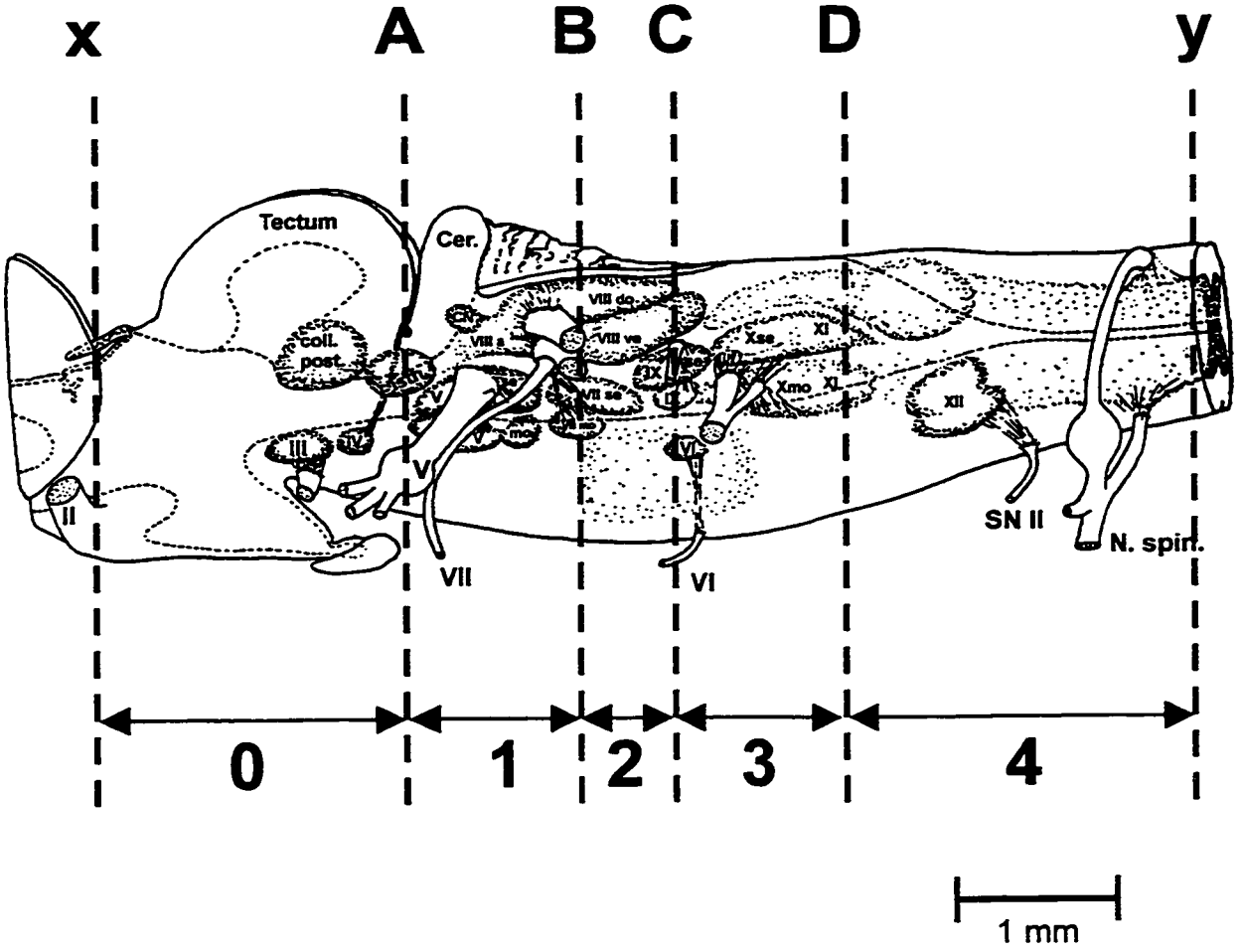


**Figure 8.1** Sagittal projection of the tadpole brainstem with serial transection sites x, A, B, C, D and y creating brainstem segments 0, 1, 2, 3 and 4. Cer. = Cerebellum; coll. Post = colliculus posterior; isth = ganglion isthmi; VIII do.=dorsal VIIIth nucleus; VIII ve = ventral VIIIth nucleus; VIII a = nuclues vestibularis anterior; CN = cerebellar nucleus; se=sensory; mo = motor; N. spin=spinal nerves

CN IX, and 3) Transection D, 1 mm caudal to Transection C. Transection A isolated the brainstem from the tectum (Segment 0). As shown in Fig. 8.1, serial transections at A, B or C and D produced three brainstem segments, each having a CN root for efferent recording as follows: Segment 1: CN VII; Segment 3: CN X; and Segment 4: SN II. Because Segment 2 lacked an external nerve, respiratory activity could not be monitored from this brainstem region. As a result, activity from this region was inferred from the behavior of CN X following Transection B and from CN VII after Transection C. Hence, when Transection B was performed, Segment 2 remained attached to Segment 3, however, following Transection C, Segments 1 and 2 remained intact.

In practice, after initial sectioning at x and y, the blade was positioned at the dorsal root of CN IX. This placement located the blade for Transection C. However, when Transection B was required, the blade was shifted 500 μm rostral from this level. To perform Transection D, the blade was positioned 1 mm caudal to Transection C. Support from the ventral cranium and intact cranial and spinal nerves facilitated brainstem sectioning by minimizing displacement and compression. Because minimal changes in the rostral-caudal dimension of the brainstem occurred with development, equivalent transection sites in pre- and post-metamorphic brainstem were obtained in constant relation to the nerve roots.

### 8.2.5 Experimental protocol

Following transfer to the recording chamber, the decerebrated brainstem was superfused in oxygenated aCSF (pH 7.8) for 30-60 min until stable rhythmic bursting activity was observed from CN VII, X and SN II roots. Respiratory motor output was recorded for 10 min at pH 7.8 and for 10 min at pH 7.4 (following equilibration of the aCSF with gas having a $P_{CO_2}$ of 45 Torr, balance $O_2$). Between 10 min recordings at each pH level, a 5 min equilibration period ensued to allow equalization of tonometer and recording chamber pH and stabilization of the brainstem response to the new superfusate pH. Rostral-to-caudal transections at A, B or C, and D were then progressively performed while suction electrodes remained attached to the nerve roots. After each transection, a 30 min recovery period ensued to ensure adequate stabilization. Following transection stabilization, efferent activity was recorded for 10 min at pH 7.8 and for 10 min at pH 7.4, with a 5 min period between to ensure pH equilibration.

### 8.2.6 Data analysis

In brainstem segments containing SN II roots, lung burst activity was identified using the SN II amplitude criterion defined in Chapter 5 and by correlative studies of spontaneously breathing decerebrate tadpoles described in Chapter 4. Lung burst activity from brainstem segments not containing SN II

roots was defined using a CN amplitude criterion and by responding to hypercapnic challenge with significantly increased frequency. For each developmental group, I analyzed the effects of hypercapnic challenge on lung ventilatory motor output frequency from CN VII, X and SN II after each transection. Within each animal, the mean lung burst frequency was measured for each 10 min recording period (pH 7.8 and 7.4) at every transection level and group means ± S.E.M. were calculated. Mean values of fictive lung frequency during hypercapnic superfusion (pH 7.4) within each animal were then expressed as the percentage change from control superfusion (pH 7.8), and group means ± S.E.M. were calculated. A Fisher Exact Test was used to assess the prevalence of the occurrence of lung bursts between pre- and post-metamorphic populations at the same transection level. The significance of pH effects both within and between developmental groups was examined at each transection level using a one-way ANOVA with repeated measures, with the criterion of statistical significance at $P<0.05$. Similarly, using a one-way ANOVA with repeated measures, significant differences in lung burst frequency as a function of transection level at each pH within a developmental group were determined. A Student–Newman-Keuls test of pairwise multiple comparisons was used to test significant differences between individuals within treatment groups when statistically significant.

## 8.3 RESULTS

All pre- (n=14) and post-metamorphic (n=13) tadpole brainstem preparations generated robust lung burst activity recorded on CN VII, X and SN II roots when superfused with aCSF of pH 7.8 or 7.4 prior to serial transection. Table 8.1 provides mean values of lung burst frequency during serial transection in pre- and post-metamorphic animals.

### 8.3.1 Pre-metamorphic transection

Lung burst generation in pre-metamorphic tadpoles was localized to caudal brainstem regions, as indicated in Table 8.1. Fig. 8.2 provides typical recordings of lung burst activity in SN II during serial transection of pre-metamorphic tadpole brainstems. Representative integrated SN II neurograms show efferent motor activity after rostral-to-caudal sectioning at A, B, C and D. In pre-metamorphic tadpoles, serial transection did not eliminate lung motor output from SN II recordings until Transection D (1 mm caudal to the root of CN IX). Thus, pre-metamorphic brainstem segments 3 and 4, in combination, were sufficient for lung rhythmogenesis. Elimination of lung bursts from CN X and SN II recordings following Transection D indicates that neither Segment 3 nor Segment 4 alone was adequate for the production of lung motor output. Rostral brainstem regions in pre-metamorphic tadpoles were unable to generate lung bursts and were not required for such generation. Following Transection B or C,

**Table 8.1** Lung ventilatory motor output from CN VII, X and SN II during sequential transection in response to superfusate pH as a function of development

| TRANSECTION | SEGMENTS | Developmental Stage | | | | | |
|---|---|---|---|---|---|---|---|
| | | Pre-Metamorphic | | | Post-Metamorphic | | |
| | | n | Lung Frequency (min-1) | | n | Lung Frequency (min-1) | |
| | | | pH 7.8 | pH 7.4 | | pH 7.8 | pH 7.4 |
| x-y | 0-1-2-3-4 | 14 | 0.95±0.55 | 0.95±0.34 | 13 | 5.31±2.27$^{*,2,3}$ | 6.86±2.57$^{*,\dagger,2,3}$ |
| A | 1-2-3-4 | 14 | 0.72±0.34 | 0.53±0.12 | 13 | 10.70±1.81$^{*,2,3}$ | 14.24±2.07$^{*,\dagger,2,3}$ |
| B | 1 | 6 | 0.00 | 0.00 | 6 | 0.00 | 0.00 |
| | 2-3-4 | 6 | 1.71±1.33 | 0.78±0.43 | 6 | 12.10±3.77$^{*,2,3}$ | 13.32±1.85$^{*,2,3}$ |
| C | 1-2 | 8 | 0.00 | 0.00 | 6 | 0.93±0.30 | 1.6±0.25$^{\dagger}$ |
| | 3-4 | 8 | 0.35±0.10$^{*}$ | 1.00±0.43$^{*}$ | 6 | 0.00 | 0.00 |
| D | 1 | 14 | 0.00 | 0.00 | 13 | 0.00 | 0.00 |
| | 1-2 | 14 | 0.00 | 0.00 | 13 | 0.93±0.30 | 1.6±0.25$^{\dagger}$ |
| | 2-3 or 3 | 14 | 0.00 | 0.00 | 13 | 0.00 | 0.00 |
| | 4 | 14 | 0.00 | 0.00 | 13 | 0.00 | 0.00 |

Data are shown as mean ± S.E.M. *Significantly different from value in corresponding developmental stage at same the pH level ($P<0.05$). †Significantly different from the value at pH 7.8 ($P<0.05$). [2]Significantly different from SN II burst frequency value at Transections C and D. [3]Significantly different from CN VII burst frequency value at Transections C and D.

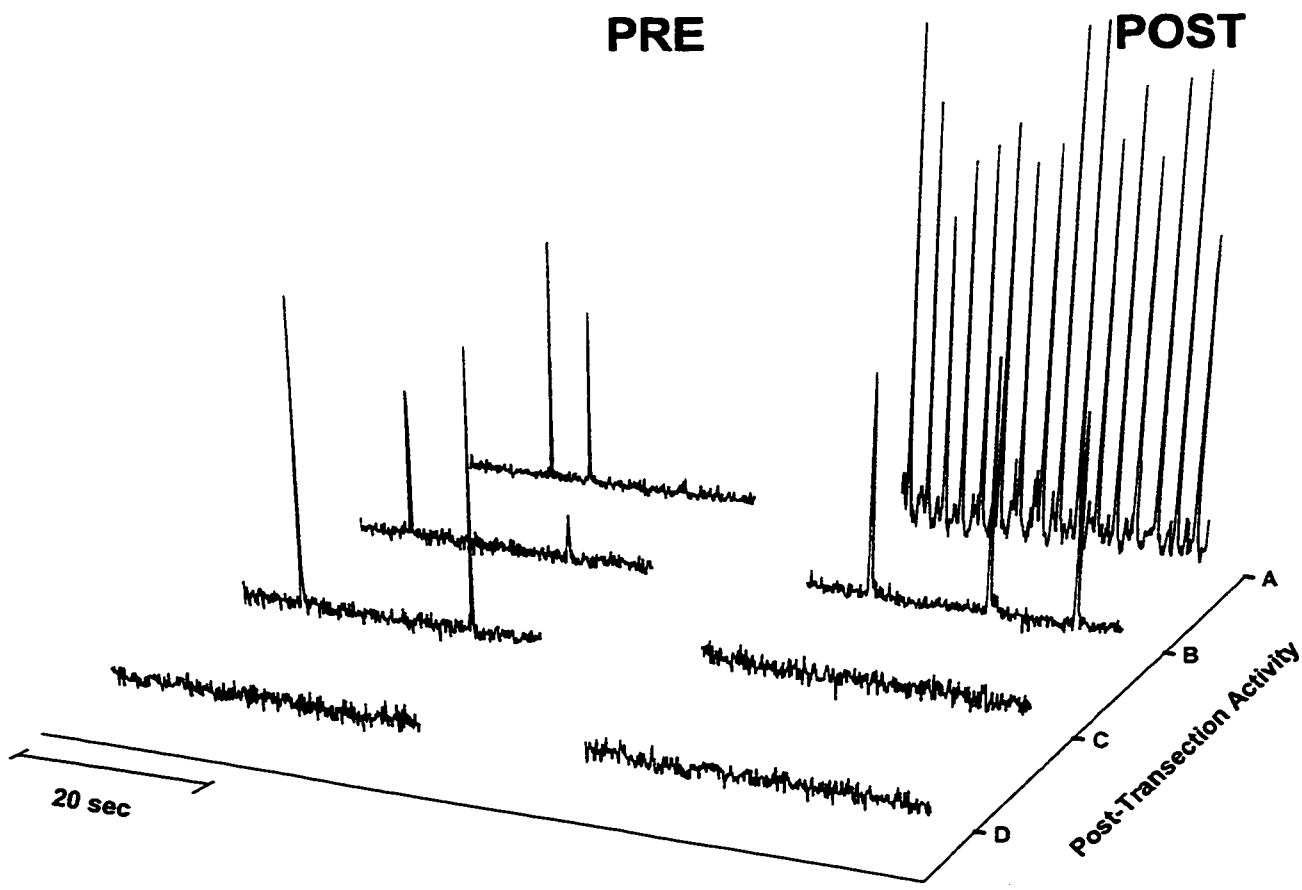


**Figure 8.2** Perturbations of SN II lung burst activity during serial brainstem transection in pre- and post-metamorphic tadpoles

fictive lung activity was absent from CN VII recordings from Segment 1 and similarly lacking from Segments 1 and 2 together after Transection C.

As displayed in Fig. 8.3 and listed in Table 8.1, lung burst frequency recorded from SN II and CN X in pre-metamorphic larvae remained unchanged after Transections A, B and C. Following Transection D, CN X and SN II lung bursts were completely eliminated ($P<0.05$).

Fig. 8.4A shows the mean lung burst frequency of SN II in pre-metamorphic tadpoles during control (pH 7.8) and hypercapnic superfusion (pH 7.4) as a function of transection level. Fictive lung ventilatory frequency recorded from CN VII, X and SN II in pre-metamorphic tadpoles was unresponsive to hypercapnic superfusion following pre-tectal brainstem sectioning, as well as Transections A, B and C.

### 8.3.2 Post-metamorphic transection

Rostral brainstem regions in post-metamorphic tadpoles generated lung burst activity (Table 8.1). As shown in Fig. 8.2, serial sectioning did not abolish recordings of lung motor output from SN II until Transection C, indicating that brainstem Segment 2, a region extending 500 μm rostral to Transection C, was necessary for lung burst generation. Further, lung bursts were recorded from CN VII after Transection C in post-metamorphic tadpoles (see Fig. 8.5). Thus, brainstem segments 1 and 2 in combination are necessary and sufficient for lung

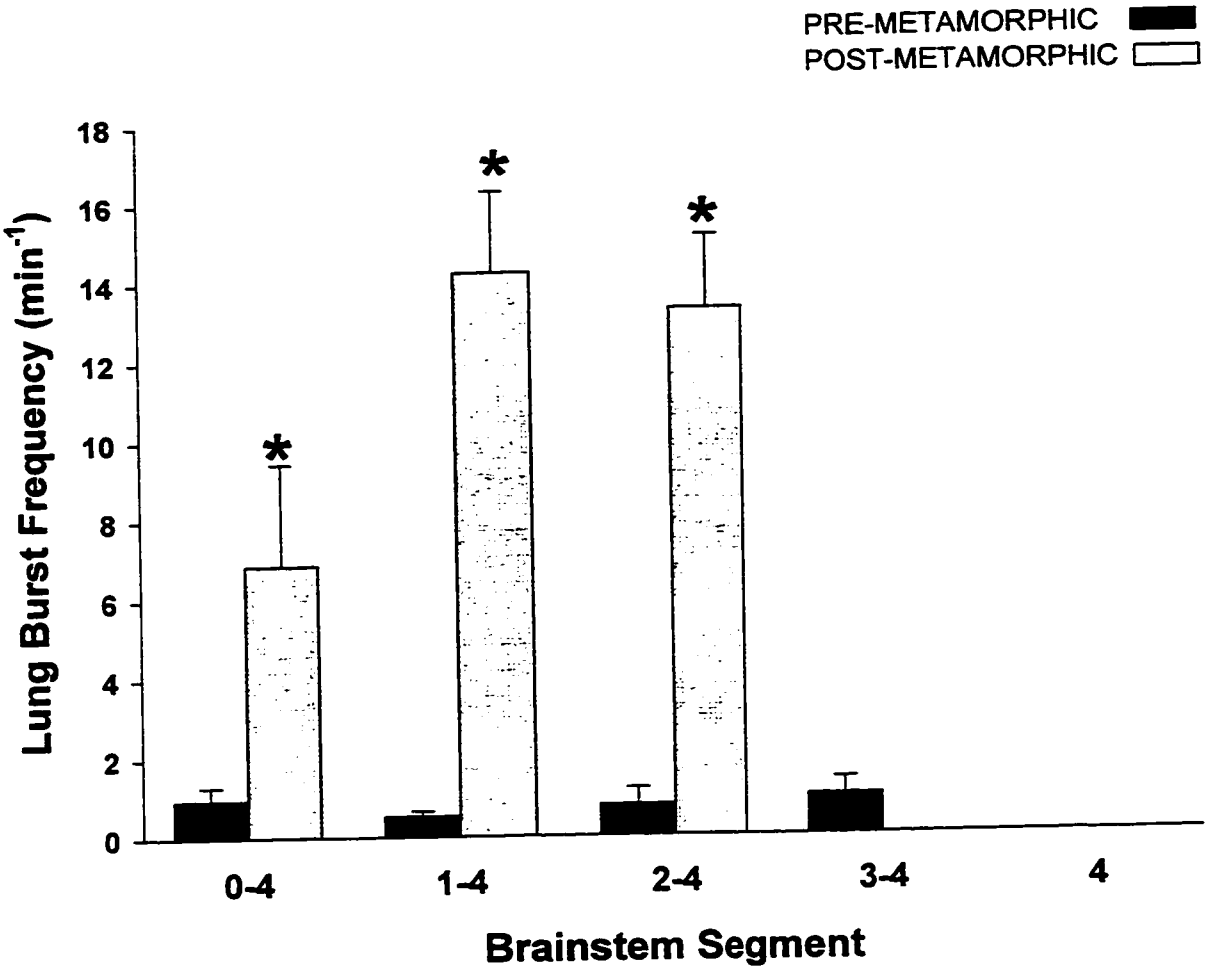


**Figure 8.3** Lung burst frequency of pre- and post-metamorphic tadpoles during serial brainstem transection. Data shown as mean ± S.E.M. *Significantly different from pre-metamorphic values at the same transection level.

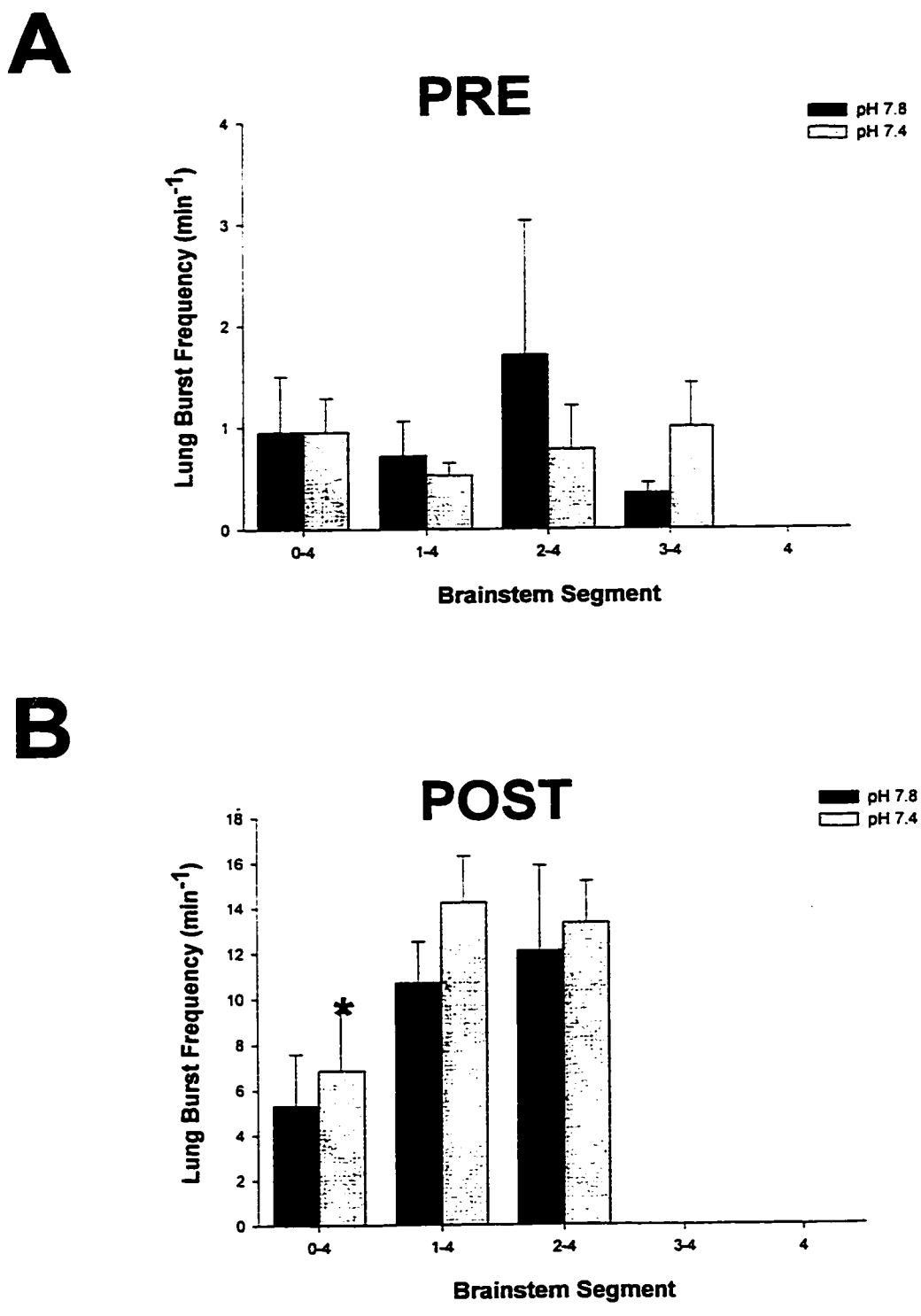


**Figure 8.4** Lung burst frequency of pre- (A) and post-metamorphic (B) tadpoles in response to hypercapnic superfusion. Data are shown as mean ± S.E.M. *Significantly different from frequency values during control superfusion at the same transection level.

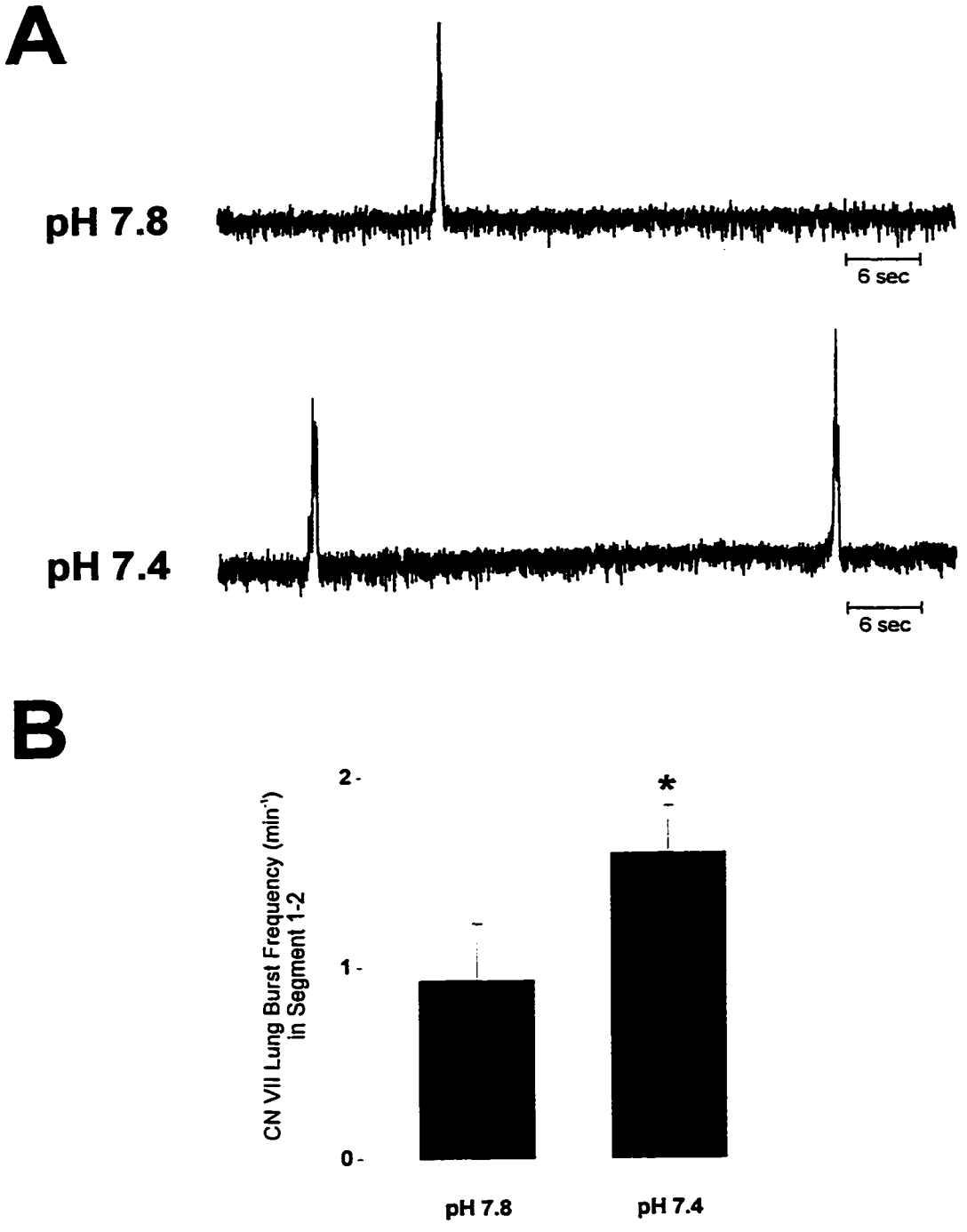


**Figure 8.5** Rostral brainstem slice sufficient to generate lung bursts in post-metamorphic tadpoles. Panel A: integrated neurograms of CN VII from the rostral brainstem segments 1 and 2 showing fictive lung bursts during control (pH 7.8) and hypercapnic (pH 7.4) superfusion. Panel B: CN VII lung burst frequency during hypercapnic superfusion significantly increased ($P<0.05$) compared to values during control superfusion.

burst generation in post-metamorphic tadpoles. By contrast, brainstem regions caudal to Transection C (Segments 3 and 4) were unable to produce fictive lung oscillations and were not required for rhythmogenesis. The prevalence of animals in the population of post-metamorphic tadpoles that displayed lung bursts recorded from CN X and SN II following Transection C (0%, 0/6) was significantly less ($P<0.001$) than observed in pre-metamorphic animals after similar sectioning (100%, 8/8).

As demonstrated in Fig. 8.3 and Table 8.1, the frequency of lung motor output was dependent on developmental stage. SN II lung burst frequency (pH 7.4) was significantly greater ($P<0.05$) in post-metamorphic tadpoles than in pre-metamorphic animals following pre-tectal transection and Transections A and B. The frequency of SN II and CN X lung bursts in post-metamorphic larvae remained unchanged after Transections A and B. and no lung bursts were observed after Transection C. (Fig. 8.3, Table 8.1). Lung burst frequency recorded in CN VII following Transection C ($0.93\pm0.30$ $min^{-1}$) in post-metamorphic tadpoles significantly decreased from that recorded after Transection A ($10.70\pm1.81$ $min^{-1}$; pH 7.8).

As shown in Fig. 8.4B, the response of fictive lung ventilation to hypercapnic superfusion varied with development stage and transection level. Lung burst frequency recorded from CN VII, X and SN II of pre-tectally transected post-metamorphic larvae significantly increased ($P<0.05$) in response

to hypercapnic superfusion. Following Transection A, hypercapnic superfusion elicited no significant increase in lung burst frequency recorded from CN X and SN II, although the trend was apparent. No response in CN X and SN II lung burst frequency to hypercapnia was observed after Transection B.

Fig. 8.5 demonstrates lung burst generation in combined brainstem segments 1 and 2 of post-metamorphic tadpoles. Integrated CN VII neurograms displayed in Panel A show lung bursts during control (pH 7.8) and hypercapnic (pH 7.4) superfusion. As illustrated in Panel B, CN VII lung burst frequency significantly increased ($P<0.05$) at pH 7.4 compared with 7.8.

## 8.4 DISCUSSION

In the present study, serial transection of the *in vitro* tadpole brainstem demonstrates that neuronal regions essential for the generation of lung motor output translocate rostrally with development. In pre-metamorphic larvae, lung burst activity was recorded from caudal brainstem nerves (CN X and SN II) following isolation of Segments 3 and 4, whereas in post-metamorphic animals this was not the case, i.e., the caudal brainstem did not display a lung rhythm after isolation of Segments 3 and 4. Lung bursts were eliminated in both CN X and SN II after Transection D, indicating the combination of both caudal segments are necessary for lung rhythmogenesis in pre-metamorphic larvae. No lung burst activity was recorded in CN VII of pre-metamorphic tadpoles following Transections B or C. In post-metamorphic tadpoles, no lung burst activity in CN X and SN II was observed following the removal of brain segments 1 and 2 (i.e., after Transection C). Neural elements in rostral brainstem segments 1 and 2 of post-metamorphic tadpole proved to be sufficient for the generation of a fictive lung rhythm and neuronal elements in Segment 2 are necessary to generate burst of lung motor output.

The transection strategy was designed to isolate thick slices of the brainstem capable of generating lung burst activity. Because the anatomy of brainstem structures in the tadpole has not been described, comparisons to the brainstem morphology of the adult frog were made (Senn, 1972). As shown in

Fig. 8.1, Transection A separated the cerebellum and brainstem (Segments 1-4) from the optic tectum (Segment 0). Although the optic tectum in the adult frog receives the bulk of its fibers from the optic nerve, transection at this level separates both efferent and afferent connections between the tectum and the superior olive and reticular neurons in the brainstem (Nieuwenhuys and Opdam, 1976). Transection B, 500 μm rostral to the root of CN IX created 2 brainstem segments; a rostral brainstem slice (Segment 1) and a caudal brainstem-spinal cord segment (Segments 2-4). Segment 1 included the cerebellum, the cerebellar nucleus, the trigeminal and facial sensory and motor nuclei and rostral portions of the superior olive (not shown) and the ventral and dorsal nucleus of CN VIII. The caudal segment (Segments 2-4) was comprised of the caudal portions of the superior olive, and the ventral and dorsal nucleus of CN VIII, as well as nuclei of the raphe (not shown), CN VI, CN IX, CN X and SN II. Transection C, at the level of CN IX and 500 μm caudal to Transection B, isolated Segment 1 and Segment 2, containing sensory and motor nuclei of CN VII, VIII and IX from Segments 3 and 4. Finally, Transection D, separated Segments 3 and 4, the former containing the roots of CN IX and X along with their sensory and motor nuclei and the other containing the SN II roots, the hypoglossal motor nucleus and the caudal portion of the vagal motor nucleus.

### 8.4.1 Lung rhythm generation in pre-metamorphic tadpoles

Prior to transection, respiratory neural output in pre-metamorphic tadpoles consisted predominantly of gill burst activity interrupted occasionally by isolated lung bursts. This characteristic pattern corresponds with respiratory patterns described in intact pre-metamorphic tadpoles (Burggren and Doyle, 1986; Infantino, 1992) and confirms previous results from isolated pre-metamorphic tadpole brainstems described in Chapter 5.

Neural elements necessary and sufficient to produce lung motor output in pre-metamorphic tadpoles were localized in brainstem regions caudal to Transection C. Sequential removal of Segments 1 and 2 caused no change in the frequency of lung bursts in CN X and SN II compared with pre-tectally transected values. However, lung burst activity was eliminated in CN X and SN II records following Transection D. These results suggest that neurons necessary for the generation of lung bursts are localized in a 1 mm region just caudal to the root of CN IX (Segment 3). This brainstem segment corresponds to the location of lung rhythmogenic areas previously reported in the adult frog (between CN VIII and X) (Langendorff, 1887; Schmidt, 1973; McLean *et al.*, 1995) but lies towards its caudal border.

No significant change in lung burst frequency occurred in response to hypercapnic superfusion prior to or following serial transection. This finding agrees with results described in Chapter 6 in the isolated pre-metamorphic

brainstem, demonstrating no response of lung burst activity to global hypercapnic superfusion.

### 8.4.2 Lung rhythm generation in post-metamorphic tadpoles

Compared to pre-metamorphic tadpoles, respiratory output in post-metamorphic animals was characterized by a predominance of lung burst activity. Prior to Transection A, the frequency of lung bursts in post-metamorphic tadpoles was significantly greater ($P<0.05$) than occurred in pre-metamorphic larvae. This pattern agrees with previous descriptions of post-metamorphic tadpole ventilation in both the isolated brainstem preparation (Chapter 5) and intact, freely swimming animals (Burrgren and Doyle, 1986; West and Burggren, 1982; Infantino, 1992).

In post-metamorphic tadpoles, neural elements necessary and sufficient to generate lung motor output were localized to Segments 1 and 2, brainstem regions rostral to Transection C. Indeed, all rostral brainstem slices displayed robust lung burst activity in CN VII, generated without perturbing the neuronal excitability of these neurons with high $[K^+]$ solutions commonly used in the neonatal rat brainstem preparation. Lung bursts from CN VII in Segments 1 and 2 were similar in duration and temporal pattern compared to those generated in the pre-tectally transected post-metamorphic brainstem, confirming that neurons in the rostral brainstem were sufficient to generate a normal lung rhythm.

In contrast to pre-metamorphic larvae, lung burst activity in post-metamorphic tadpoles was completely absent in the caudal two segments combined (i.e., Transection C). Lung motor output was similarly absent from both CN X and SN II recordings following Transection D. Hence, these findings indicate that neurons necessary for the generation of lung motor output in post-metamorphic tadpoles are distributed within Segment 3, a 500 μm region just rostral to the root of CN IX. This area roughly corresponds to brainstem areas between CN VIII and X, determined important for lung burst generation in the adult frog (Langendorff, 1887; Schmidt, 1973; McLean *et al.*, 1995) and is comparable to the location of the pre-Bötzinger complex in the isolated brainstem of the neonatal rat, the lung rhythmogenic region just caudal to the CN VII motor nucleus (Smith *et al.*, 1991). Compared with Segment 3, the brainstem region necessary for lung burst generation in pre-metamorphic animals, the corresponding area in post-metamorphic tadpoles, Segment 2, was shifted 500 μm rostrally, indicating a translocation of lung rhythmogenic function with development. Whether such translocation of function represents a development shift in the anatomical position of the rhythmogenic neurons or rather a developmental plasticity in the membrane or synaptic properties of neurons is unknown. Early developmental studies by Senn (1972) demonstrated that differentiation and formation of nerve centers in the growing medulla and spinal cord markedly depends on cellular migration.

Unlike pre-metamorphic tadpoles, lung burst activity in post-metamorphic larvae was influenced by central respiratory chemoreceptors. Pre-tectally transected brainstems of post-metamorphic tadpoles displayed significant increases in CN VII, CN X and SN II lung burst frequency in response to pH reduction, reflecting findings described in Chapter 6 of similar stage tadpoles. Following Transection A, no significant increase in lung burst frequency was observed in response to hypercapnic superfusion, although an obvious trend was apparent. These findings correspond with results from Chapter 7 in which central respiratory chemoreceptor (CRC) regions were anatomically localized within the post-metamorphic brainstem. Chapter 7 described post-metamorphic CRC regions distributed throughout the rostral medulla between the root of CN IX and an area 500 μm rostral to CN V. Accordingly, CRC influence on CN X and SN II lung burst activity was apparent after Transection A, where CRC elements were left intact, but was eliminated following the removal of Segment 1, where the majority of CRC regions were distributed.

CN VII lung burst frequency recorded from rostral brainstem segments 1 and 2 of post-metamorphic tadpoles significantly increased in response to hypercapnic superfusion. These results support previous findings reported in Chapter 7 that CRC elements in post-metamorphic tadpoles were localized in medullary regions rostral to the root of CN IX. Hence, neurons necessary and sufficient for lung burst generation and central respiratory chemoreceptors

appear to be co-localized in the medulla rostral to the root of CN IX in post-metamorphic tadpoles. Clearly, further investigation is required to ascertain whether respiratory neurons in the tadpole brainstem are themselves chemosensitive. In the isolated brainstem of the neonatal rat, Kawai *et al.* (1996) provided evidence that "synaptically isolated" respiratory neurons in the VRG depolarized in response to acid challenge.

It is concluded that neuronal regions essential for lung rhythmogenesis in the tadpole brainstem translocate rostrally with development. This anatomical shift parallels the developmental movement of CRC function and necessitates further study to establish whether lung respiratory neurons in the tadpole are intrinsically chemosensitive. The rostral medullary slice from post-metamorphic tadpoles developed in these studies contains an isolated, functionally active circuit *in vitro* and may be a viable alternate to the intact brainstem preparation. Without question, this slice will further facilitate the investigation of mechanisms underlying the generation and transmission of lung oscillations in tadpoles.

# *CHAPTER NINE*

## *General Discussion*

Collectively, the studies of this thesis describe a larval amphibian brainstem model useful for the elucidation of basic mechanisms of central respiratory chemoreception and rhythmogenesis and perhaps providing specific insight into fundamental principles underlying respiratory control in vertebrates. The *in vitro* tadpole brainstem preparation offers distinct advantages for the study of endogenously generated rhythms underlying complex respiratory behavior. The brainstem preparation retains the circuitry necessary for the generation of spontaneous rhythmic motor output in the absence of peripheral feedback mechanisms. Nerve roots containing peripheral input fibers are accessible for stimulation. Stable neural recordings can be obtained in the absence of cardio-perturbations, and reasonable control can be gained over the

extracellular milieu, allowing pharmacological manipulations of the neuronal environment.

However, a primary concern of superfused isolated brainstem tissues relates to the adequacy of respiratory gas exchange in that all $CO_2$ and $O_2$ transport occurs as diffusive exchange at the surface. Similar superfused *in vitro* brainstem preparations of mammals sustain severe tissue acidosis (Okada *et al.*, 1990; Voipio and Ballanyi, 1997) and anoxia (Fujii *et al.*, 1982; Brockhaus *et al.*, 1993). Such abnormalities have been shown to alter the membrane properties of neurons (Fugiwara *et al.*, 1987; Haddad and Donnelley, 1990) and, in addition, to induce gasping, a respiratory pattern fundamentally different from normal eupnic breathing (Lumsdem, 1923a, b, c, St. John, 1990). In contrast to mammalian preparations, pH and $P_{O_2}$ measurements of the *in vitro* tadpole brainstem show that, although moderately acidic, all tissue layers are well oxygenated. This finding represents the first demonstration of an *in vitro* brainstem that exhibits rhythmic respiratory motor output not associated with tissue hypoxia, thereby confirming the physiological usefulness of the tadpole preparation.

Because all tissue layers within the tadpole brainstem were fully oxygenated, the development of substantial pH gradients measured within the tissue presumably results from the accumulation of $CO_2$ produced by aerobic metabolism. Theoretical calculation of $P_{CO_2}$ using pH and $P_{O_2}$ data assuming

constant metabolic rate and uniform bicarbonate distribution, predict substantial gradients reaching maximal values between 36-49 Torr. These predictions were considerably lower than those measured by Voipio and Ballanyi (1997) in the anoxic *in vitro* neonatal rat brainstem, where values as high as 106 Torr were recorded. The high $P_{CO_2}$ in such hypoxic preparations is thought to reflect generation of $CO_2$ from bicarbonate ion caused by the metabolic acidosis of anaeorbic metabolism. By contrast, my calculations indicate that most of the $CO_2$ gradient in the well oxygenated tadpole brainstem results from aerobic metabolism.

Compared with normoxic tissue $P_{O_2}$ (30-40 Torr), the isolated tadpole brainstem was hyperoxic; I found a minimum tissue $P_{O_2}$ of 240 Torr. While the effect of hyperoxia on respiratory neurons in the brainstem is unknown, recent studies have suggested the possibility of oxygen toxicity by free radical formation (Enokido *et al.,* 1992) and nitric oxide formation (Leone *et al.,*1991). The latter may present a significant source of stimulation to the generation of respiratory motor output in the tadpole model. Nitric oxide (NO) has been shown to enhance the excitability and spontaneous discharge rates of respiratory–related neurons throughout the CNS (Ma *et al.,* 1995; Travagli and Gillis, 1994; Ling *et al.,* 1992). Thus, because molecular oxygen is a substrate for NO synthesis, tissue hyperoxia could lead to increased NO production, thereby stimulating respiratory motor output. Additionally, since NO binds to hemoglobin, the lack of

NO removal by the blood in the isolated brainstem may contribute to the accumulation of tissue NO.

Spontaneous rhythmic motor output generated in the *in vitro* tadpole brainstem demonstrates a coordinated sequence of rhythmic bursts related to gill and lung ventilation that are unequivocally identified using SN II recordings. Isolated tadpole brainstems generated one of two general bursting patterns: Pattern 1, high-frequency, low-amplitude bursts, and Pattern 2, low-frequency, high-amplitude bursts. The spatial and temporal characteristics of these neural bursting patterns recorded from CN V, VII, X, SN II and XI bear striking resemblance to those recorded from CN V, VII and SN II in the spontaneously breathing, decerebrate tadpole in which gill and lung ventilation were mechanically defined. The high frequency, low amplitude and rostral to caudal sequence of Pattern 1 bursts *in vitro* resembled neural recordings in the decerebrate tadpole that occurred in phase with oropharyngeal pressure oscillations when intrapulmonary pressure was constant. Similarly, the low frequency, high amplitude and more synchronous activity of Pattern 2 bursts, in addition to a characteristic appearance of SN II *in vitro,* coincided with *in vivo* neural recordings that occurred during phasic increases in intrapulmonary pressure. Accordingly, because of their close correspondence to the *in vivo* patterns, Pattern 1 was classified as fictive gill ventilation and Pattern 2 as fictive lung ventilation.

Accompanying the transition from water to air breathing, the isolated tadpole brainstem demonstrates a developmental shift in the pattern of respiratory motor output. In pre-metamorphic tadpoles, respiratory neural output consisted predominately of gill burst activity interrupted occasionally by isolated lung bursts. By contrast, fictive ventilation in post-metamorphic tadpoles was characterized by a predominance of lung burst activity, interspersed with rhythmic gill output. Further, fictive gill and lung ventilatory patterns in post-metamorphic tadpoles differ in burst onset latency from pre-metamorphic tadpole patterns and resemble fictive oropharyngeal and pulmonary burst cycles in adult frogs.

The present investigation has demonstrated the existence of central respiratory chemoreceptors (CRCs) in the *in vitro* tadpole brainstem that exert a developmentally dependent influence on fictive gill and lung ventilation. Global hypercapnic superfusion has a significant augmenting influence on the amplitude and frequency of fictive gill ventilation in pre-metamorphic and metamorphic tadpoles (stages 10-14 and 15-19), but not in the post-metamorphic tadpoles (stages 20-25). While the response of gill ventilation to $H^+/CO_2$ has been previously described in fishes and tadpoles, the role of central chemoreceptors has not been identified (see Shelton *et al.*, 1986 for review). Acidic superfusion of isolated carp, lamprey, and lung fish brainstems, produced no response in fictive gill bursts (Hughes and Shelton, 1962; Rovainen, 1977; Burleson *et al.*,

1996). Thus, the first unequivocal demonstration of CRC influence on gill ventilation in fish or amphibians is provided by the results of this thesis.

In contrast to gill motor output, significant stimulation of fictive lung ventilation by global hypercapnic superfusion occurred in metamorphic and post-metamorphic tadpoles (stages 15-19 and 20-25). These results correspond to studies by Infantino (1992) showing that the frequency of lung ventilation in similar stage intact tadpoles increased by raising $CO_2$ levels. Overall, therefore, global hypercapnic stimulation of CRCs in the isolated tadpole brainstem initiates changes in the amplitude and frequency of respiratory motor output and these changes are transferred from the gills to lungs with development.

Central respiratory chemoreceptive areas identified by discrete microinjection of hypercapnic aCSF were distributed throughout the tadpole brainstem and became more prevalent with development. Further, paralleling the shift in CRC influence from gill to lung regulation, the location of CRC function translocates rostrally with development. Systematic exploration of the pre-metamorphic tadpole identified CRC areas in caudal brainstem regions between the roots of CN IX and SN II. Discrete injection of hypercapnic aCSF into these chemosensitive regions evoked mixed lung and gill ventilatory responses. In contrast to results for global hypercapnic superfusion in pre-metamorphic tadpoles, these data suggest that there is no specialization of chemoreceptive elements that specifically drive gill and lung burst activity in

early tadpoles, providing evidence for the existence of a common respiratory chemoreceptor. Why pre-metamorphic brainstems produce lung bursts in response to discrete hypercapnic microinjection and not during global hypercapnic superfusion is uncertain. Global hypercapnic superfusion may stimulate CRC elements and depress lung motor control systems. Hence, stimulation of the total population of chemoreceptive elements, like that produced by global hypercapnic superfusion, might inhibit the summation of CRC activity that selectively evokes lung bursts. Another possibility is that the chemoreceptor mechanism or the respiratory control system in the pre-metamorphic tadpole might show accommodation during sustained acidosis. Slow acidification of the brainstem that occurs with global hypercapnic superfusion may cause the chemoreceptive elements to adapt and thereby raise the threshold for lung responses.

In post-metamorphic tadpoles, CRC regions were located in more rostral brainstem segments from the level of CN IX to an area 500 μm rostral to CN V. Further, the prevalence of CRC regions in post-metamorphic tadpoles was significantly greater than that in pre-metamorphic tadpoles. These results not only confirm previous studies of global hypercapnic superfusion that demonstrate progressive central chemoreceptive influence driving fictive lung ventilation but additionally reflect a functional shift in the distribution of central chemoreceptors regulating fictive gill ventilation. Discrete hypercapnic stimulation in post-

metamorphic tadpoles evoked lung bursts and not gill bursts. This result agrees with data generated in post-metamorphic tadpoles during hypercapnic superfusion and indicates that as development proceeds, CRC function influences lung motor output only.

Serial brainstem transection has established that those neurons essential for the generation of lung motor output in the tadpole parallel the movement of central respiratory chemoreceptive function and translocate rostrally with development. Further, neural elements in the vicinity of CN VII are sufficient to generate fictive lung ventilation. In pre-metamorphic tadpoles, the combination of the two caudal-most brainstem segments 3 and 4, a region extending between CN IX and 1 mm caudal to SN II, is necessary and sufficient for lung burst generation. The rostral-most brainstem segments 1 and 2, an area between the cerebellar bar and CN IX, do not generate fictive gill or lung ventilation. By contrast, in post-metamorphic animals, the combination of rostral brainstem segments 1 and 2 is necessary and sufficient to generate lung motor output, while caudal brainstem regions, Segments 3 and 4, do not produce lung bursts. Further, Segment 2, an area extending 500 μm from the level of CN IX is necessary for lung rhythmogenesis in post-metamorphic tadpoles. This area roughly corresponds to brainstem areas between CN VIII and X, determined important for lung burst generation in the adult frog (Langendorff, 1887; Schmidt, 1973; McLean *et al.*, 1995), and compares to the location of the pre-

Bötzinger complex, the mammalian lung rhythmogenic region just caudal to the CN VII motor nucleus, of the neonatal rat (Smith *et al.,* 1991), adult rat (Ellenberger an Feldman, 1990) and cat (Connelly *et al.,* 1992; Schwarzacher *ert al.,* 1991). Such correlation indicates that the location of the respiratory rhythm generator may be conserved throughout the vertebrate phylum.

Perhaps the most striking result of the thesis research is the excellent correspondence of CRC with CPG regions in pre- and post-metamorphic tadpoles. As illustrated in Fig 9.1A, both CRC and CPG elements of pre-metamorphic tadpoles were localized in brainstem regions caudal to the root of CN IX. By contrast, CRC and CPG elements of post-metamorphic tadpoles were distributed in brainstem regions rostral to the level of CN IX as shown in Fig 9.1B. Hence, neurons necessary and sufficient for lung burst generation and central respiratory chemoreceptors appear to be co-localized in the brainstem, translocating from caudal regions in immature larvae to rostral brainstem regions in post-metamorphic tadpoles. Co-localization of central chemoreception and respiratory rhythmogenesis has been suggested in numerous mammalian studies. Onimaru *et al.* (1989) reported that synaptically isolated Pre-I neurons below the ventral medullary surface of the in *vitro* neonatal rat were involved in both respiratory rhythm generation and $CO_2$ chemoreception. Issa and Remmers (1992) demonstrated similar co-localization of chemoreceptive areas sensitive to local changes in $P_{CO_2}$ in the ventral medulla of the *in vitro* neonatal rat. Further,

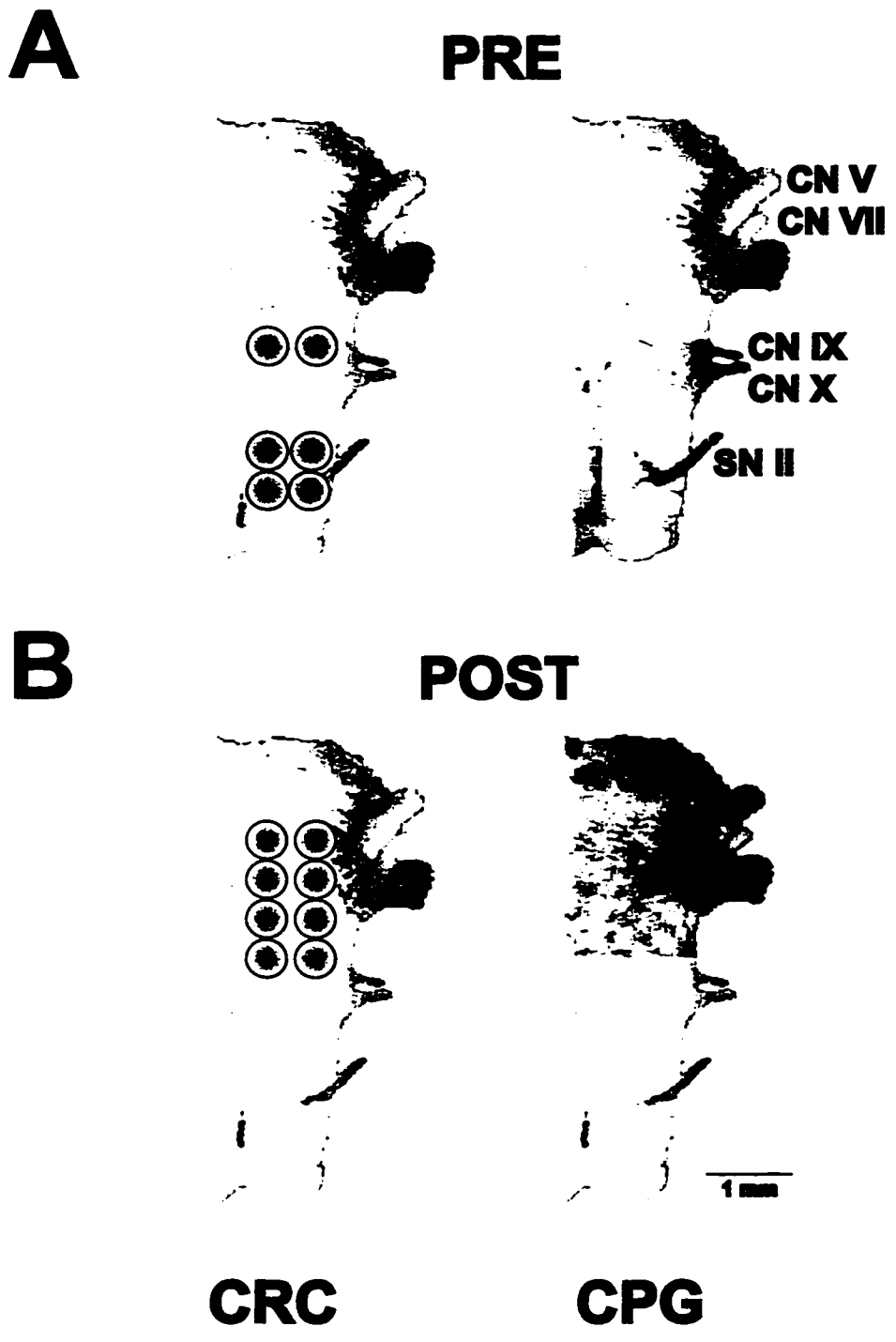


**Figure 9.1** Localization of central respiratory chemoreceptor (CRC) and lung central pattern generator (CPG) function (red) in the isolated brainstem of pre- (Panel A) and post-metamorphic (Panel B) tadpole.

using an *in vivo* cat preparation, Coates *et al.* (1993) localized chemoreceptors in the rostral ventrolateral medulla by application of AZ beneath the surface. Accordingly, if respiratory rhythmogenesis and central chemoreception are indeed co-localized and their functions intimately associated, one possible explanation may be that brainstem respiratory neurons are intrinsically chemosensitive. Recently, Kawai *et al.* (1996) showed in the *in vitro* brainstem of the neonatal rat that "synaptically isolated" respiratory neurons in the VRG depolarized (inspiratory neurons) or (hyperpolarized) expiratory neurons in response to acid challenge. A variety of investigational approaches, including the *in vitro* tadpole brainstem will likely facilitate answering this and related questions.

## *CHAPTER TEN*

## *Bibliography*

Adams, W.E. (1958). *The Comparative Morphology of the Carotid Body and Carotid Sinus.* Springfield, IL, Thomas.

Aota, S., Holmgren, K.D., Gallaugher, P. & Randall, D.J. (1990). A possible role of catecholamines in the ventilatory responses associated with internal acidosis or external hypoxia in rainbow trout *Oncorhynchus mykiss. J. Exp. Biol.* **151**: 57-70.

Atkinson, B.G. & Just, J.J. (1975). Biochemical and histological changes in the respiratory system of *Rana catesbeiana* larvae during normal and induced metamorphosis. *Dev. Biol.* **45**: 151-165.

Bartlett, D., Remmers, J.E. & H. Gautier. (1973). Laryngeal regulation of respiratory airflow. *Respir. Physiol.* **18**: 194-204.

Becker, K. B., Stephens, K. C., Davey, J. C., Schneider, M. J., & Galton, V. A. (1997). The type 2 and type 3 iodothyronine deiodinases play important roles in coordinating development in Rana catesbeiana tadpoles. *Endocrinology*, **138,** 2989-97.

Bernard, D. G., Li, A. & Nattie, E. E. (1996). Evidence for central chemoreception in the midline raphe. *Journal of Applied Physiology* **80,** 108-15.

Bianchi, A., Denavit-Saubié, & J. Champagnat. (1995). Central control of breathing in mammals: neuronal circuitry, membrane properties, and neurotransmitters. *Physiol. Rev.* **75**: 1-45.

Branco, L.G.S., Glass, M.L. & A. Hoffman. (1992). Central chemoreceptor drive to breathing in unanesthetized toads, *Bufo paracnemis. Respir. Physiol.* **87**, 195-204.

Brockhaus, J., Ballanyi, K., Smith, J.C. & D.W. Richter (1993). Microenvironment of respiratory neurons in the *in vitro* brainstem-spinal cord of neonatal rats. J. Physiol. **462**: 421-445.

Brown, T.G. (1911). The intrinsic factors in the acts of progression in mammal. *Proc. R. Soc. Bio.* **84**: 380-319.

Burggren, W.W. (1984). Transition of respiratory processes during amphibian metamorphosis: from egg to adult. In: Respiration and Metabolism of Embryonic Vertebrates, edited by R.J. Seymour. pp. 31-50. Boston: Dr. W. Junk Publishers.

Burggren, W.W. (1989). Lung structure and function: Amphibians. In *Comparative Pulmonary Physiology: Current Concepts* (ed. S.C. Wood). pp. 153-192. New York: Marcel Dekker.

Burggren, W.W. & M. Doyle. (1986). Ontogeny of the regulation of gill and lung ventilation in the bullfrog, *Rana catesbeiana. Respir. Physiol.* **66**: 279-291.

Burggren, W.W. & R.L Infantino (1994). The respiratory transition from water to air breathing during amphibian metamorphosis. *Amer. Zool.* **34**: 238-246.

Burggren, W.W. & A. Mwalukoma. (1983). Influence of chronic hypoxia and hyperoxia on gas exchange processes in larval and adult bullfrogs (*Rana catesbeiana*) I. Morphological responses of the lungs, skin and gills. *J. Exp. Biol.* **105**: 191-203.

Burggren, W.W. & N.H. West. (1982). Changing respiratory importance of gills, lungs and skin during metamorphosis in the bullfrog Rana catesbeiana. *Respir. Physiol.* **47(2)**: 151-64.

Burleson, M.L. & N.J. Smatresk. (1989). The effect of decerebration and anesthesia on the reflex responses to hypoxia in catfish. *Can. J. Zool.* **67**: 630-635.

Cameron, J.N. (1978). Regulation of blood pH in teleost fish. *Respir. Physiol.* **33**: 129-144.

Cherniak, J.S., von Euler, C., Homma, I. & F.F. Kao. (1979). Graded changes in central chemoreceptor input by local temperature changes on the ventral surface of the medulla. *J. Physiol. (London).* **287**: 191-211.

Coates, E. L., Li, A. & E.E. Nattie. (1993). Widespread sites of brain stem ventilatory chemoreceptors. *J. Appl. Physiol.* **75**: 5-14.

Connelly, C.A., Dobbins, E.G. & J.L. Feldman. (1992). Pre-Bötzinger complex in cats: respiratory neuronal discharge patterns. *Brain Res.* **590**: 337-340.

Dean, J. B., Bayliss, D. A., Erickson, J. T., Lawing, W. L., & D.E. Millhorn. (1990). Depolarization and stimulation of neurons in nucleus tractus solitarii by carbon dioxide does not require chemical synaptic input. *Neuroscience*, **36**: 207-16.

DeJongh, H.J. (1968). Functional morphology of the jaw apparatus of larval and metamorphosing *Rana temporaria*. *Neth. J. Zool.* **18**: 1-103.

DeJongh, H.J. & C. Gans. (1969). On the mechanism of respiration in the bullfrog, *Rana catesbeiana*. A reassessment. *J. Morph.* **127**: 259-290.

Dejours, P. (1975). Principles of Comparative Respiratory Physiology. Amsterdam, Elsevier Publishing Company.

Dejours, P. (1988). Respiration in Water and Air. Adaptations-Regulation-Evolution. Amsterdam, New York, Oxford: Elsevier, p.179.

De Marneffe-Foulon, C. (1962). Contribution à l'étude du méchanisme et du contrôle des mouvements respiratoires chez *Rana*. *Ann. Soc. Roy. Zool. Belgique.* **91**(1): 81-132.

Dittmer, D.S. & R.M Grebe (1956). Handbook of Respiration. American Elsevier Publishing Co., Inc., New York. p. 150.

Dively, J.L., Mudge, J.E., Neff, W.H. & A. Anthony. (1977). Blood $P_{O_2}$, $P_{CO_2}$, and pH changes in brook trout (*Salvelinus fontinalis*) exposed to sublethal levels of acidity. *Comp. Biochem. Physiol.* **57A**: 347-351.

Douse, M.A. & G.S. Mitchell. (1990). Episodic respiratory related discharge in turtle cranial motoneurons: in vivo and in vitro studies. *Brain Res.* **536**: 297-300.

Duellman, W.E. & L. Trueb. (1986). (eds.) *Biology of Amphibians.* McGraw-Hill, New York, USA; pp.219.

Eddy, F.B. (1976). Acid-base balance in rainbow trout (*Salmo gairdneri*) subjected to acid stresses. *J. Exp. Biol.* **64**: 159-171.

Ellenberger, H.H. & J.L. Feldman. (1990). Subnuclear organization of the lateral tegmental field of the rat. I. Nucleus ambiguous and ventral respiratory group. *J. Comp. Neurol.* **294**: 202-211.

Enokido, Y., Y. Akaneya, M. Niinobe, K. Mikoshiba & H. Hatanaka (1992). Basic fibroblast growth factor rescues CNS neurons from cell death caused by high oxygen atmosphere in culture. *Brain Res.* **599**: 261-271.

Evans, B. K. & G. Shelton. (1984). Ventilation in *Xenous laevis* after lung or carotid labyrinth denervation. *Proc. IUBS: Comp. Physiol. Biochem.* **1**: A75.

Ezure, K. (1990). Synaptic connections between medullary respiratory neurons and considerations on the genesis of respiratory rhythm. *Prog. Neurobiol.* **35**: 429-450.

Feldman, J.L & J.C. Smith. (1989). Cellular mechanisms underlying modulation of breathing pattern in mammals. *Ann. N.Y. Sci.* **563**: 114-130.

Feldman, J.L., Smith, J.C., Ellenberger, H.H., Connelly, C.A., Liu, G.S., Greer, J.J., Lindsay, A.D. & M.R. Otto. (1990). Neurogenesis of respiratory rhythm and pattern: emerging concepts. *Am. J. Physiol.* **259**: R879-886.

Feldman, J. L., Smith, J. C., & G. Liu. (1991). Respiratory pattern generation in mammals: in vitro en bloc analyses. *Current Opinion in Neurobiology*, **1**: 590-4.

Fugiwara, N., Higashi, H., Shimoji, K. & M. Yoshimura. (1987). Effects of hypoxia on hippocampal neurons *in vitro*. *J. Physiol. (London)* **384**: 131-151.

Fujii, T., H. Baumgärtl & D.W. Lübbers (1982). Limiting section thickness of guinea pig olfactory cortical slices studies from tissue $P_{O_2}$ and electrical activities. *Pflügers Arch.* **393**: 83-87.

Funk, G.D. & J.L. Feldman. (1995). Generation of respiratory rhythm and pattern in mammals: insights from developmental studies. *Curr. Opin. Neurobiol.* **5**: 778-785.

Galante, R.J., L. Kubin, A.P. Fishman & A.I. Pack (1996). Role of chloride-mediated inhibition on respiratory rhythmogenesis in an *in vitro* brainstem of tadpole *Rana catesbeiana*. *J. Physiol. (London)* **492**: 545-558.

Gans, C. (1970). Strategy and sequence in the evolution of the external gas exchangers of ectothermal vertebrates. *Forma. Functio.* **3**: 61-104.

Gans, C., De Jongh, H.J. & J. Farber. (1969). Bullfrog (Rana catesbeiana) ventilation: how does the frog breathe? *Science* **163(872)**: 1223-5.

Getting, P.A. (1988). Comparative analysis of invertebrate central pattern generators. In: *Neural Control of Rhythmic Movements in Vertebrates*. ed. Cohen, A.H., Rossignol, S. & S. Grillner. Sprigner-Verlag Press, New York, USA; pp. 101-127.

Gleeson, M. & V. Molony. (1989). Control of Breathing. In: *Form and Function in Birds (Vol. 4)*, ed. King, A.S. & J. McLelland. Academic Press, New York, USA; pp. 439-484.

Gradwell, N. (1971). Ascaphus tadpole: experiments on the suction and gill irrigation mechanisms. *Can. J. Zool.* **49(3)**: 307-32.

Gradwell, N. (1972a). Gill irrigation in Rana catesbeiana. I. On the anatomical basis. *Can. J. Zool.* **50(5)**: 481-99.

Gradwell, N. (1972b). Gill irrigation in Rana catesbeiana. II. On the musculoskeletal mechanism. *Can. J. Zool.* **50(5)**: 501-21.

Gradwell, N. & B. Walcott. (1971). Dual function and structural properties of the interhyoideus muscle of the bullfrog tadpole (*Rana catesbeiana*). *J. Exp. Biol.* **176**: 193-197.

Haddad, G.G. & D.F. Donnelly. (1990). $O_2$ deprivation induces a major depolarization in brainstem neurons in the adult but not in the neonatal rat. *J. Physiol. (London)* **429**: 411-428.

Harada, Y., M. Kuno & Y.Z. Wang (1985). Differential effects of carbon dioxide and pH on central chemoreceptors in the rat *in vitro*. *J. Physiol. (London)* **368**: 679-693.

Hargis, J.R. (1976). Ventilation and metabolic rate of young rainbow trout (*Salmo gairdneri*) exposed to sublethal environment pH. *J. Exp. Zool.* **196**: 39-44.

Heisler, N., Toews, D.P. & G.F. Holeton. (1988). Regulation of ventilation and acid-base status in the elasmobranch *Scyliorhinus stellaris* during hyperoxia-induced hypercapnia. *Respir. Physiol.* **71**: 227-246.

Helff, O.M. (1932). Studies on amphibian metamorphosis. X. Hydrogen-ion concentration of the blood of anuran larvae during involution. *Biol. Bull. Mar. Biol. Lab.*, Woods Hole. **63**: 405-418.

Henke, K.G., Arais, A., Skatrud, J.B. & J.A. Dempsey. (1988). Inhibition of inspiratory muscle activity during sleep. Chemical and nonchemical influences. *Am. Rev. Respir. Dis.* **138**(1): 8-15.

Hill, A.V. (1928). The diffusion of oxygen and lactic acid through tissues. *Roy. Soc. Proc., B.* **104**: 39-96

Hughes, G.M & G. Shelton. (1962). Respiratory mechanisms and their nervous control in fish. *Adv. Comp. Physiol. Biochem.* **1**: 275-364.

Infantino, R.L., Jr. (1990). Ventilatory responses to inspired gas variation in larval bullfrogs. *The Physiologist*, **33**: A35.

Infantino, R.L., Jr. (1992). Ontogeny of ventilatory regulation in the bullfrog *Rana catesbeiana,* (Doctoral dissertation), University of Massachusetts, Amherst, Massachusetts.

Ishii, K. & K. Ishii. (1970). Efferent innervation to the chemoreceptor of the carotid labyrinth of the toad. *Tohoku J. Exp. Med.* **102**: 113-119.

Ishii, K. & K. Ishii. (1976). The chemoreceptors of amphibians. *In* A. S. Paintal (Ed.), *Morphology and Mechanics of Chemoreceptors* (pp. 265-274). New Dehli, India.

Ishii, K., Ishii, K. & T. Kusakabe. (1985). Chemo- and baroreceptor innervation of the aortic trunk of the toad *bufo vulgaris*. *Respir. Physiol.* **60**: 365-375.

Issa, F.G. & J.E. Remmers (1992). Identification of a subsurface area in the ventral medulla sensitive to local changes in $P_{CO_2}$. *J. Appl. Physiol.* **72**: 439-446.

Ito, F. & S. Watanabe. (1962). Localization and organization of respiratory neurons in the brainstem of the toad, with reference to activate, with reference to activities of slow motor system. *Jap. J. Physiol.* **12**: 611-622.

Jackson, D.C. & B.A. Braun. (1979). Respiratory control in bullfrogs: cutaneous versus pulmonary response to selective $CO_2$ exposure. *J. Comp. Physiol.* **129**: 339-342.

Janssen, R.G. & D.J. Randall. (1975). The effects of changes in pH and $P_{CO_2}$ in blood and water on breathing in rainbow trout *Salmo gairdneri*. *Respir. Physiol.* **25**: 235-245.

Jia, X. & W.W. Burggren. (1989). Developmental changes in gill ventilation reflexes in larvae of *Rana catesbeiana*. *Amer. Zool.* **29**: 56A.

Johansen, K. (1970). Cardiorespiratory adaptations in the transition from water breathing to air breathing. *Fedn. Proc. Fedn. Am. Socs exp. Biol* **29**: 1118-1119.

Jones, D. R. & C. Chu. (1988). Effect of carotid denervation of carotid labyrinths on breathing in unrestrained *Xenopus laevis*. *Respir. Physiol.* **73**: 243-256.

Jones, D. R. & W. K. Milsom. (1982). Peripheral receptors affecting breathing and cardiovascular function in non-mammalian species. *J. Exp. Biol.* **100**: 59-91.

Just, J.J., Gatz, R.N. & E.C. Crawford, Jr. (1973). Changes in respiratory functions during metamorphosis of the bullfrog, *Rana catesbeiana. Respir. Physiol.* **17**(3): 276-82.

Kawai, A., Ballantyne, D., Muckenhoff, K. & P. Scheid. (1996). Chemosensitive medullary neurones in the brainstem-spinal cord preparation of the neonatal rat. *J. Physiol.* **492**: 277-92.

Kimura, N., & J.E. Remmers. (1997). Unpublished results.

Kimura, N., Perry, S. F. & J.E. Remmers. (1997). Strychnine eliminates reciprocation and augmentation of respiratory bursts of the *in vitro* frog brainstem. *Neurosci. Lett.* **224**: 1-4.

Kinkead, R. (1995). The control of breathing in the bullfrog (*Rana catesbeiana*). Ph.D. Dissertation. The University of British Columbia.

Kinkead, R., & W.K. Milsom. (1994). Chemoreceptors and control of episodic breathing in the bullfrog (Rana catesbeiana). *Respir. Physiol.*, **95**: 81-98.

Kinkead, R. & W.K. Milsom. (1997). Role of pulmonary stretch receptor feedback in control of episodic breathing in the bullfrog. *Am. J. Physiol.* **272**: R497-508.

Kinkead, R. & S.F. Perry. (1991). The effects of catecholamines on ventilation in rainbow trout during hypoxia or hypercapnia. *Respir. Physiol.* **84**: 77-92.

Knowlton, G.C. & M.G. Larrabee. (1946). A unitary analysis of pulmonary volume receptors. *Am. J. Physiol.* **147**: 100-114.

Kogo, N., S.F. Perry & J.E. Remmers (1994). Neural organization of the ventilatory activity of the frog, *Rana catesbeiana.* I. *J. Neurobiol.* **25**: 1067-1079.

Kogo, N. & J.E. Remmers (1994). Neural organization of the ventilatory activity in the frog, *Rana catesbeiana.* II. *J. Neurobiol.* **25**: 1080-1094.

Kuhlmann, W.D. & M.R. Fedde. (1979). Intrapulmonary receptors in the bullfrog: sensitivity to $CO_2$. *J. Comp. Physiol.* **132A**: 69-75.

Langendorff, O. (1887). Die automatie des atemzentrums. *Arch. Anat. Physiol.* 285-295.

Leone, A.M., Palmer, R.M.J., Knowles, R.G., Francis, P.L., Ashton, D.S. & S. Moncada. Constitutive, and inducible nitric oxide synthases incorporate molecular oxygen into both nitric oxide and citrulline. *J. Biol. Chem.* **266**: 23790-23795.

Li, A. & E.E. Nattie. (1997). Focal central chemoreceptor sensitivity in the RTN studied with a $CO_2$ diffusion pipette *in vivo*. *J. Appl. Physiol.* **83**(2): 420-428.

Liao, G. S., Kubin, R. J. Galante, A. P. Fishman & A. I. Pack (1996). Respiratory activity in the facial nucleus in an *in vitro* brainstem of tadpole, *Rana catesbeiana*. *J. Physiol (London)* **492**: 529-544.

Ling, L., Karius, D.R., Fiscus, R.R. & D.F. Speck. (1992). Endogenous nitric oxide required for an integrative respiratory function in the cat brain. *J. Neurophysiol.* **68**: 1910-1912.

Little, C. (1983). The Colonization of Land: Origins and Adaptations of Terrestrial Animals. Cambridge; New York: Cambridge University Press.

Loeschcke, H.H., De Lattre, J., Schlaefke, M.E. & C.O. Trouth. Effects on respiration and circulation of electrically stimulating the ventral surface of the medulla oblongata. *Respir. Physiol.* **10**: 184-197.

Lumsden, T. (1923a). Observations on the respiratory centres in the cat. *J. Physiol. (London)* **57**: 153-160.

Lumsden, T. (1923b). Observations on the respiratory centres. *J. Physiol. (London)* **57**: 354-367.

Lumsden, T. (1923c). The regulation of respiration. Part I. *J. Physiol. (London)* **58**: 82-91.

Lumsden, T. (1924). Chelonian respiration (tortoise). *J. Physiol. (London)* **58**: 259-266.

Ma, S., Abboud, F.M. & R.B. Felder. (1995). Effects of L-arginine-derived nitric oxide synthesis on neuronal activity in nucleus tractus solitarius. *Am. J. Physiol. (Regul. Integr. Comp. Physiol.)* **268**: R487-R491.

MacIntyre, D.H. & Toews, D.P. (1976). The mechanics of lung ventilation and the effects of hypercapnia on respiration in *Bufo marinus*. *Can. J. Zool.* **54**: 1364-1374.

McLean, H.A., N. Kimura, N. Kogo, S.F. Perry & J.E .Remmers (1995a). Fictive respiratory rhythm in the isolated brainstem of frogs. *J. Comp. Physiol.* **176**: 703-713.

McLean, H.A., S.F. Perry & J.E. Remmers (1995b). Two regions in the isolated brainstem of the frog that modulate respiratory -related activity. *J. Comp. Physiol.* **177**: 135-144.

McLean, H. A. & J.E. Remmers. (1995). Respiratory motor output of the sectioned medulla of the neonatal rat. *Respir. Physiol.*, **96**: 49-60.

McMahon, B.R. (1969). A functional analysis of the aquatic and aerial respiratory movements of an African lungfish, Protopterus aethiopicus, with reference to the evolution of the lung-ventilation mechanism in vertebrates. *J. Exp. Biol.* **51**(2): 407-30.

Milsom, W. K. (1991). Intermittent breathing in vertebrates. *Annual Review of Physiology*, **53**: 87-105.

Milsom, W.K. (1995). Regulation of ventilation in lower vertebrates: role of $CO_2$/pH chemoreceptors. In *Advances in Environmental and Comparative Physiology* (ed. R. Gilles). pp. 1-74.

Milsom, W.K. & D.R. Jones. (1977). Carbon dioxide sensitivity of pulmonary receptors in the frog. *Experientia*. **33**: 1167-1168.

Mitchell, R. A., Loeschcke, H. H., Massion, W. H., & J.W. Severinghaus. (1963). Respiratory response mediated through superficial chemosensitive areas on the medulla. *J. Appl. Physiol.*, **18**: 523-533.

Mouritzen, D.A. (1979). Shrinkage of the brain during histological procedures with fixation in formaldehyde solutions of different concentrations. *J. Hirnforschung* **20**: 115-119.

Nattie, E. E., Li, A. & E.E. Coates. (1995). Central chemoreceptor location and the ventrolateral medulla. In *Ventral Brainstem Mechanisms and Control of Respiration and Blood Pressure*, ed. Trouth, C. O., Millis, R. M., Kiwull-Schöne, H. F. & Schläfke, M. E., pp. 131-150. Marcel Dekker, Inc., New York.

Nattie, E. E. & A. Li. (1996). Central chemoreception in the region of the ventral respiratory group in the rat. *J. Appl. Physiol.* **81**: 1987-95.

Nicholson, C. (1985). Diffusion from an injected volume of a substance in brain tissue with arbitrary volume fraction and tortuosity. *Brain Research* **333**: 325-329.

Nieuwenhuys, R. & P. Opdam. (1976). Structure of the brainstem. In *Frog Neurobiology*, ed. Llinas, R. & Precht, W., pp. 811-47. Springer-Verlag Press, New York, USA.

Nishizaki, T., R. Yamauchi, M. Tanimoto & Y. Okada (1988). Effects of temperature on the oxygen consumption in the thin slices from different brain slices. *Neurosci. Lett.* **86**: 301-305.

Norris, D.O. (1985). *Vertebrate Endocrinology. Second Edition.* Lea & Febiger, Philadelphia.

Oka, K. (1958a). The influence of the transection of the brain upon the respiratory movement of the frog. *Jap. J. Physiol.*, **20**: 513-519.

Oka, K. (1958b). Further studies on the localization of the respiratory centers of the frog. *Jap. J. Physiol.*, **20**: 520-524.

Okada, Y., G. Mückenhoff, G. Holtermann, H. Acker & P. Scheid (1993). Depth profiles of pH and $P_{O_2}$ in the isolated brain stem-spinal cord of the neonatal rat. *Respir. Physiol.* **93**: 315-326.

Onimaru, H., Arata, A. & I. Homma. (1989). Firing properties of respiratory rhythm generating neurons in the absence of synaptic transmission in rat medulla *in vitro*. *Experimental Brain Research* **76**: 530-536.

Orem, J. & E.H. Vidruk. (1998). Activity of medullary respiratory neurons during ventilator-induced apnea in sleep and wakefulness. *J. Appl. Physiol.* **84**(3): 922-932.

Pack, A. I., Galante, R. J., Walker, R. J., Kubin, L. K., & A.P. Fishman. (1993). Comparative approach to neural control of respiration. *In* D. F. Speck, M. S. Deakin, W. R. Revelette, & D. T. Frazier (Eds.), *Respiratory Control: Central and Peripheral Mechanisms.* (pp. 52-57). Lexington: The University Press of Kentucky.

Pineda, J., & G.K. Aghajanian. (1997). Carbon dioxide regulates the tonic activity of locus coeruleus neurons by modulating a proton- and polyamine-sensitive inward rectifier potassium current. *Neuroscience*, **77**: 723-43.

Randall, H., Burggren, W. W., Farrell, A.P. & M.S. Haswell. (1981). *The Evolution of Breathing in Vertebrates.* Cambridge; NewYork: Cambridge University Press.

Randall, D.J. & D.R. Jones. (1973). The effect of deafferentation of the pseudobranch on respiratory response to hypoxia and hyperoxia in the trout (*Salmo gairneri*). *Respir. Physiol.* **17**: 291-301.

Richerson, G. B. (1995). Response to CO2 of neurons in the rostral ventral medulla in vitro. *J. Neurophysiol.*, **73**: 933-44.

Richter, D.W. (1982). Generation and maintenance of the respiratory rhythm. *J. Exp. Biol.* **199**: 93-107.

Richter, D.W. & D. Ballantyne. (1983). A three phase theory about the basic respiratory pattern generator. In: *Central Neurone Environment*, ed. M.E. Schläfke, H.P. Koepchen & W.R. See. Springer-Verlag, Berlin, Germany; pp. 167-174.

Romer, A.S. (1958). Tetrapod limbs and early tetrapod life. *Evolution.* **12**: 365-369.

Rovainen, C.M. (1977). Neural control of ventilation in the lamprey. *Fedn. Proc. Fedn. Am. Socs. Exp. Biol.* **36**: 2386-2389.

Rovainen, C.M. (1985). Respiratory bursts at the midline of the rostral medulla of the lamprey. *J. Comp. Physiol.* **157A**: 303-309.

Sakakibara, Y. (1984). The pattern of respiratory nerve activity in the bullfrog. *Jap. J. Physiol.* **34**(2): 269-82.

Sakakibara, Y. (1984). Trigeminal nerve activity and buccal pressure as an index of total inspiratory activity in the bullfrog. *Jap. J. Physiol.* **34**(5): 827-38.

Schläfke, M.E., See, W.R., & H.H. Loeschcke. (1970). Ventilatory responses to alterations of $H^+$-ion concentration in small areas of the ventral medullary surface. *Respir. Physiol.* **10**: 198-212.

Schmidt, R. S. (1973). Central mechanisms of frog calling. *American Zoologist* **13**: 1169-1117.

Schmidt, R. S. (1992). Neural correlates of frog calling: production by two semi-independent generators. *Behavioural Brain Research* **50**: 17-30.

Schwarzacher, S.W., Smith, J.C. & D.W. Richter. (1991). Respiratory neurons in the Pre-Bötzinger region of cats. *Pflügers Arch.* **418**: R17.

Senn, D.G. (1972). Development of tegmental and rhombencephalic structures in a frog (*Rana temporaria* L.). *Acta. Anat.* **82**:525-548.

Shelton, G., Jones, D.R. & W.K. Milsom. (1986). Control of breathing in ectothermic vertebrates. In *Handbook of Physiology*, section. 3. *The Respiratory System.*, vol. II., *Control of breathing.* part II (ed. A.P. Fishman, N.S. Cherniak, J.G. Widdicombe and S.R. Geiger), pp. 857-909. Bethesda: American Physiological Society.

Shi, Y. (1994). Molecular biology of amphibian metamorphosis. *Trends. Endocrinol. Metab.*, **5**: 14-20.

Shibata, M. & C.M. Blatteis (1991). High perfusate $P_{O_2}$ impairs thermosensitivity of hypothalamic thermosensitive neurons in slice preparations. *Brain Res. Bulletin* **26**: 467-471.

Smatresk, N.J. (1990). Chemoreceptor modulation of endogenous respiratory rhythms in vertebrates. *Am. J. Physiol.* **259**: R887-897.

Smatresk, N.J. & A.W. Smits. (1991). Effects of central and peripheral chemoreceptor stimulation in ventilation in the marine toad, *Bufo marinus*. *Respir. Physiol.* **83**: 223-238.

Smith, F. M., & D.R. Jones. (1982). The effect of changes in blood oxygen-carrying capacity on ventilation volume in the rainbow trout (Salmo gairdneri). *J. Exper. Biol.*, **97**: 325-34.

Smith, J.C. & J.L. Feldman (1987). In-vitro brain stem-spinal cord preparations for study of motor systems for mammalian respiration and locomotion. *J. Neurosci. Methods* **21**: 321-333.

Smith, J.C., Ellenberger, H.H., Ballanyi, K., Richter, D.W. & J.L. Feldman. (1991). Pre-Botzinger complex: a brainstem region that may generate respiratory rhythm in mammals. *Science* **254**: 726-29.

Smyth, D.M. (1939). The central and reflex control of respiration in the frog. *J. Physiol. (London).* **95**: 305-327.

Southard, T. L., Huang, R. Q., & J.B. Dean. (1995). Electrophysiological properties of neurons in chemosensitive areas of the dorsal and ventral brainstem. *Soc. Neurosci. Abstracts*, **21**: 1883.

St. John, W.M. (1990). Neurogenesis, control and functional significance of gasping. *J. Appl. Physiol.*, **68**: 1305-1315.

Stuesse, S. L., Cruce, W.L.R. & K. S. Powell. (1984). Organization within the cranial IX-X complex in ranid frogs: a horseradish peroxidase transport study. *J. Comp. Neurol.* **222**: 358-365.

Suzue, T. (1984). Respiratory rhythm generation in the *in vitro* brain stem-spinal cord preparation of the neonatal rat. *J. Physiol. (London)* **354**: 174-183.

Takeda, R., Remmers, J.E., Baker, J.P. & J.P. Farber. (1986). Postsynaptic potentials of bulbar respiratory neurons of the turtle. *Respir. Physiol.* **64**: 149-160.

Taylor, A.C. and J. Köllros (1946). Stages in the normal development of *Rana pipiens* larvae. *Anat. Record* **94**: 7-24.

Taylor, E.W. (1985). Control and co-ordination of gill ventilation and perfusion. *Symposia of the Society for Experimental Biology* **39**:123-61.

Tenney, S.M. & J.C. Leiter. (1995). The control of breathing: an uninhibited survey from the perspective of comparative physiology. In: *Regulation of Breathing, Second Edition* (edited by J.A. Dempsey & A.I. Pack). *Lung Biology in Health and Disease, Vol. 79* (ed. Claude Lenfant). Pp. 3-36. New York; Basel; Hong Kong, Marcel Dekker, Inc.

Thomas, S. (1983). Changes in blood acid-base balance in trout (*Salmo gairdneri*) following exposure to combined hypoxia and hypercapnia. *J. Comp. Physiol.* **152B**: 53-57.

Thomas, S. & H. LeRuz. (1982). A continuous study of rapid changes in blood acid-base status of trout during variations of water $P_{CO_2}$. *J. Comp. Physiol.* **148B**: 123-130.

Travagli, R.A. & R.A. Gillis. (1994). Nitric oxide-mediated excitatory effect on neurons of dorsal motor nucleus of vagus. *Am. J. Physiol. (Gastrointest. Liver Physiol.)* **266**: G154-G160.

Van Vliet, B.N. & N.H. West. (1986). Cardiovascular responses to electrical stimulation of the recurrent laryngeal nerve in conscious toads (*Bufo marinus*). *J. Comp. Physiol.* **156B**: 363-375.

Van Vliet, B.N. & N.H. West. (1987). Response characteristics of pulmocutaneous arterial baroreceptors in the toad, *Bufo marinus*. *J. Physiol. (London)* **388**: 55-70.

Van Vliet, B.N. & N.H. West. (1992). Functional characteristics of arterial chemoreceptors in an amphibian (*Bufo marinus*). *Respir. Physiol.* **88**(1,2): 113-127.

Voipio, J. & K. Ballanyi. (1997). Interstitial $P_{CO_2}$ and pH, and their role as chemostimulants in the isolated respiratory network of neonatal rats. *J. Physiol. (London)* **499**(2): 527-542.

Von Euler, C. (1983). On the origin and pattern control of breathing rhythmicity in mammals. *Symposia of the Society for Experimental Biology*, **37**: 469-85.

Walker, R., Galante, R.J., Fishman, A.P. & A.I. Pack. (1990). Effect of GABA on gill and lung ventilation in an *in vitro* isolated brainstem preparation in the tadpole. *Physiologist* **33**: A35.

West, N.H. & W.W. Burggren. (1982). Gill and lung ventilation responses to steady-state aquatic hypoxia and hyperoxia in the bullfrog tadpole. *Respir. Physiol.* **47**(2): 165-76.

West, N.H. & W.W. Burggren. (1983). Reflex interactions between aerial and aquatic gas exchange organs in larval bullfrogs. *Am. J. Physiol.*, **244**(13): R770-R777.

West, N.H. & W.W. Burggren. (1984). Control of pulmonary and cutaneous blood flow in the toad, *Bufo marinus*. *Am. J. Physiol.* **64**: 25-38.

West, N.H. & D.R. Jones. (1975). Breathing movements in the frog *Rana pipiens*. I. The mechanical events associated with lung and buccal ventilation. *Can. J. Zool.* **53**(3): 332-44.

West, N.H., Topor, Z.L. & B.N. Van Vliet. (1987). Hypoxemic threshold for lung ventilation in the toad. *Respir. Physiol.* **70**: 377-390.

Wood, C.M., Turner, J.D., Munger, R.S. & M.S. Graham. (1990). Control of ventilation in the hypercapnic skate *Raja oscellata*. II Cerebrospinal fluid and intracellular pH in the brain and other tissue. *Respir. Physiol.* **80**: 279-298.

# IMAGE EVALUATION
# TEST TARGET (QA-3)

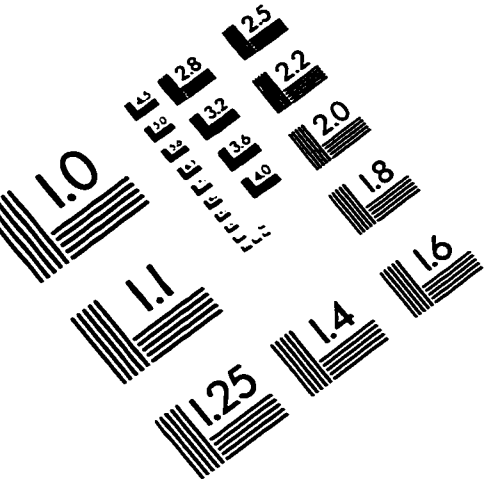


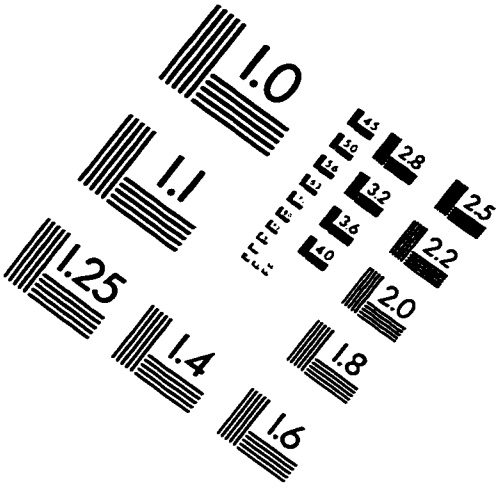


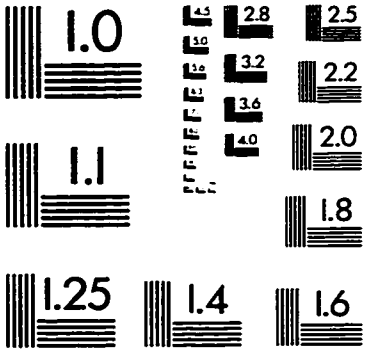


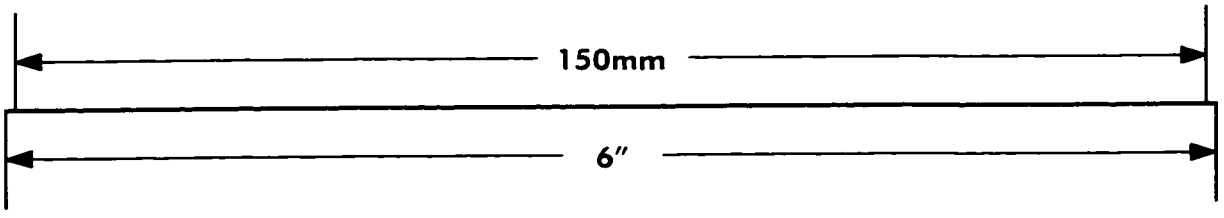


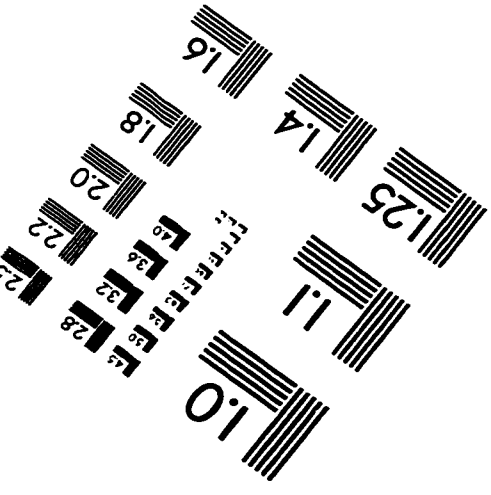


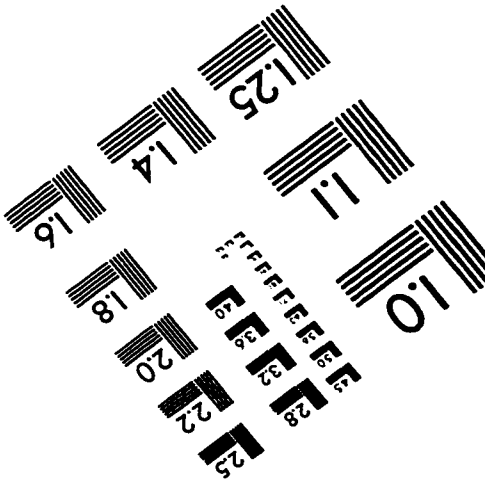


APPLIED IMAGE, Inc
1653 East Main Street
Rochester, NY 14609 USA
Phone: 716/482-0300
Fax: 716/288-5989